Simulation and Techno-Economic Analysis of the AChT Green Methanol Process

by

Sean Christopher McCaul

A thesis
presented to the University of Waterloo
in fulfillment of the
thesis requirement of the degree of
Master of Applied Science
in
Chemical Engineering

Waterloo, Ontario, Canada, 2019

Author’s Declaration

I hereby declare that I am the sole author of this thesis. This is a true copy of the thesis, including any required final revisions, as accepted by my examiners.

I understand that my thesis may be made electronically available to the public.

Abstract

Methanol is a valuable commodity with many uses. It is used to manufacture other chemicals such as olefins, formaldehyde, and methyl-tert-butyl ether (MTBE). Methanol is also being researched as an alternative fuel for vehicles. Global methanol demand is increasing, making it a valuable chemical to manufacture.

Methanol production requires three main steps: syngas production, methanol production, and methanol purification. Syngas is a mix of carbon monoxide and hydrogen that can be made through the reforming of natural gas. The production of syngas is done through many methods. Three primary methods are steam methane reforming (SMR), partial oxidation (POX), and autothermal reforming (ATR). Once syngas is produced, it is sent to a methanol reactor where three main reactions occur: the hydrogenation of CO, the hydrogenation of CO_2, and the water-gas shift reaction. A product stream with methanol is then purified in using distillation.

The company Technology Convergence Inc. (TCI) made a process for manufacturing methanol in 2004 called the Green Methanol Process. This process involved the use of a POX reformer and an electrolyser to provide the required hydrogen and oxygen. TCI is now known as Advanced Chemical Technologies (AChT), and they have since updated their Green Methanol Process. The new process still uses an electrolyser to generate hydrogen and oxygen, but now uses an ATR for syngas production.

Aspen Plus was used in this work to simulate the updated AChT process. Heat integration was successfully implemented into the simulation. Additionally, the syngas production method was changed over from POX to ATR. An initial analysis of the amine reboiler of a CO_2 capture unit was done. Finally, it was discovered that the waste stream contained a large amount of hydrogen. To remedy this, a method of hydrogen purification was studied called pressure swing adsorption (PSA). A version of the methanol process simulation was done with the PSA hydrogen recycle system added.

An economic analysis looked into the OPEX and CAPEX of the process with and without PSA hydrogen recycling. Without hydrogen recycling, the CAPEX and OPEX were found to be $248 CAD/metric tonne (MT) methanol and $300 CAD/MT methanol, respectively, while producing 217 MTPD (metric tonne per day) of methanol. This resulted in a combined overall cost of $548 CAD/MT methanol produced. With hydrogen recycling, the CAPEX and OPEX were found to be $223 CAD/MT methanol and $280 CAD/MT methanol respectively, while producing 249 MTPD of methanol. This resulted in a combined cost of $503 CAD/MT methanol. Overall, it was found that the implementation of a PSA hydrogen recycle system was a good investment.

Additionally, hourly Ontario electricity price (HOEP) data from 2018 were used to determine on average the most expensive consecutive 11-day period. Since the plant was planned to be shut down for 11 days for maintenance, this would inform when the best time to shut down would be to save the most on electricity. The best day to start the maintenance was found to be January 5th. The next most expensive periods started on December 4th and April 9th.

Acknowledgments

I would like to express my immense gratitude to my supervisor, Prof. Eric Croiset, for his relentless patience, his continuous encouragement, and his vast knowledge. This thesis was a challenging task, but without him it would have been an impossible one.

I would also like to thank Doug Beynon and Seth Brouwers at Advanced Chemical Technologies for their help and support throughout the process of completing this thesis.

Table of Contents

Author's Declaration ii
Abstract iii
Acknowledgments iv
Table of Contents v
List of Figures viii
Chapter 1 Figures viii
Chapter 2 Figures viii
Chapter 3 Figures viii
Chapter 4 Figures viii
Chapter 5 Figures ix
Appendix A Figures ix
Appendix B Figures ix
List of Tables x
Chapter 3 Tables x
Chapter 4 Tables x
Chapter 5 Tables x
Appendix A Tables xi
Appendix B Tables xi
Chapter 1: Introduction 1
1.1 Advanced Chemical Technologies (AChT) Process 2
1.2 Thesis Approach 3
1.3 Thesis Outline 3
Chapter 2: Literature Review 4
2.1 Conventional Methanol Synthesis Process 4
2.1.1 Low Pressure Methanol Synthesis 4
2.1.2 CO2 as Feedstock to the Methanol Process 6
2.1.3 Methanol Reactors 7
2.2 Electrolysis 11
2.3 Syngas Production 12
2.3.1 Autothermal Reforming 13
Chapter 3: Model Development 16
3.1 AChT Methanol Process 16
3.2 Electrolyser 17

3.3 Syngas Production Section 18
3.3.1 Feedstocks 20
3.3.2 Adiabatic Pre-Reformer 21
3.3.3 Autothermal Reformer 22
3.3.4 Steam Generator 22
3.4 Methanol Synthesis Section 23
3.4.1 Methanol Reactor 24
3.4.2 Recycle 25
3.5 Methanol Purification Section 26
3.6 Heat Integration 27
3.6.1 Steam Generator Configuration 27
3.6.2 Cooling Sections 28
3.6.3 Fired Heater 30
3.6.4 Heating Sections 31
3.7 CO_2 Capture 32
Chapter 4: Simulation Results 33
4.1 ATR Section 33
4.1.1 Steam-to-Carbon Ratio Design Specification 34
4.1.2 CO_2 to ATR 35
4.1.3 ATR Syngas Stream Results 37
4.2 Methanol Reactor Section 38
4.2.1 Methanol Recycle 39
4.2.2 Hydrogen Recycle 42
4.2.3 Pressure Swing Adsorption 42
4.2.4 Electrolyser Hydrogen Recovery 43
4.2.5 Hydrogen Recycle Split Percentage 44
4.3 Heat Integration 45
4.3.1 Post-ATR Cooling Section 45
4.3.2 Post-Methanol Reactor Cooling Section 47
4.3.3 Fired Heater Section 48
4.3.4 Remaining Hot Streams 49
4.3.5 Hydrogen Recycle Heat Integration 49
4.4 CO_2 Capture 51
4.4.1 CO_2 Emitted by the Methanol Process 51
4.4.2 Amine Reboiler Steam Generator 52

4.4.3 Reboiler Steam Requirement 55
4.4.4 CO_2 Solutions Capture Unit Simulation 55
Chapter 5: Economic Evaluation 56
5.1 Capital and Operating Cost Comparison with and without PSA Hydrogen Recycling 56
5.1.1 CAPEX of Scenario 1 57
5.1.2 OPEX of Scenario 1 58
5.1.3 Total Scenario 1 Costs 60
5.1.4 CAPEX of Scenario 2 60
5.1.5 OPEX of Scenario 2 61
5.1.6 Total Scenario 2 Costs 61
5.1.7 Scenario 1 and 2 Comparison 62
5.2 Payback Period 62
5.2.1 Scenario 1 Payback Period 63
5.2.2 Scenario 2 Payback Period 63
5.2.3 Payback Period Comparison 63
5.3 Internal Rate of Return 64
5.4 Sensitivity Analysis 65
5.4.1 Scenario 1 Sensitivity Analysis 65
5.4.1 Scenario 2 Sensitivity Analysis 66
5.5 Electrolyser Shutdown 68
Chapter 6: Conclusions and Recommendations 69
6.1 Conclusions 69
6.2 Recommendations 70
References 71
Appendix A: Scenario 1 ASPEN Stream Results 74
Appendix B: Scenario 2 Aspen Simulation Results 85

List of Figures

Chapter 1 Figures

Figure 1.1 Traditional methanol manufacturing process [6]. 2
Figure 1.2 2010 Green Methanol Process [6]. 2

Chapter 2 Figures

Figure 2. 1 ICI quench reactor [17]. 8
Figure 2.2 ICI methanol synthesis loop [17]. (a) Recycle compressor; (b) heat exchanger; (c) reactor; (d) boiler feed water (BFW) preheater; (e) cooler/condenser; (f) separator; (g) start-up heater. 8
Figure 2.3 Lurgi methanol synthesis loop [17]. (a) Recycle compressor; (b) heat exchanger; (c) reactor; (d) cooler/condenser; (e) separator. 9
Figure 2.4 The three main methanol synthesis reactor types and their temperature profiles [1].10
Figure 2.5 Illustration of an ATR reactor [7]. 14

Chapter 3 Figures

Figure 3.1 The AChT methanol synthesis process. 16
Figure 3. 2 Electrolyser simulation. 17
Figure 3.3 Typical layout of the autothermal reforming section with an adiabatic pre-reformer in a GTL plant [7]. 18
Figure 3. 4 Aspen Plus simulation of the syngas production section. 19
Figure 3.5. Zoomed-in view of the adiabatic pre-reformer 22
Figure 3.6 Aspen simulation of the methanol synthesis section. 23
Figure 3.7 Aspen Plus simulation of the methanol purification section. 26
Figure 3.8 Steam generator configuration for post-ATR cooling. 28
Figure 3.9 Steam generation and cooling of the syngas stream. 29
Figure 3.10 Steam generator configuration for post-methanol reactor cooling. 30
Figure 3.11 Amine reboiler and steam generator simulation in Aspen Plus. 32

Chapter 4 Figures

Figure 4.1 CO2 bypass percentage vs. ATR heat duty. 35
Figure 4.2 CO_2 bypass percentage vs. syngas ratio. 36
Figure 4.3 CO2 bypass percentage vs. methanol output. 36
Figure 4.4 ATR syngas result stream. 37
Figure 4.5 Methanol reactor section. 38
Figure 4.6 Methanol output vs. methanol recycle split to recycle. 40
Figure 4. 7 Recycle stream flowrate vs. methanol recycle split to recycle. 41
Figure 4. 8 Reactor conversion vs. methanol recycle split to recycle. 41
Figure 4.9 Methanol synthesis section with PSA hydrogen recovery 43
Figure 4. 10 Recovery of electrolyser hydrogen. 43
Figure 4. 11 Recycle split to hydrogen recycle vs. hydrogen recycle flowrate. 45
Figure 4. 12 Heat integration of the steam generated from the post-ATR cooling section. 46

Figure 4. 13 Steam generator configuration for post-methanol reactor cooling. 47
Figure 4. 14 Heat integration of the fired heater hot stream 48
Figure 4.15 Hydrogen recycle heat integration. 50
Figure 4.16 Amine reboiler steam generator iteration loop. 51
Figure 4.17 Amine reboiler and steam generator simulation in Aspen Plus. 52

Chapter 5 Figures

Figure 5.1 Scenario 1 sensitivity of CAPEX. 65
Figure 5.2 Scenario 1 sensitivity of OPEX. 66
Figure 5.3 Scenario 2 sensitivity of CAPEX. 66
Figure 5.4 Scenario 2 sensitivity of OPEX. 67
Figure 5.5 Average HOEP of every consecutive 11-day period in 2018. 68

Appendix A Figures

Figure A.1 Scenario 1 Aspen simulation part 1: Electrolyser and ATR section 74
Figure A.2 Scenario 1 Aspen simulation part 2: Methanol reactor section 75
Figure A.3 Scenario 1 Aspen simulation part 3: Amine reboiler 76

Appendix B Figures

Figure B.1 Scenario 2 Aspen simulation with PSA part 1: Electrolyser and ATR section. 85
Figure B.2 Scenario 2 Aspen simulation with PSA part 2: Methanol reactor section. 86
Figure B.3 Scenario 2 Aspen simulation with PSA part 3: Amine reboiler section. 87

List of Tables

Chapter 3 Tables

Table 3.1 Feed natural gas composition....20
Table 3.2 Reaction rate constants....24
Table 3.3 Adsorption equilibrium constants....24
Table 3.4 Reaction equilibrium constants....25

Chapter 4 Tables

Table 4.1 STMSEP-1 steam separation results (380°C, 35 atm).....34
Table 4.2 Combined steam and methane flow to the ATR. 34
Table 4.3 CO_2 bypassing ATR vs. ATR heat duty, syngas ratio, and methanol output. 35
Table 4.4 Test with 88% CO_2 bypass. 37
Table 4.5 SYNGAS-6 stream composition at 231°C and 70 atm. 38
Table 4.6 Methanol recycle split percentage test results. 40
Table 4.7 Molar flow and mole fraction composition of methanol, recycle, and waste streams. .42
Table 4.8 Results of hydrogen recycle split percentage tests. 44
Table 4.9 Remaining hot streams.....49
Table 4.10 CO_2 emissions per CO_2 source. 51
Table 4.11 CO_2 capture to heat duty conversion rates found from literature. 53
Table 4.12 Final CO_2 capture iteration results. 54
Table 4.13 Total CO_2 captured. 54
Table 4.14 Remaining hot streams vs. reboiler steam requirement. 55
Table 4.15 CO_2 Solutions capture results. 55

Chapter 5 Tables

Table 5.1 Simulation results with and without hydrogen recycling. 56
Table 5.2 Key economic parameters. 57
Table 5.3 Scenario 1 CAPEX values. 57
Table 5.4 Scenario 1 annualized CAPEX values. 57
Table 5.5 Scenario 1 CAPEX cost of methanol values. 58
Table 5.6 Scenario 1 natural gas cost. 58
Table 5.7 Scenario 1 cost of electricity. 59
Table 5.8 Scenario 1 cost of water to electrolyser. 59
Table 5.9 Scenario 1 miscellaneous costs. 59
Table 5.10 Scenario 1 total OPEX.....59
Table 5.11 Scenario 1 total costs. 60
Table 5.12 Scenario 2 CAPEX. 60
Table 5.13 Scenario 2 OPEX 61
Table 5.14 Scenario 2 total costs. 61
Table 5.15 Scenarios 1 and 2 total cost comparison. 62
Table 5.16 Scenario 1 payback period calculation. 63
Table 5.17 Scenario 2 payback period calculation. 63
Table 5.18 IRR calculations for scenarios 1 and 2. 64

Appendix A Tables

Table A.1 Scenario 1 Aspen simulation results. 76

Appendix B Tables

Table B.1 Scenario 2 Aspen simulation stream results.....87

Chapter 1: Introduction

Methanol is an important chemical that has many uses. It is used in the manufacturing of products like olefins, formaldehyde, and methyl-tert-butyl ether (MTBE) [1] [2]. Methanol is also being researched as an alternative fuel for vehicles [1]. Global methanol demand has increased significantly over the past few years, from 72.6 million tonnes in 2014 to an estimated 98.0 million tonnes in 2019 [3].

Methanol is conventionally manufactured through three main steps:

1. Syngas production
2. Methanol production
3. Methanol purification

Syngas production involves the reformation of hydrocarbon (usually from the reforming of natural gas or coal) with some combination of steam and/or oxygen in order to create syngas. Syngas, or synthesis gas, is made up primarily of hydrogen and carbon monoxide. Syngas is used in methanol manufacturing, where it is a key feedstock. The primary methods of syngas production from natural gas include [4]:

- Steam methane reforming (SMR): endothermic reaction of methane with steam.
- Partial oxidation (POX): exothermic reaction of methane with sufficiently low amount of oxygen to avoid combustion of methane.
- Autothermal reforming (ATR): combination of SMR and POX where heat is neither consumed nor removed.

Once syngas is produced, it can be used to make methanol. In a methanol reactor, three main reactions occur. These are the hydrogenation of CO, the hydrogenation of CO_2, and the water-gas shift reaction, shown below [5].

$$CO + 2H_2 \leftrightarrow CH_3OH \quad \text{Equation 2.1}$$
$$CO_2 + 3H_2 \leftrightarrow CH_3OH + H_2O \quad \text{Equation 2.2}$$
$$CO_2 + H_2 \leftrightarrow CO + H_2O \quad \text{Equation 2.3}$$

Additionally, syngas should be delivered to the methanol reactor at a specific ratio, known as the syngas ratio or module 'M' [6] [7], shown in Equation 2.4. The syngas ratio should equal 2 based on the stoichiometry of the hydrogenation of CO reaction (Equation 2.1). It offers the ideal ratio of reactants for the process of methanol synthesis [6]. This is an important factor when designing syngas production for methanol manufacturing.

$$M = \frac{H_2 - CO_2}{CO + CO_2} \quad \text{Equation 2.4}$$

After this, the product of the methanol reactor is purified in order to separate unreacted material from product methanol. This is typically done through distillation.

1.1 Advanced Chemical Technologies (AChT) Process

Traditional methanol manufacturing can create carbon dioxide (CO_2) emissions, a well-known greenhouse gas. Syngas production methods require feedstocks like natural or coal, as well as steam and/or oxygen. This is shown in Figure 1.1. When oxygen is required, it is usually produced using air separation technology, but that method is expensive.

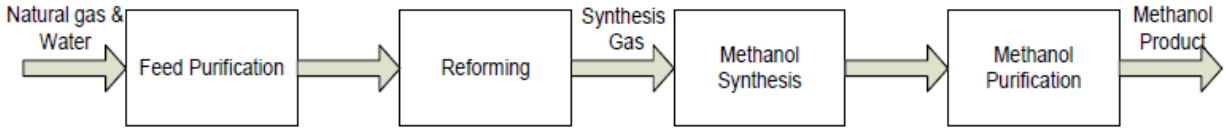

Figure 1.1 Traditional methanol manufacturing process [6].

The company Technology Convergence Inc. (TCI) developed what was called the Green Methanol Process [8], which was the subject of a 2010 report by Lalitnorasate & Croiset [6].

The 2010 TCI process used partial oxidation (POX) as the syngas manufacturing method. This means that a feed of methane, oxygen, and steam was required. The fundamental difference between traditional methanol manufacturing and the Green Methanol Process is the source of these feedstock materials for the syngas production process. Instead of using a feed of just steam and natural gas for the POX, a water electrolysis unit was added. This electrolyser would use electricity to convert water into hydrogen and oxygen. The oxygen was fed to the POX reformer, and the hydrogen was used to supplement the syngas. This is shown in figure 1.2. Given that the electrolyser produces nearly zero carbon emissions in Ontario because electricity is primarily generated from nuclear power plants and hydroelectric dams, it was a nearly emissions-free way to supplement both the POX and methanol feeds.

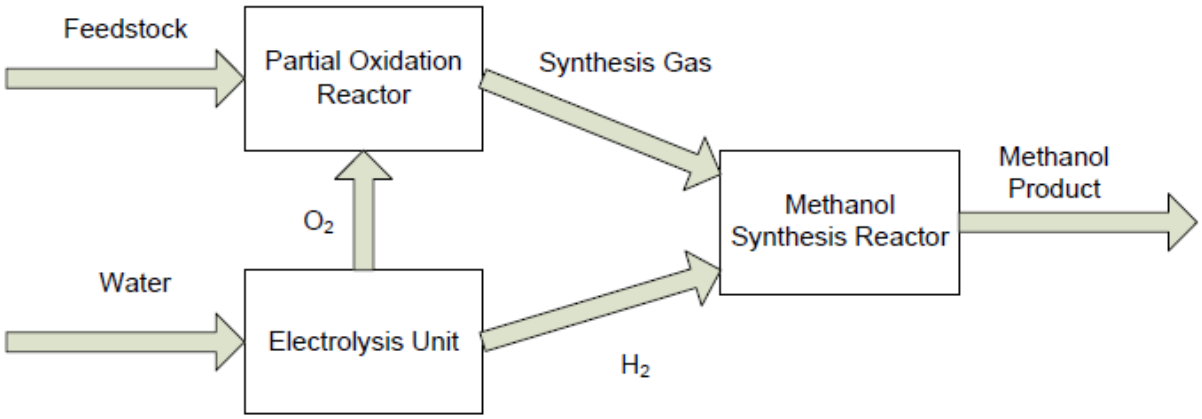

Figure 1.2 2010 Green Methanol Process *[6]*.

TCI is now known as Advanced Chemical Technologies Inc. (AChT), and the AChT Green Methanol Process has been further developed since that time. In the new version, the syngas production method has been changed from POX to autothermal reforming (ATR). This change fundamentally alters the syngas production section of the process. Additionally, the original TCI process included a feed of CO_2 to the POX reformer in order to maintain a syngas ratio of 2.

The newer version of the process has a more specific notion for the CO_2 feedstock. This feed of CO_2 is now meant to be a combination of captured CO_2 from a neighbouring plant operation plus the captured CO_2 from the Green Methanol Process itself. These changes are meant to improve the carbon footprint of the process by making it less reliant on the burning of natural gas.

1.2 Thesis Approach

The first goal of this thesis was to simulate the updated AChT Green Methanol Process in Aspen Plus. This meant starting with the Aspen simulation that was developed in the TCI process and described in Lalitnorasate & Croiset, then updating it to reflect the changes to the process. The main change was moving from a POX reformer to an ATR for syngas production. The scale chosen was a pilot plant that produces 230 MTPD (300 kmol/hr) of methanol.

Moving forward with the Aspen simulation, there were goals to make other changes. These included added heat integration to the model and testing CO_2 capture. The last planned step was to do an economic evaluation of the process.

1.3 Thesis Outline

This thesis consists of six chapters:

Chapter 1: Introduction

Chapter 2: Literature Review.

> A study into the background of chemical engineering topics relevant to this work. Related studies are also described.

Chapter 3: Model Development.

> This chapter describes the setup of the process simulation. It goes into detail on the operating conditions of the many blocks and streams.

Chapter 4: Simulation Results.

> In this chapter, the process simulation was analysed based on its behaviour. Results are processed, and developments to the simulation are applied and suggested.

Chapter 5: Economic Evaluation.

> This chapter looks into the overall capital and operating expenditures (CAPEX and OPEX) required to install and run this process. It also features some economic testing of cost-saving changes to the simulation.

Chapter 6: Conclusions and Recommendations.

Chapter 2: Literature Review

This chapter overviews key chemical engineering subjects relevant to this work, starting with methanol synthesis, followed by electrolysis, and then syngas production. In each section, relevant studies are discussed.

2.1 Conventional Methanol Synthesis Process

Methanol was discovered in 1661 by Robert Boyle [9]. A process to synthesize methanol was later developed in 1857 [9]. This initial synthesis process involved distilling methanol from wood, leading some to refer to methanol as “wood alcohol”. This highly inefficient process was eventually replaced with a 1913 patent from Badische Anilin-und-Soda-Fabrik (BASF) for a method of synthesizing methanol from a feed of CO, CO_2, and H_2 over a zinc/chromium oxide catalyst [9]. This process occurred at a temperature of 300 to 400°C and pressures between 100 and 250 atm, and was the origin of what became known as high-pressure methanol synthesis [9] [6] [10].

In 1923, BASF constructed the first commercial plant using the high-pressure methanol synthesis process [9] [1]. This process was widely used for a long period of time, with Commercial Solvents Corporation and DuPont also developing commercial methanol synthesis plants in 1927 [9]. DuPont’s plant in Belle, West Virginia, manufactured methanol and ammonia in tandem, with the waste gases from the methanol process being used as the feedstock for the ammonia process [9]. At the time, coal was the preferred carbon feedstock for the methanol synthesis process, however natural gas took its place starting around the 1940s [9]. Coal would later have a resurgence in popularity starting in the 1980s [9].

Researchers devoted a great amount of time trying to improve the high-pressure methanol synthesis process [6] [10] [11] [12] [13] [5] [14] [2]. It was understood early on that copper-based catalysts were much more efficient than the zinc/chromium oxide catalysts that were used at the time, however copper catalysts were too easily poisoned by sulfur contamination [15]. In the 1960s, sulfur removal technology experienced a leap in efficacy, allowing for the introduction of copper-based catalysts to the methanol synthesis process [9] [10]. In 1966, Imperial Chemistry Industries Ltd. (ICI) introduced a copper/zinc oxide catalyst that allowed the process to operate at 250-300°C and 50-100 atm [9] [10]. This was the birth of the low-pressure methanol synthesis process, the basis of the modern methanol synthesis industry [9] [10].

2.1.1 Low Pressure Methanol Synthesis

Today, methanol is manufactured on an industrial scale. As a feedstock in other processes, it has many uses. It is used in the production of chemicals like formaldehyde, methyl-tert-butyl ether (MTBE), and acetic acid [1], and is used to manufacturing olefins [2]. Methanol has also been suggested as a potential alternative fuel for use in vehicles [1]. As of 2014, the annual production of methanol was 62 million tonnes per year [2]. The basis of industrial methanol production is the low-pressure methanol synthesis process, developed by ICI in the 1960s. It traditionally involves a feed of CO, CO_2, and H_2 mixtures over a $Cu/ZnO/Al_2O_3$ catalyst [2]. However, research continues to work to improve the process year after year [1] [2] [5] [6] [10] [11] [12] [13] [14].

Understanding copper-based methanol synthesis catalysts in terms of catalyst type and applied reaction conditions is an active area of industrial and academic research [2] [5] [12]. Van de Water et al. [2] studied methanol synthesis from CO/H_2 feeds over Cu/CeO_2 catalysts, exploring the methanol formation in detail. Their results indicate that the active site and reaction mechanism for methanol synthesis over Cu/CeO_2 are different from the conventional $Cu/ZnO/Al_2O_3$ catalyst. While the carbon source for the traditional $Cu/ZnO/Al_2O_3$ catalyst is CO_2, it was discovered that the carbon source for Cu/CeO_2 catalysts is instead CO. Additionally, they presented catalyst poisoning gradients for Cu/CeO_2 catalysts, showing that CO_2 generated during CeO_2 reduction by CO acts as a poison for the Cu/CeO_2 catalyst. Even small amounts of CO_2 added to the feed would lead to uniform deactivation across the catalyst. It was found that changes to the CO content in the feed could control this deactivation. The reason for these differences between the tested Cu/CeO_2 catalyst and the traditional $Cu/ZnO/Al_2O_3$ catalyst was found to be the lack of CO_2 and H_2O re-adsorption on the $Cu/ZnO/Al_2O_3$ catalyst during catalyst activation.

Li and Jens [12] studied a new catalyst system that functions at lower temperature and pressure than the traditional methanol synthesis process. The catalyst system was produced in situ by the reaction of $Cu(CH_3COO)_2$, NaH, and methanol. While the conventional methanol synthesis process operates at 250-300°C and 50-100 atm, this new catalyst system operates at 60-120°C and 10-20 atm. It was shown that the catalyst suffers from intolerance to poisons such as CO_2 and H_2O, which is an issue that still needs to be solved. However, given the drastic decrease in operating pressure and temperature, further exploration may be valuable.

A paper by Seidel et al. [5] looked to describe a new kinetic model for the low-pressure methanol synthesis process. They studied traditional methanol synthesis from $H_2/CO_2/CO$ using a $Cu/Zn/Al_2O_3$ catalyst, but took into account different active surface species for CO and CO_2 hydrogenation than most established kinetic models. Varying the amounts of these surface species played an important role for the dynamic transient behaviour. The model showed suitability for methanol production under changing feed conditions employed, for example, in novel applications for chemical energy storage. The kinetic model was applied to experimental data for varying CO/CO_2 feed ratios. This work forms a basis for future work on model-based design of methanol reactors for chemical energy storage with a wide range of CO-to-CO_2 ratios.

Clausen et al. [14] reported on their work designing methanol production process configurations based on renewable energy sources. Simulating the configurations in the process simulation tool DNA, six different configurations were tested - each with a unique and renewable method of producing syngas. The syngas production methods involved various combinations of the following: gasification of biomass, electrolysis of water, CO_2 from post-combustion capture, and autothermal reforming of natural gas or biogas. Underground gas storage of hydrogen and oxygen was used to ensure the constant production of methanol while the operation of the electrolyser followed the daily variations in the electricity price. Each process was highly heat integrated, resulting in high energy efficiencies for the plants. The plants were compared by specific methanol costs as well as by methanol exergy efficiency.

Alarifi et al. [1] worked to optimize and model the gas-phase methanol synthesis process. Emphasis was placed on four main factors:

- A comparison between single and double tube industrial methanol synthesis reactors.
- Optimization and simulation of a quench adiabatic reactor for use in the methanol synthesis process, with a focus on methanol production and CO_2 usage.
- Displaying the capabilities of derivative-free search algorithm-based methods when scaled to industrial cases.
- Designing and analyzing a hybrid metaheuristics algorithm to quickly determine the optimal operating conditions for the methanol synthesis process while undergoing catalyst deactivation.

2.1.2 CO2 as Feedstock to the Methanol Process

Nowadays it is understood that the CO_2 in the $CO/CO_2/H_2$ feed to the methanol process is what provides the dominant path to synthesizing methanol [10] [5]. However, this was not always the case. Operators of the original ICI process in the 1960s were so convinced that methanol came from the hydrogenation of CO and not CO_2 that CO_2 was even scrubbed from the reactant mixture at the time. It was only after the CO_2 scrubber failed and CO_2 was accidentally leaked into the CO/H_2 mixture that a large increase in methanol production was noticed, leading to CO_2 being incorporated into the feed mixture [10]. Today, the traditional feed to the methanol process is comprised of $CO/CO_2/H_2$, and it is generally understood that it is the hydrogenation of CO_2 that produces the methanol.

CO_2 as a carbon feedstock presents both environmental and industrial benefits - especially when combined with CO_2 capture methods. Li et al. discovered a hybrid oxide catalyst comprising of manganese oxide nanoparticles supported on mesoporous spinel cobalt oxide, and were able to catalyze the conversion of CO_2 to methanol at high yields [13]. Through control experiments, they found that the catalyst's chemical nature and architecture were key factors in enabling the enhanced methanol synthesis production.

Uctug et al. looked at optimizing CO_2 emission usage for methanol synthesis plants [16]. They used the modelling software General Algebraic Modelling Systems (GAMS) to optimize from among three options: purchasing carbon emission credits on the carbon market, investing in carbon capture and sequestration (CCS) technology, or some combination of the two. The key question was at what price would investing in CCS infrastructure be cheaper than purchasing credits for excess CO_2 emissions? They found that for CCS to be a good investment, carbon credit prices needed to be above 15 Euros per ton. At the time, the actual prices were approximately 5 Euros per ton, meaning that CCS was not yet a good investment.

A different process was explored by Abbas et al. [11]. They looked at combining enhanced gas recovery (EGR) with CO_2 utilization via methanol production in a combined CCS/CCU process. By adding the captured CO_2 to the natural gas feed stream, a relatively high 23.2% molar CO_2 was successfully integrated into the feed. They also observed improvements in CO_2 abatement intensity when compared to conventional scenarios. Whatever captured CO_2 could not be fed to the methanol synthesis process was stored using geo-sequestration by way of EGR to recover natural gas from the ground.

Alarifi et al. simulated and optimized multiple versions of the gas-phase methanol synthesis process with CO_2 as a feedstock [1]. In the work, they present the findings of three individual but related research papers. In the second work in particular, they optimize the operating conditions of the methanol synthesis process by simulating the capture and reutilization of the CO_2 produced from natural gas-fueled syngas reforming. Using an elitist and non-dominated sorting genetic algorithm, CO_2 was optimally reinjected into the methanol reactor at various points. This resulted in 3% improvement in methanol production and prevention of 3,430 MTPD of CO_2 when compared to a base-case ICI reactor.

Additionally, the third work looks into improving the optimization of reusing the CO_2 emitted from natural gas-fed syngas reforming in a Lurgi type methanol reactor. Operating conditions for the methanol reactor are determined to find the best use of captured and recycled CO_2 as a feedstock, as well as the optimal shell coolant temperature, while not breaking any process constraints. Alarifi et al. proposed a new optimization algorithm by combining genetic algorithm (GA) with generalized pattern search (GPS) derivative-free methodologies in order to solve this optimization problem. The simulation results showed that the proposed optimization implemented with a 5% recycle ratio of CO_2 improved the methanol production by approximately 2.5% compared to the base case operating conditions.

2.1.3 Methanol Reactors

Methanol is generally synthesized via hydrogenation of carbon monoxide and carbon dioxide in a reactor over a Cu/Zn based catalyst [1]. In terms of reactors, there are three primary reactor designs: ICI quench adiabatic converter, Lurgi converter, and the more recent Mitsubishi superconverter [1].

The ICI reactor, shown in Figure 2.1, is a single vessel with multiple layers of catalyst that are intermittently cooled with quench gas through lozenge distributors [1] [17]. Most of the reactor feed gas is preheated and fed into the reactor from above. The small remainder of feed gas is fed to the reactor from below without preheating so it may act as quench gas [17]. The cooling of each catalyst stage except the bottommost results in a temperature gradient known as a “saw tooth” diagram (see Fig. 2.4) [6] [17]. Figure 2.2 shows how the ICI reactor is used in a methanol synthesis loop.

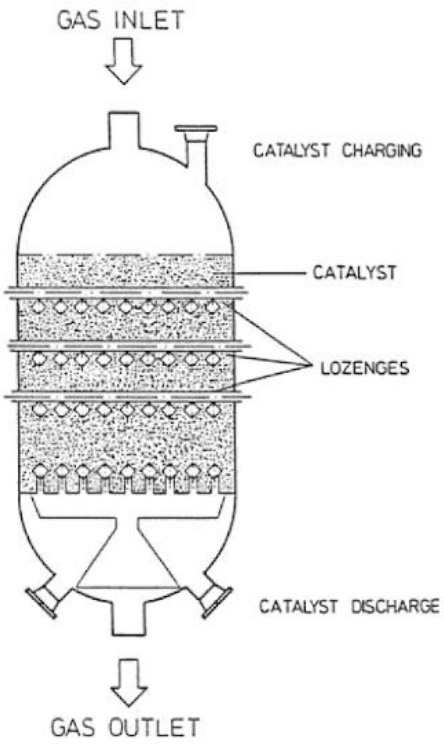

Figure 2. 1 ICI quench reactor [17].

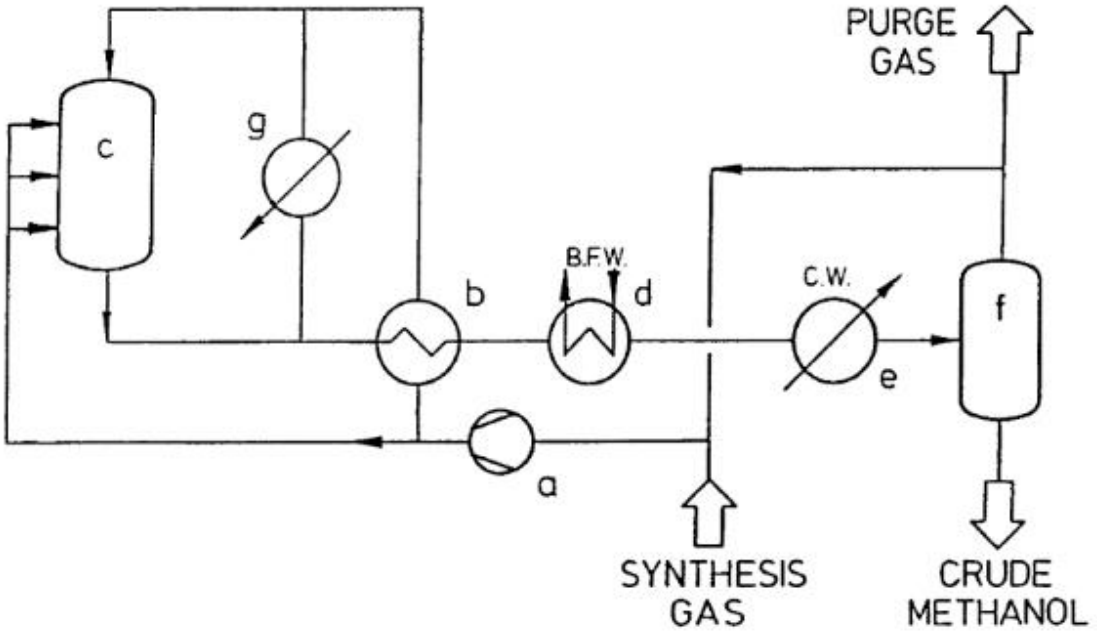

Figure 2.2 ICI methanol synthesis loop [17]. (a) Recycle compressor; (b) heat exchanger; (c) reactor; (d) boiler feed water (BFW) preheater; (e) cooler/condenser; (f) separator; (g) start-up heater.

The Lurgi process involves a tubular packed bed reactor with boiling water cooling. The shell and tube reactor has catalyst packed into the tube side and coolant water on the shell side [6] [1] [17]. Some advantages of the Lurgi reactor design include the fact that its temperature profile does not drop more than 10-12 °C along the tube [1]. This nearly isothermal profile provides high selectivity and means that less catalyst is required when compared to the ICI quench converter [1]. Figure 2.3 shows how the Lurgi reactor is used in a methanol synthesis loop. Figure 2.4 shows the typical temperature gradient of a Lurgi reactor.

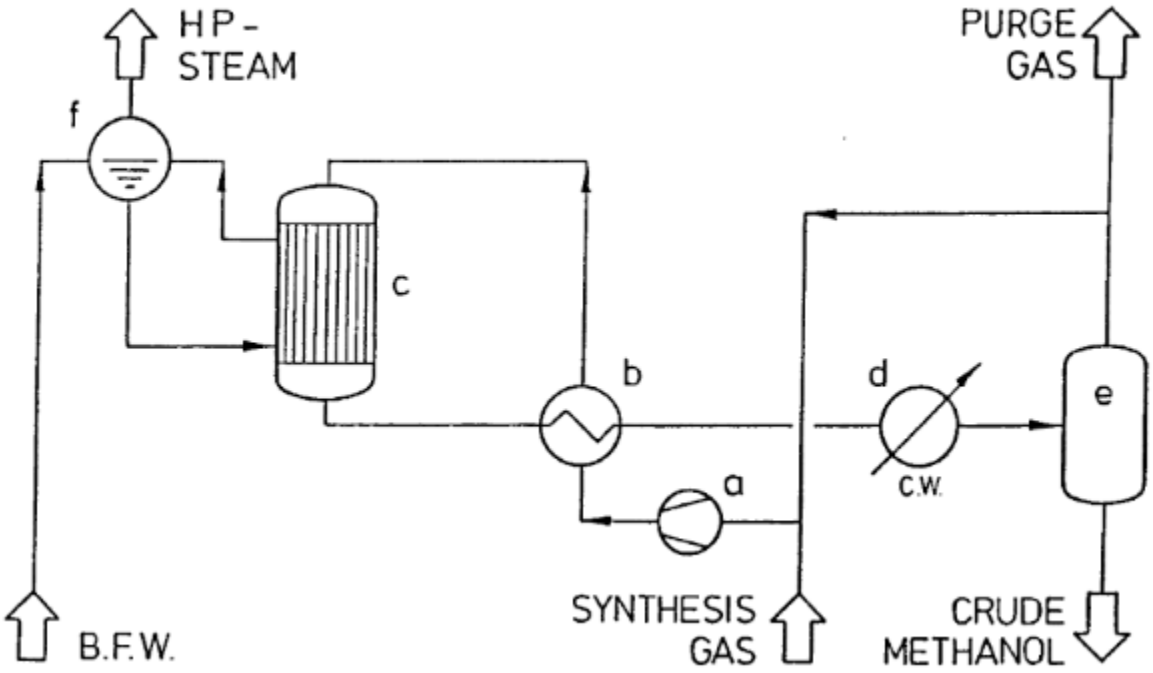

Figure 2.3 Lurgi methanol synthesis loop [17]. (a) Recycle compressor; (b) heat exchanger; (c) reactor; (d) cooler/condenser; (e) separator.

Developed by Mitsubishi Gas Chemical Company (MGC) and Mitsubishi Heavy Industries, Ltd. (MHI), the Mitsubishi superconverter design is the newest development in methanol reactor. It is based on double-tube type vertical heat exchanger design featuring an inner section and an outer annular section [1]. The catalyst is packed in the tube side, and the boiler water is in the shell side. The feed gas enters through the bottom and flows through the center of the reactor, where it is preheated by the reactions occurring in the annular outer section. Once it reaches the top of the reactor, the gas flows to the bottom through the catalyst bed in the annular outer section of the reactor [1]. Figure 2.4 shows the typical temperature profile of a Mitsubishi superconverter.

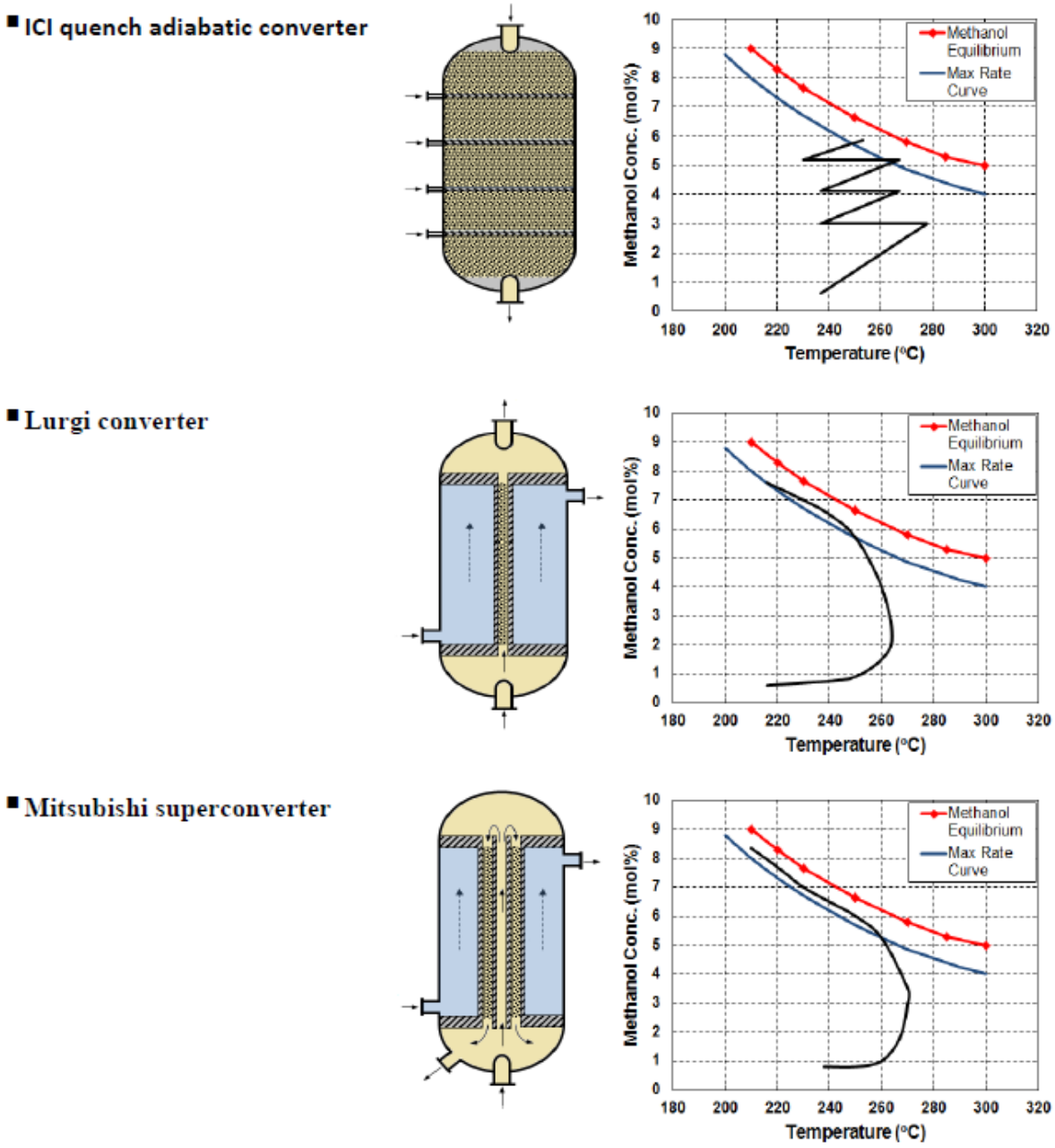

Figure 2.4 The three main methanol synthesis reactor types and their temperature profiles [1].

2.2 Electrolysis

Electrolysis of water is the process of running an electric current through a sample of water in order to decompose it into oxygen and hydrogen [18]. It was first discovered in 1789 by van Troostwijk and Deiman [19]. There are two primary methods of water electrolysis: alkaline electrolysis and polymer electrolyte membrane (PEM) electrolysis [18] [20]. A third method is emerging, called anion exchange membrane (AEM) electrolysis, but it is still a developing technology [21] [22]. Today, electrolysis is being looked at as a key source of oxygen and hydrogen [18] [23] [20], as well as syngas in some cases [24] [25]. Assuming the required electricity comes from renewable resources, electrolysis can be a carbon-free method of generating these gases, making it an attractive option to reduce carbon emissions [18] [23] [20].

Guerra et al. in 2018 researched the production of syngas by water electrolysis [25]. Using renewable electric energy as well as liquefied biomass as a carbon source, they demonstrated and optimized the process for production of renewable fuels like methane, methanol, dimethyl ether, and more.

Electrolysis is being used to reduce carbon emissions in other ways. Huang et al. (2015) simulated hydrogen production scenarios for fuel cell electric vehicle hydrogen refueling stations by examining an electrolysis hydrogen production system powered by small wind turbines and a photovoltaic system [23]. Using purely renewable electricity sources, the electrolysis would provide the hydrogen that would fuel an electric vehicle. The study simulated different operating conditions in order to determine the optimal system temperature based on the required solar and wind power in each scenario.

In 2009, Liu projected the economic and structural requirements of a hydrogen economy in Ontario based on the use of hydrogen fuel cell vehicles [18]. Many hydrogen generation methods were considered and compared, including steam reforming of methane, water electrolysis, high-temperature electrolysis, and thermochemical cycle hydrogen production. While steam reforming of methane is the most common hydrogen generation method, it was ruled out due to the CO_2 pollution is creates. High-temperature electrolysis and thermochemical cycle methods were still being researched at the time and were not efficient enough. Water electrolysis could be powered by any variety of electricity source, was free of carbon emissions if powered by carbon-free electricity sources, and had been proven commercially. These factors made water electrolysis the hydrogen production method of choice in the study. Of water electrolysis as the hydrogen generation method of choice, Liu said that it was a good option both early in a transitional period to a hydrogen economy, and late once that economy is more matured. Once hydrogen fuel cell vehicles become the norm, centralized hydrogen production plants will be needed, and water electrolysis plants can fill that need.

A 2017 paper by Alsubaie investigated the use of PEM electrolyzers for power-to-gas (PtG) energy storage [20]. The study examined the use of surplus baseload power generation from Ontario's energy system to convert electricity into hydrogen (power-to-gas) via water electrolysis. This electrolytic hydrogen was then employed for gasoline manufacturing in order to reduce the carbon intensity of traditional transportation fuel production in Ontario. While the study found that traditional steam methane reforming generated hydrogen at a lower cost than the outlined power-to-gas process, the electrolytic hydrogen showed promise as a carbon-reduction substitute. It was

found that PtG could meet the hydrogen need of every gasoline refinery in Ontario using a fraction of the surplus baseload power available. This use of electrolysis was found to reduce the amount of natural gas used in gasoline production by 4.6% overall, as well as lowering the yearly greenhouse gas emissions in the province by 0.26 megatons when compared to annual gasoline sales in Ontario.

Al-Zakwani (2018) also looked into applications of PtG technology [22]. Calling the electrolyzer "the first and central brick of PtG systems," the study investigated utilization of Ontario's surplus baseload power generation for generation of hydrogen through electrolysis. From there, the electrolytic hydrogen was theoretically allocated to four different pathways: mobility fuel, industrial use, use as hydrogen-enriched natural gas, and renewable natural gas. Five scenarios of differing hydrogen allocation to the four different pathways were considered based on their economic and environmental aspects. The results found that the 2017 Ontario surplus baseload electricity could have been converted to 170-227 kilo-tonnes (depending on the hydrogen production capacity assumption used) of hydrogen. Additionally, the power-to-gas to mobility fuel pathway presented a profitable business case while also resulting in 2,215,916 tonnes of CO_2 removed every year from road travel. Electrolytic hydrogen production via PtG technology was still found to be costly when compared to traditional steam methane reforming.

The 2011 paper by Ebbesen et al. studied the use of Solid Oxide Electrolysis Cell (SOEC) stacks for electrolysis of steam and CO_2 simultaneously in order to generate hydrogen and syngas [24]. They tested the long-term feasibility of the SOEC stacks in terms of electrolysis cell degradation and found them to be practical.

2.3 Syngas Production

There are multiple methods of reforming hydrocarbons into syngas. Some prominent methods are steam methane reforming (SMR), partial oxidation (POX), and autothermal reforming (ATR) [4].

SMR is the most popular method of syngas reforming, requiring methane (typically via coal or natural gas) and steam as the feedstocks [7] [26]. The methane and steam are mixed at high temperatures in a reactor over a catalyst, where they are reformed into syngas [7] [26]. This typically occurs around 800-900°C and 15-30 atm on a nickel-based catalyst [26]. SMR produces syngas through the equation below [6] [7].

$$CH_4 + H_2O \leftrightarrow CO + 3H_2 \qquad \text{Equation 2.1}$$

Partial oxidation involves mixing steam and oxygen with a methane feedstock, such as coal or natural gas, in a reactor [4] [7]. At very high temperatures, usually around 1300-1400°C, they react homogeneously, without the need for a catalyst [4] [7]. While the need for oxygen and the high operating temperatures lead to soot formation, POX also produces less CO_2 than other methods [4]. POX creates syngas through the equation below.

$$CH_4 + O_2 \leftrightarrow CO_2 + 2H_2 \qquad \text{Equation 2.2}$$

Autothermal reforming effectively combines the reaction methods of SMR and POX. Initially the reactions are carried out homogeneously in a burner, as in POX, and then completed heterogeneously on a catalyst, as in SMR [7]. ATR involves a feed of methane (via coal or natural gas), oxygen, and steam at around 850-1100°C and 20-70 atm [7] [26] [27]. The need for oxygen in the ATR process can be accomplished through air separation or water electrolysis. ATR produces syngas through the three equations below [7].

Combustion	$CH_4 + 1.5O_2 \rightarrow CO + 2H_2O$	Equation 2.3
Reforming	$CH_4 + H_2O \leftrightarrow CO + 3H_2$	Equation 2.4
Shift	$CO + H_2O \leftrightarrow CO_2 + H_2$	Equation 2.5

This section will focus on the ATR method of syngas production, as it is what was used in the simulation of the methanol manufacturing process.

2.3.1 Autothermal Reforming

Autothermal reforming (ATR) is a syngas reforming process that has been in use for decades [7]. It takes in a carbon source like natural gas or coal, in addition to some steam, and generates a combination of $CO/CO_2/H_2$ known as syngas. Throughout the 1950's and 60's, autothermal reformers were used to generate syngas for ammonia and methanol production [7]. Early ammonia plants operated at steam-to-carbon (S/C) ratios ranging from 2.5 to 3.5 on a molar basis - very high by today's standard of around 0.6 [7]. A lower S/C ratio is desired because steam is a very expensive component in these types of processes, but soot formation can occur if the ratio goes too low [7]. In the 1990's, the technology was further developed to achieve lower steam-to-carbon ratios, with improved burners enabling safe, soot-free operation while still maintaining high on-stream factors [7]. Operation at a S/C ratio of 0.6 has been demonstrated in at pilot and industrial scale [7].

As shown in Fig. 2.5, the major components of an ATR reactor are the burner, the combustion chamber, the fixed catalyst bed section, the refractor lining, and the pressure shell [7]. The two key elements of the ATR are the burner and the catalyst [7]. The burner provides proper mixing of the feed streams, and the fuel-rich combustion is taking place as a turbulent diffusion flame [7]. Intensive mixing is essential in order to avoid soot formation. Meanwhile, the catalyst balances the synthesis gas and eliminates soot precursors. In order to design a compact reactor, catalyst particle size and shape is optimized to achieve high activity and low pressure [7].

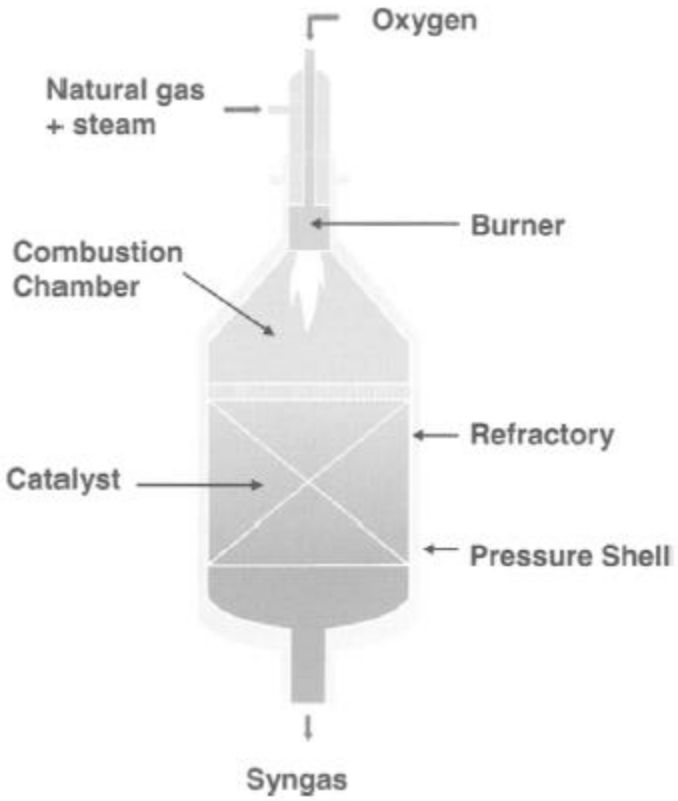

Figure 2.5 Illustration of an ATR reactor [7].

Some studies from 10-15 years ago focused on the impact of natural gas composition on the ATR process [28] [29]. Chan and Wang (2001) looked into how natural gas composition affected the carbon monoxide yield in the products of the ATR process [28]. They ran a simulation to randomize natural gas compositions within certain boundaries, then ran them through an ATR. From this, they were able to determine the correlation between various natural gas compositions and CO yield.

Meanwhile, Hoang and Chan (2007) investigated how natural gas composition affected the overall performance of autothermal reforming [29]. By testing natural gas with varying concentrations of C_2H_6 and CO_2, they were able to determine the relationship between those concentrations and the required air-to-fuel ratios and water-to-fuel ratios. These ratios are indicators of reforming performance.

More recent reports looked at the autothermal reforming of biogas for the purpose of hydrogen production from the generated syngas [30]. Rau et al. (2017) constructed and investigated a pilot plant for hydrogen production for use as hydrogen refueling stations for fuel cell transportation [30]. The plant was based on the autothermal reforming of biogas with a noble metal catalyst. They found that this process was an applicable and sustainable way to produce hydrogen for the demand of individual transport technologies of the future. In terms of cost, the process was found to be less expensive than electrolysis for the purpose of hydrogen production, but more expensive than large-scale steam reforming.

In 2018, Al-Sobhi et al. simulated a framework for optimal downstream usage of natural gas [4]. One branch of this network was methanol synthesis from syngas. They compare ATR to other syngas reforming methods, namely catalytic steam methane reforming (SMR), two-step reforming, partial oxidation (POX), combined reforming (CR), ceramic membrane reforming (CMR), and dry reforming (DR). In their description of the system, they determined that autothermal reforming was one of the best methods of producing syngas, stating that ATR can be scaled up to large-scale scenarios while also being cost-effective. For the purpose of their simulation, they consider only ATR and SMR as their competing syngas reforming technologies. One potential improvement they described for ATR technology was the tight integration of an oxygen plant with the ATR unit in order to decrease the impact of the currently large investment required for air separation.

Chapter 3: Model Development

The simulation model of the Green Methanol process was done in Aspen Plus. It was based on the preliminary Aspen Plus simulation developed by Lalitornasate and Croiset [6]. Three major changes were made to the original simulation:

1. The syngas production method was changed from partial oxidation (POX) to autothermal reforming (ATR).
2. Heat integration was added.
3. Reduced wasted hydrogen in the methanol reactor loop.

This chapter will break down the development of the Aspen Plus model.

3.1 AChT Methanol Process

The AChT methanol process is composed of four main sections:

1. The electrolyser
2. The syngas production section
3. The methanol production section
4. The methanol purification section

Figure 3.1 shows how these sections are organized.

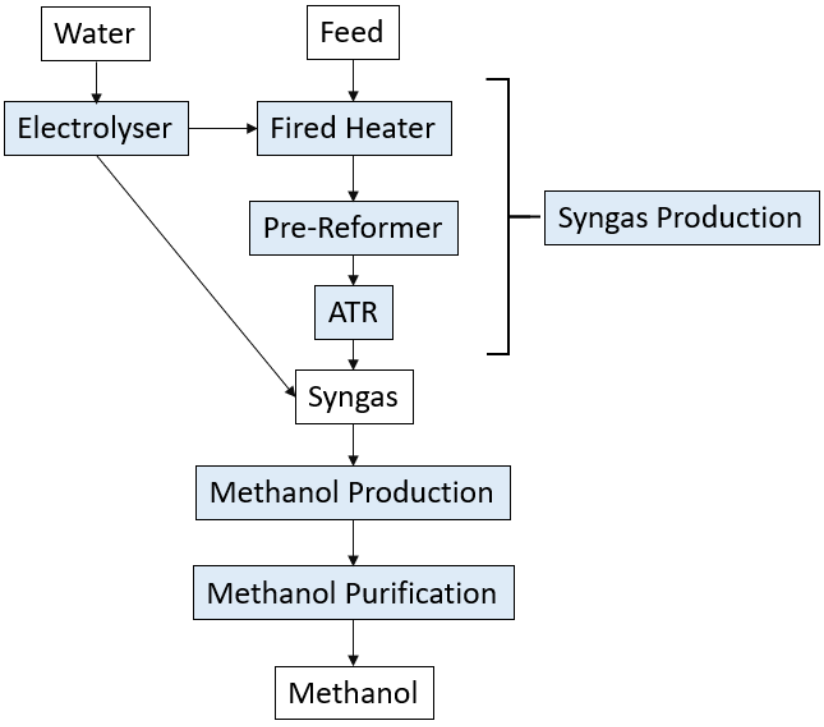

Figure 3.1 The AChT methanol synthesis process.

Syngas, or synthesis gas, is a gas mixture of CO, H_2, and CO_2, generated using one of a few available syngas production methods from a carbon source (usually coal or natural gas) [27] [7] [9]. Syngas is the key feedstock to the methanol synthesis process. For stoichiometric reasons, it is desirable for syngas to be delivered to the methanol reactor in the following molar ratio [6] [7] [14]:

$$M = \frac{H_2 - CO_2}{CO + CO_2} = 2 \qquad \text{Equation 3.1}$$

Equation 3.1 shows the so-called module ‘”M” or syngas ratio.

The model developed in Lalitornasate and Croiset [6] used partial oxidation for the syngas production method. The model developed in this work uses autothermal reforming instead. This means that much of the syngas preparation section was changed from the Lalitornasate and Croiset simulation. On the other hand, the core methanol reactor and purification sections remain largely the same. While the methanol reactor section received the addition of heat balancing and hydrogen recycling, the methanol reactor itself was largely kept intact in terms of design and kinetics.

3.2 Electrolyser

The electrolyser simulation is shown in Figure 3.2. Water (stream H2O) is fed at 288.6 kmol/hr, 25°C, and 1 atm. It is composed of pure water. The block ELECTRO simulates the power requirement of the electrolysis reaction, and also pressurizes the stream to 35 atm. The pressure was chosen based on literature [31], and the fact that all feeds in the ATR section will be pressurized to 35 atm. The separator SEP-1 splits the water into an oxygen stream (O2-1) and a hydrogen stream (H2-1).

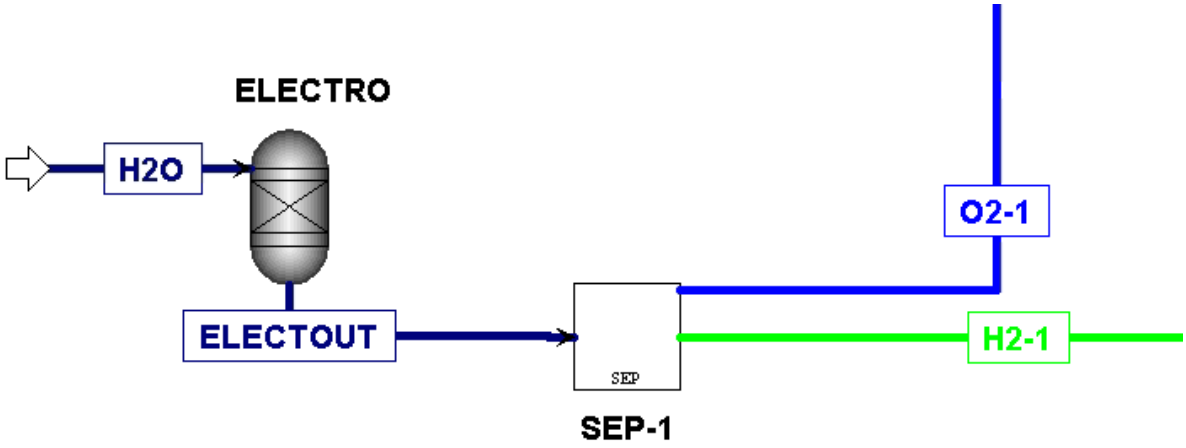

Figure 3. 2 Electrolyser simulation.

3.3 Syngas Production Section

The syngas production method used for this simulation is autothermal reforming (ATR). The design of this section was based on the description of a typical ATR syngas generation unit used in gas-to-liquid (GTL) processes by Aasberg-Petersen et al. [7], and which is shown in Figure 3.3. According to literature, ATR occurs at temperatures of 850°C to 1100°C and pressures of 20 atm to 70 atm [27] [7]. The autothermal reforming in this work was simulated at a temperature of 1050°C and a pressure of 35 atm.

Figure 3.3, taken from Aasberg-Petersen et al. [7], shows the key steps in the ATR syngas production process: sulfur removal from natural gas, adiabatic prereforming, fired heater, autothermal reforming, and steam production.

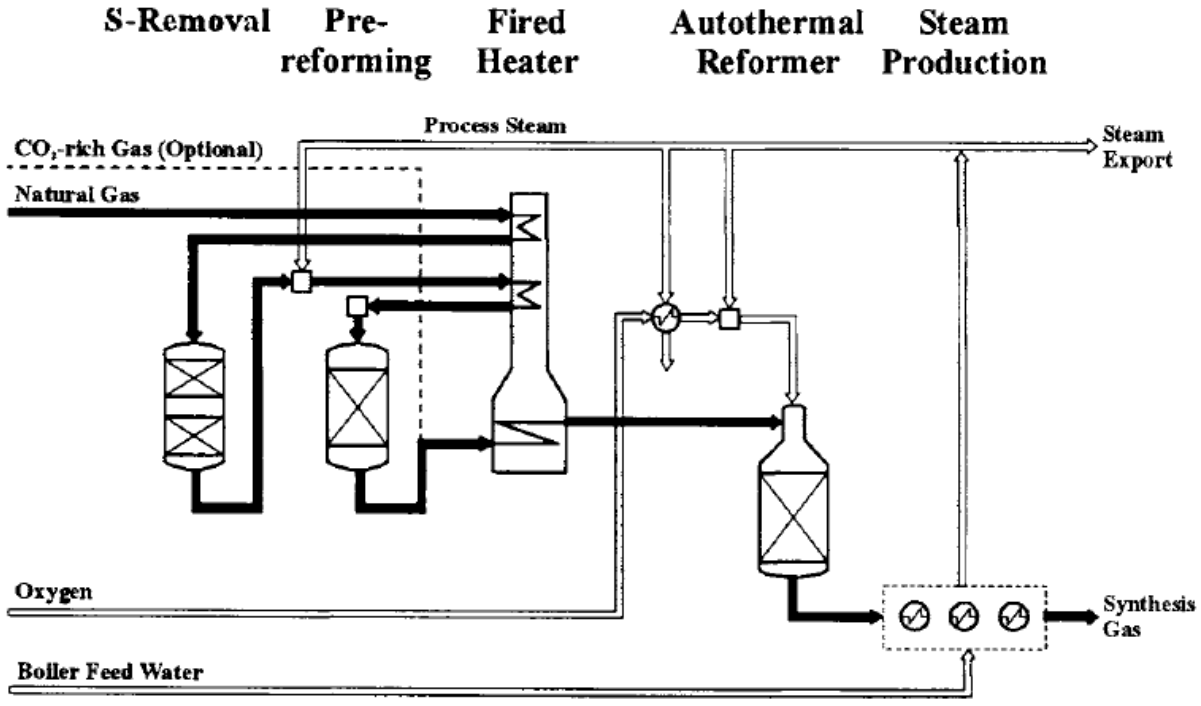

Figure 3.3 Typical layout of the autothermal reforming section with an adiabatic pre-reformer in a GTL plant [7].

Figure 3.4 shows the actual simulation of the syngas production section in Aspen Plus based on the process shown in Figure 3.3.

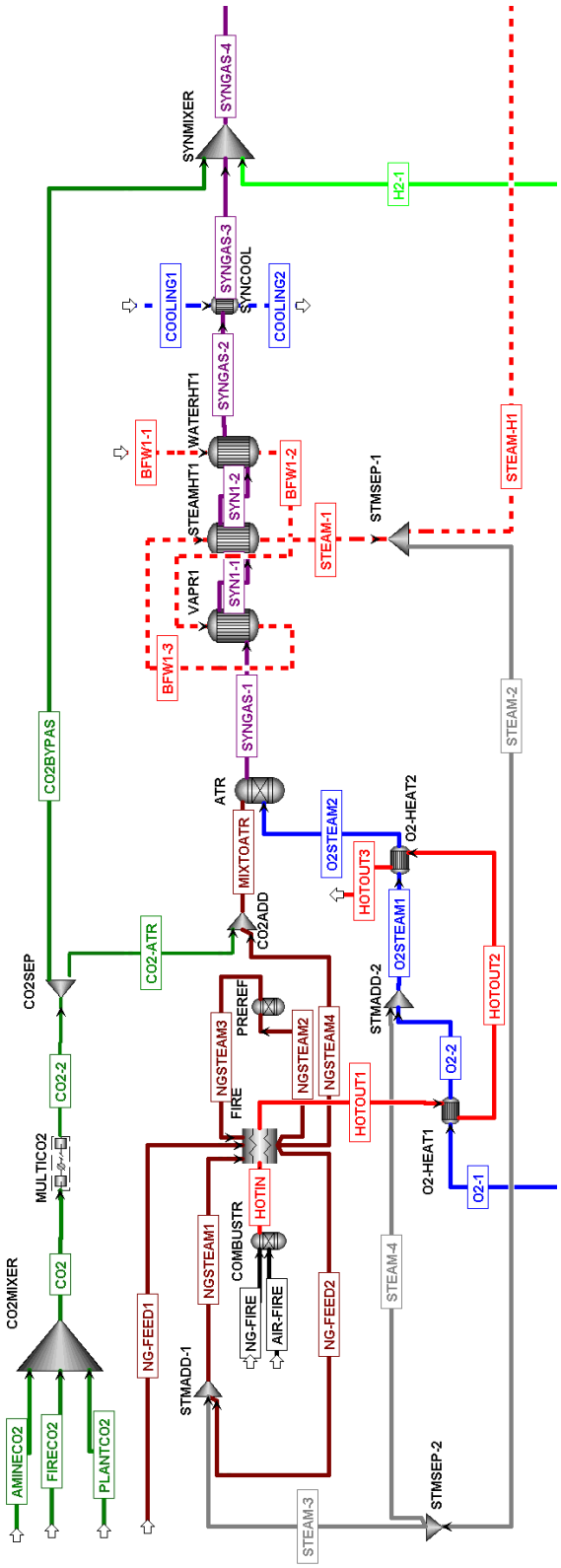

Figure 3.4 Aspen Plus simulation of the syngas production section.

The adiabatic pre-reformer is labelled as PREREF, the fired heater is labelled as FIRE, the autothermal reformer is labelled as ATR, and the steam production occurs over the heat exchangers labelled as VAPR1, STEAMHT1, and WATERHT1. Sulfur removal from the natural gas was not included in this work.

3.3.1 Feedstocks

The most common feeds used to prepare syngas for methanol synthesis are coal and natural gas [7]. This model uses natural gas as the primary carbon source in the feedstock. It was simulated to be delivered to the process at a temperature of 30°C and a pressure of 35 atm (NG-FEED1 stream in Figure 3.4). This pressure was chosen because natural gas is typically delivered around 40 atm, and all feeds to the ATR needed to be pressurized to 35 atm. The chemical composition of the natural gas used in the process was provided by AChT and is shown in Table 3.1.

Table 3.1 Feed natural gas composition.

Component	Mole Fraction
CH_4	0.950521
CO_2	0.00501
O_2	0.000193
N_2	0.017736
C_2H6	0.024226
C_2H_4	0.00231

Water was fed to the steam generator via the stream BFW1-1 and the cooler SYNCOOL via the stream COOLING1. Both of these streams exist for heat integration purposes (see Section 3.6). BFW1-1 was fed at 121°C and 35 atm. The temperature was tuned to ensure proper steam production in the 3-part steam generator, and the pressure was chosen because the steam will eventually be mixed with both natural gas and oxygen entering the ATR at 35 atm. COOLING1 was fed at 20°C and 1 atm strictly for the purposes of sufficiently cooling the syngas stream.

CO_2 was also a feedstock to the process. In the AChT process the CO_2 comes partly from the capture and recycling of its own generated CO_2, and partly from the flue gas stream of a neighbouring plant. This is simulated with three different CO_2 streams (AMINECO2, FIRECO2, and PLANTCO2 in Figure 3.4) being fed and mixed to the system. PLANTCO2 represents the constant feed of CO_2 from a neighbouring plant at 58.2 kmol/hr. FIRECO2 represents the CO_2 from the flue gas stream out of the fired heater (the CO_2 from HOTOUT3). AMINECO2 represents the CO_2 from the flue gas of the steam generator by burning natural gas for the amine reboiler in the CO_2 capture plant. This capture plant is sized in Section 4.4, which determines the flowrate of AMINECO2. These streams were simulated to be delivered at 30°C and 1 atm, but the mixed stream is pressurized immediately to 35 atm. This is because the ATR operates at the pressure of 35 atm. The stream composition is 100% CO_2. A majority of the CO_2 bypasses the ATR, instead mixing with the syngas after the autothermal reforming is complete. A small amount of the CO_2 feed is delivered to the ATR. This is due to the autothermal requirement of the ATR – all heat required for the reaction must be provided by the reaction. In other words, the ATR must have a heat duty of 0 kW. The addition of some CO_2 to the ATR helped to adjust the heat duty to approximately 0 kW. This is further explained in Chapter 4. As

shown in Figure 3.3, CO_2 is delivered by the stream CO2. It is then split into CO2-ATR, which goes to the ATR, and CO2BYPAS, which bypasses the ATR and is added to the syngas afterwards.

Natural gas and air are also feedstocks, being burned together and fed to the fired heater. Both streams, NG-FIRE and AIR-FIRE respectively, are fed at 30°C and 1 atm. The natural gas is fed such that it achieves the minimal amount of heating required for the fired heater in order to minimize CO_2 emissions. The air is fed so that the mixture of air and natural gas in the stream HOTIN contains 3% oxygen, by mole (i.e. ~18% excess air).

The products of the electrolyser the syngas production sections via the streams O2-1 and H2-1. They both enter at 25°C and 35 atm. The hydrogen stream is mixed in the mixer SYNMIXER with the syngas product and the CO_2 that bypassed the ATR. The oxygen stream is heated from 25°C to 360°C in the heat exchanger O2-HEAT1. It is then mixed with steam in the mixer STMADD-2. This mixture of steam and oxygen is heated further to 422°C in the exchanger O2-HEAT2 before entering the ATR.

3.3.2 Adiabatic Pre-Reformer

Adiabatic pre-reforming is a well-established step in the ammonia and methanol industries, for hydrogen production in refineries, and to produce syngas for a variety of other chemicals [7] [32]. The adiabatic pre-reformer has three key features when applied to syngas production:

- It converts all higher hydrocarbons down to simpler elements in advance of the syngas reformer [32].
- It removes all sulphur remaining in the feedstocks. This is due to the lower temperature of the pre-reformer, which favors the removal of sulphur [32].
- It reduces the temperature requirement for the syngas reformer [32].

According to Christensen [32], these features lead to many advantages in the syngas production process, including increased production capacity, smaller reformer furnace, feedstock flexibility, increased catalyst lifetime, increased tube life, elimination of problems of carbon formation and hot banding in tubular reformers, and advanced processes featuring low energy consumption and investment [32].

According to literature, the typical operating temperature of an adiabatic pre-reformer is between 350 and 550°C [7] [32].

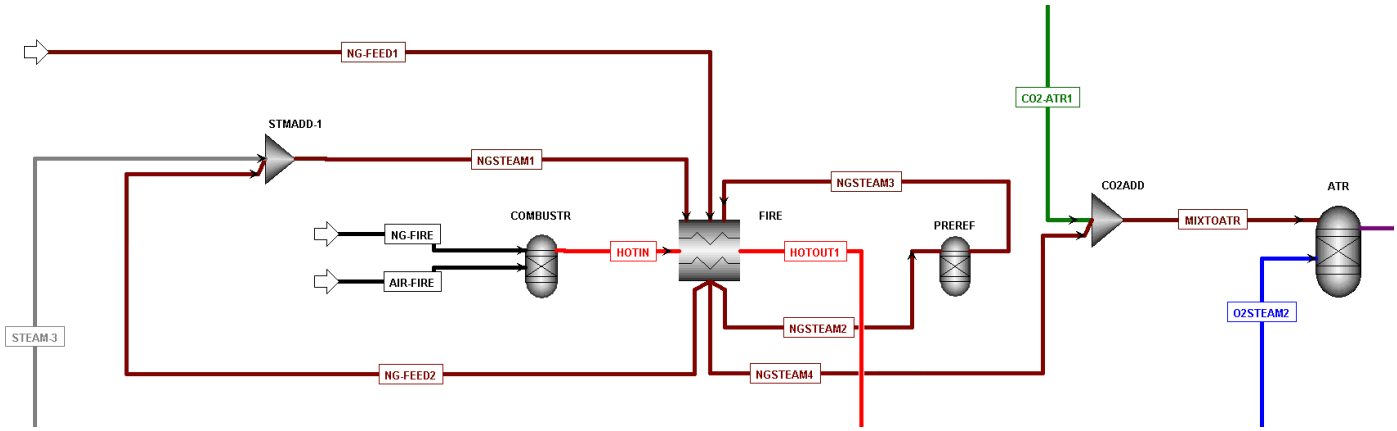

Figure 3.5. Zoomed-in view of the adiabatic pre-reformer

Figure 3.5 shows how this was implemented in the Aspen Simulation. The feedstock natural gas (NG-FEED1) was preheated in a fired heater (FIRE) to 380°C. It was then mixed with steam (STEAM-3) and heated through the fired heater again before entering the pre-reformer (PREREF) at 450°C. This is in accordance with the conclusion from literature that an adiabatic pre-reformer should operate at 350-550°C. After leaving the pre-reformer, the stream was again heated in the fired heater to 655°C and mixed with the inlet CO_2 before entering the ATR. It is heated to 655°C, as this was the highest temperature the fired heater could heat the stream to while still minimizing the natural gas requirements of the fired heater.

3.3.3 Autothermal Reformer

There are three feeds to the ATR: the fraction of CO_2 that does not bypass the ATR, the mix of steam and oxygen from the electrolyser, and the mix of natural gas and steam that went through the pre-reformer. In Aspen Plus, the ATR is represented by a RGIBBS reactor, which is based on Gibbs free energy minimization. According to literature, autothermal reforming occurs at operating temperatures of 850°C to 1100°C and pressures of 20 atm to 70 atm [7] [27]. For this work, the operating temperature and pressure were chosen to be 1050°C and 35 atm, respectively.

Given the autothermal requirement of the ATR, the heat required for the reaction must be provided by the feeds themselves. In Aspen Plus, this means that the ATR must operate with a heat duty of 0 kW. This was achieved by adjusting the steam and CO_2 input to the ATR, as well as by maximizing the temperatures of the feed streams.

The resultant stream from the ATR is the syngas stream, SYNGAS-1, which is cooled in the 3-part steam generator and mixed with H_2 and the CO_2 that bypassed the ATR.

3.3.4 Steam Generator

The 3-part steam generator is made up of the blocks VAPR1, STEAMHT1, and WATERHT1. The purpose of this steam generator is to simultaneously cool the exit stream from the ATR

while also generating steam that can be used to heat other areas of the process. The design of this steam generator is explained in Section 3.6.

The steam leaving the steam generator via the stream STEAM-1 is at 380°C and 35 atm. It is separated in the separator STMSEP-1, with an amount of steam sent to the ATR to maintain a steam-to-carbon ratio of 0.6. This is detailed in Section 4.1.1. The rest of the separated steam goes to heat integration. The ATR steam (STEAM-2) is split again at the separator STMSEP-2, with some going to mix with the oxygen feed to the ATR, and the rest going to mix with the natural gas feed to the ATR. Based on AChT design recommendation, 80% of the steam goes to mix with the natural gas, and 20% goes to mix with the oxygen.

3.4 Methanol Synthesis Section

The methanol synthesis section simulated in Aspen Plus is shown in Figure 3.6. The input to this section is the syngas stream from the ATR (SYNGAS-4). The water is removed using a flash drum, FLASH in Figure 3.6. The remaining mix of CO, CO_2, and H_2 is further pressurized from 35 atm to 70 atm before entering the methanol synthesis section. 70 atm is the typical operating pressure for a methanol production reactor, and was the pressure used in the design of the methanol reactor in Lalitornasate and Croiset [6].

The methanol synthesis section has one output and one recycle stream. The output is the crude methanol stream (METH-6), which is later refined in the purification section. The recycle stream (RECYCLE1, RECYCLE2 RECYCLE3 is implemented to reuse unreacted material. It loops back and reconnects with the syngas feed at the inlet of the methanol reactor. The syngas ratio must equal 2 at SYNGAS-6.

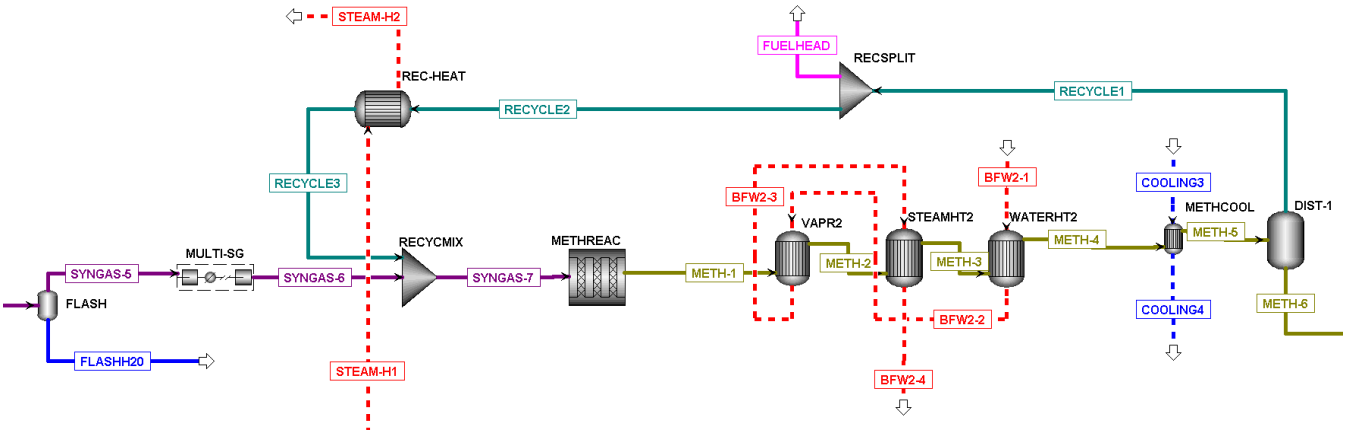

Figure 3.6 Aspen simulation of the methanol synthesis section.

3.4.1 Methanol Reactor

The syngas reaches the methanol synthesis section at 231°C and 70 atm. The recycle stream is mixed in via the mixer RECYCMIX. From there, the stream heads into the methanol reactor.

The methanol reactor simulation in Aspen Plus is taken from the simulation in Lalitornasate and Croiset [6]. The same reaction kinetics developed in that simulation were used with this simulation. The following is the description of the reaction kinetics from Lalitornasate and Croiset [6].

In the simulation, the kinetics expressions of methanol synthesis of Cu/Zn/Al were based on the LHHV approach. The expression rate and data of these kinetic reactions were based on Graaf et al. (1989) and the rates of methanol synthesis reactions and details about reaction constants are listed below.

Hydrogenation of CO:

$$r_1 = \frac{k_1 K_{CO}[f_{CO} f_{H_2}^{3/2} - f_{CH_3OH}/f_{H_2}^{1/2} K_{P1}]}{(1+K_{CO} f_{CO}+K_{CO_2} f_{CO_2})[f_{H_2}^{1/2}+(K_{H_2O}/K_{H_2}^{1/2}) f_{H_2O}]} \quad \text{Equation 3.2}$$

Hydrogenation of CO_2:

$$r_2 = \frac{k_2 K_{CO_2}[f_{CO_2} f_{H_2}^{3/2} - f_{CH_3OH} f_{H_2O}/f_{H_2}^{3/2} K_{P2}]}{(1+K_{CO} f_{CO}+K_{CO_2} f_{CO_2})[f_{H_2}^{1/2}+(K_{H_2O}/K_{H_2}^{1/2}) f_{H_2O}]} \quad \text{Equation 3.3}$$

Reverse gas-shift reaction:

$$r_3 = \frac{k_3 K_{CO_2}[f_{CO_2} f_{H_2} - f_{H_2O} f_{CO}/K_{P3}]}{(1+K_{CO} f_{CO}+K_{CO_2} f_{CO_2})[f_{H_2}^{1/2}+(K_{H_2O}/K_{H_2}^{1/2}) f_{H_2O}]} \quad \text{Equation 3.4}$$

Table 3.2 Reaction rate constants

$k = A \exp(\frac{B}{RT})$	A	B
k_1	(4.89 ± 0.29) × 10^7	−113,000 ± 300
k_2	(1.09 ± 0.07) × 10^5	−87,500 ± 300
k_3	(9.64 ± 7.30) × 10^{11}	−152,900 ± 11,800

Table 3.3 Adsorption equilibrium constants

$K = A \exp(\frac{B}{RT})$	A	B
K_{CO}	(2.16 ± 0.44) × 10^{-5}	46,800 ± 800
K_{CO_2}	(7.05 ± 1.39) × 10^{-7}	61,700 ± 800
$(K_{H_2O}/K_{H_2}^{1/2})$	(6.37 ± 2.88) × 10^{-9}	84,000 ± 1,400

Table 3.4 Reaction equilibrium constants

$K_P = 10^{((\frac{A}{T})-B)}$	A	B
K_{P1}	5,139	12.621
K_{P2}	3,066	10.592
K_{P3}	−2,073	−2.029

These data were converted and added into the reactions block in Aspen Plus. Then, the results of the literatures and the Aspen Plus simulation were compared using the same feed and same configuration of reactor.

The stream exiting the methanol reactor is cooled and distilled in order to separate the methanol from the unreacted H_2, CO, and CO_2. The methanol stream is sent to the purification section, while the unreacted material is recycled.

3.4.2 Recycle

Due to the relatively low single-pass conversion of the methanol reactor, the unreacted material is looped back (RECYCLE1 in Figure 3.6). Some percentage of the recycle stream by molar flowrate is bled off to waste (FUELHEAD) in order to prevent buildup. This percentage is determined in Section 4.2.1 to be 7%. The rest (RECYCLE2) is heated back to operating temperature (231°C) and mixed back into the syngas mixture.

3.5 Methanol Purification Section

After being distilled initially, the raw methanol stream is distilled two more times. This is shown in Figure 3.7.

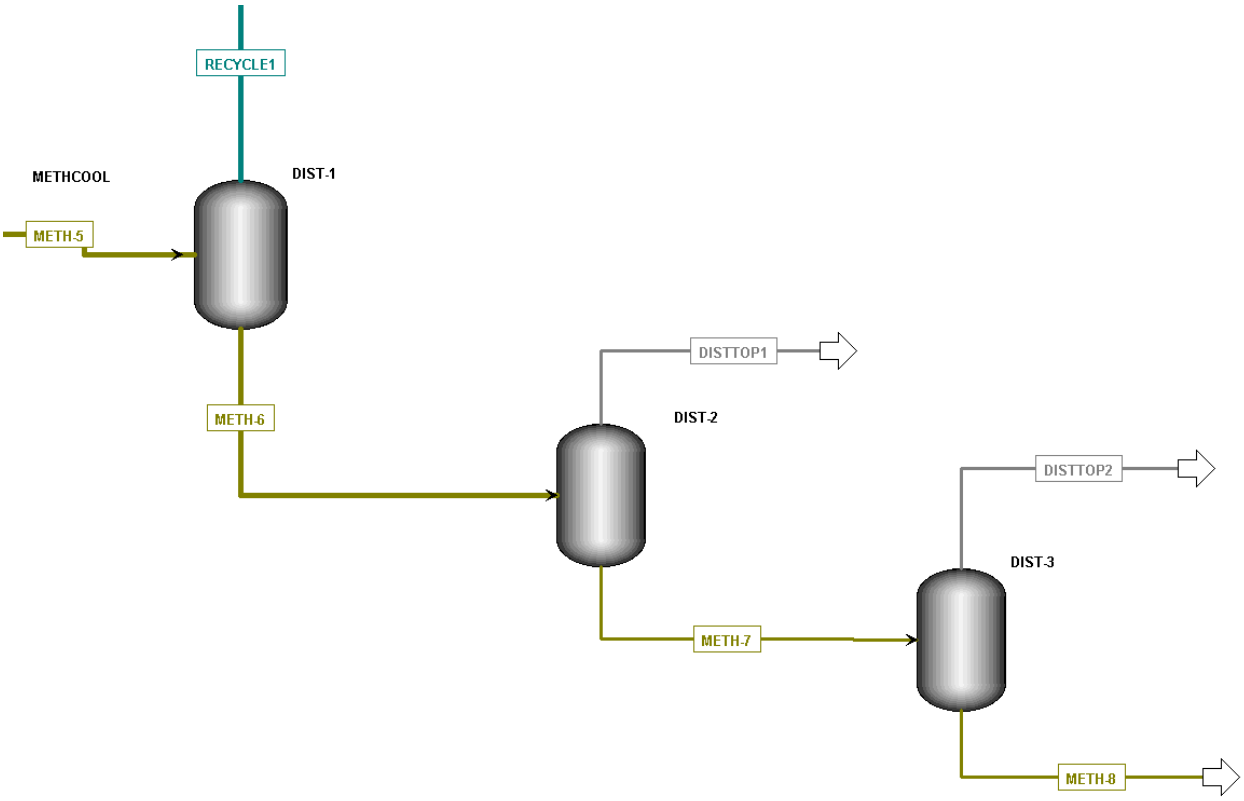

Figure 3.7 Aspen Plus simulation of the methanol purification section.

The raw methanol stream exits the methanol reactor, is cooled, and then enters the purification section. The stream METH-5 enters the first distillation column at 40°C and 70 atm. The distillation purifies the methanol in the stream, so it is more highly concentrated when it leaves the process. The streams DISTTOP1 and DISTTOP2 are mostly unreacted CO_2, methane, and some methanol losses.

3.6 Heat Integration

The entire process has sections of heating and cooling. Heat integration takes heat recovered from a cooling section and reuses it to heat streams in other sections. This recycling of heat minimizes the need for heat generation via fuel combustion, thereby reducing CO_2 emissions.

This section describes how heat balancing was applied in this work. First, the configuration of the steam generator is detailed. This is followed by a look at the heaters and coolers specific to this process.

3.6.1 Steam Generator Configuration

There are cooling locations in the process where heat is extracted. This heat is stored and transported in the form of steam. By exchanging heat with liquid water, the hot stream can be cooled while also generating steam. A steam generating heat exchanger network was developed based on Chapter 15 of Lieberman & Lieberman [33].

The configuration of this steam generating network is made up of the following three heat exchanger subsections that each implements a different step in converting water to steam:

1. Heating water
2. Vaporizing water into steam
3. Heating steam

This means that water is fed into the first heat exchanger where it is heated just below its vaporization temperature. Then, the hot water is fed to a second exchanger where its latent heat requirement is fulfilled, vaporizing it completely into steam. The newly-formed steam then goes to the third exchanger, where it is heated further. This steam can then go on to heat other sections of the process.

The heat delivered at each of the three exchangers comes from a single hot process stream. As this hot process stream passes through each heat exchanger, it cools down as needed and simultaneously heats the water/steam. As per Lieberman & Lieberman [33], the hot stream first heats the vaporization section, then the steam heating section, then finally the water heating section.

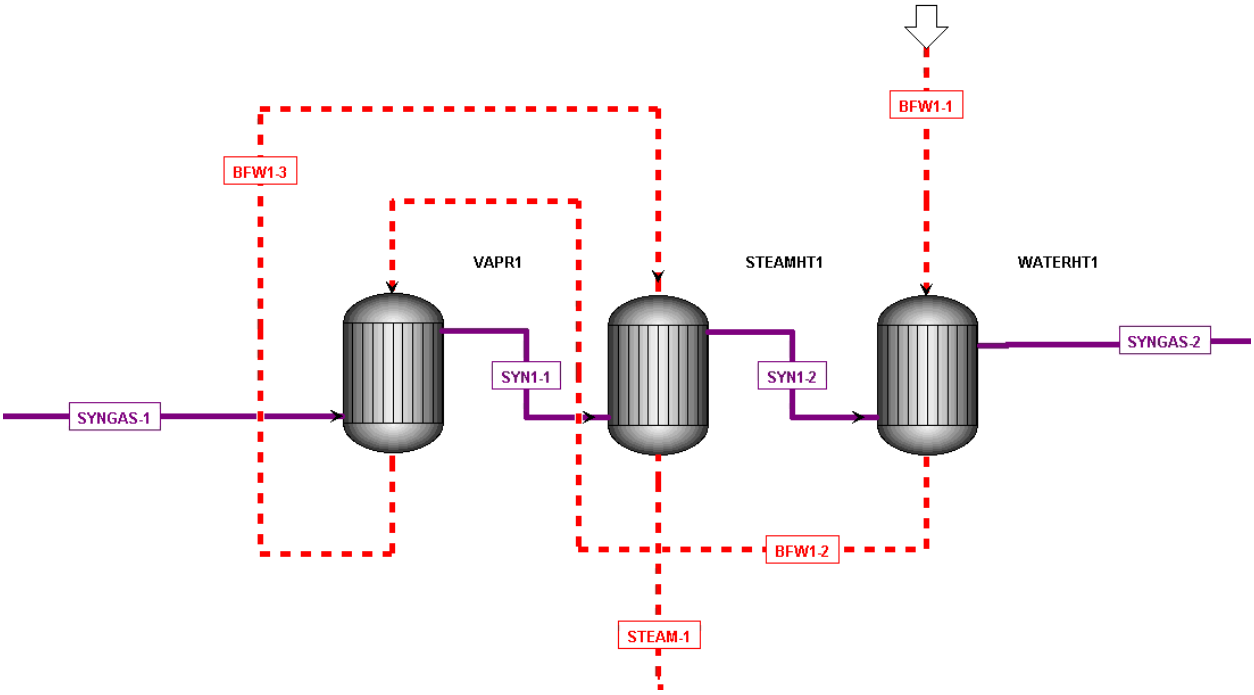

Figure 3.8 Steam generator configuration for post-ATR cooling.

Figure 3.8 shows how this setup was applied in the simulation. The three heat exchangers, VAPR1, STEAMHT1, and WATERHT1, represent the water vaporizer, the steam heater, and the water heater, respectively. The red dotted lines represent the cold stream of water that is turned into steam, starting with BFW1-1. The purple line represents the hot stream that is cooled. In this case, it is the hot syngas just leaving the ATR, starting with SYNGAS-1.

3.6.2 Cooling Sections

There are two cooling sections in this process where heat is recovered: the post-ATR cooler and the post-methanol reactor cooler. Both of these areas use the steam generator configuration described in the previous section to recover heat in the form of steam.

Post-ATR Cooling Section

The post-ATR cooling section occurs immediately after the ATR. This is shown in Figure 3.9. The stream of syngas from the ATR is treated as the hot stream. It enters the 3-part steam generator at a temperature and pressure of 1050°C and 35 atm, respectively. The boiler feed water (BFW) is the cold stream, and it enters the 3-part steam generator at a temperature and pressure of 121°C and 35 atm, respectively. The water is at this pressure because some of the generated steam will later be mixed with feedstocks to the ATR that are also at 35 atm. At this high pressure, water boils at approximately 243°C, so the BFW is delivered at a higher temperature. It is assumed that the BFW is heated and pressurized outside of the simulation.

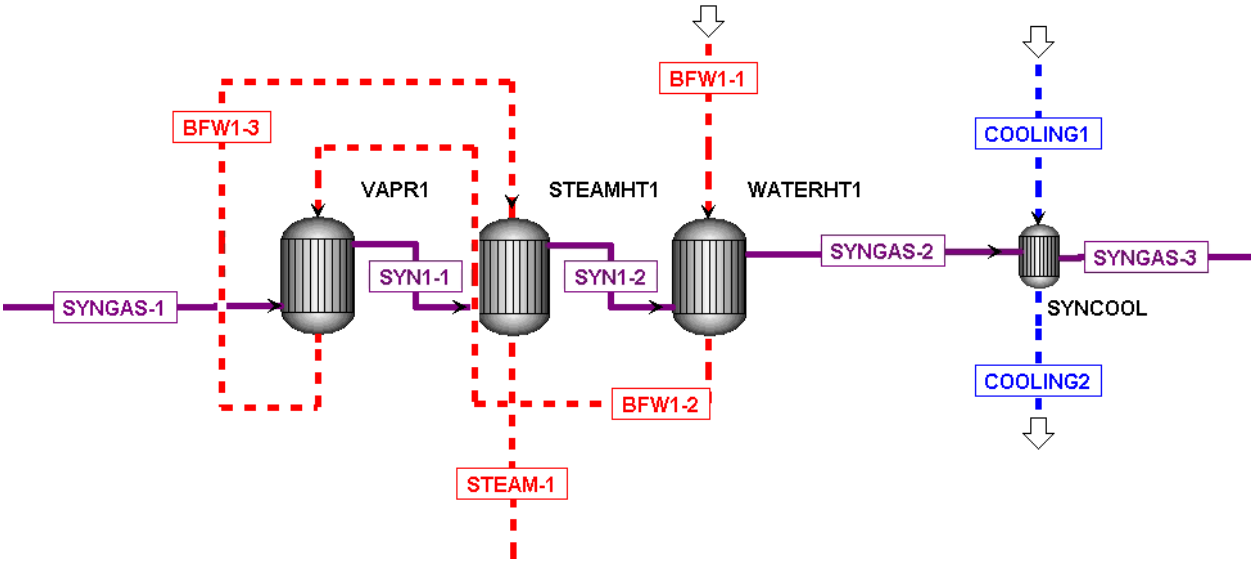

Figure 3.9 Steam generation and cooling of the syngas stream.

The BFW is heated to 240°C, because the vaporization temperature of water at 35 atm is approximately 243°C. The BFW is then vaporized at 243°C and heated to 380°C. A portion of the resultant steam (STEAM-1) is sent to heat integration, and the rest is sent to mix with the natural gas and oxygen feeds to the ATR. The reason the steam is heated to 380°C is because of the portion of the steam that will be mixed with the oxygen and natural gas feedstocks to the ATR. When the steam mixes with natural gas, the natural gas is at 380°C. When the steam mixes with oxygen, the oxygen is at 360°C. By heating the steam to 380°C, the maximum amount of steam is generated at the minimum possible temperature so as to not lower the temperature of the oxygen or natural gas streams upon mixing.

The hot syngas stream is cooled to 154°C at the end of the steam generation section (SYNGAS-2). The syngas needs to be further cooled to 40°C so that it may be later distilled, so additional cooling is needed. A stream of cold water (COOLING1) at 20°C and 1 atm is added to cool the syngas at the heat exchanger SYNCOOL stream to achieve this.

Post-Methanol Reactor Cooling Section

This cooling section occurs immediately after the methanol reactor, shown in Figure 3.10. The unrefined methanol stream (METH-1) from the methanol reactor acts as the hot stream, entering the steam generation section at 251°C and 70 atm. The BFW (BFW2-1) functions as the cold stream, entering at 50°C and 1 atm.

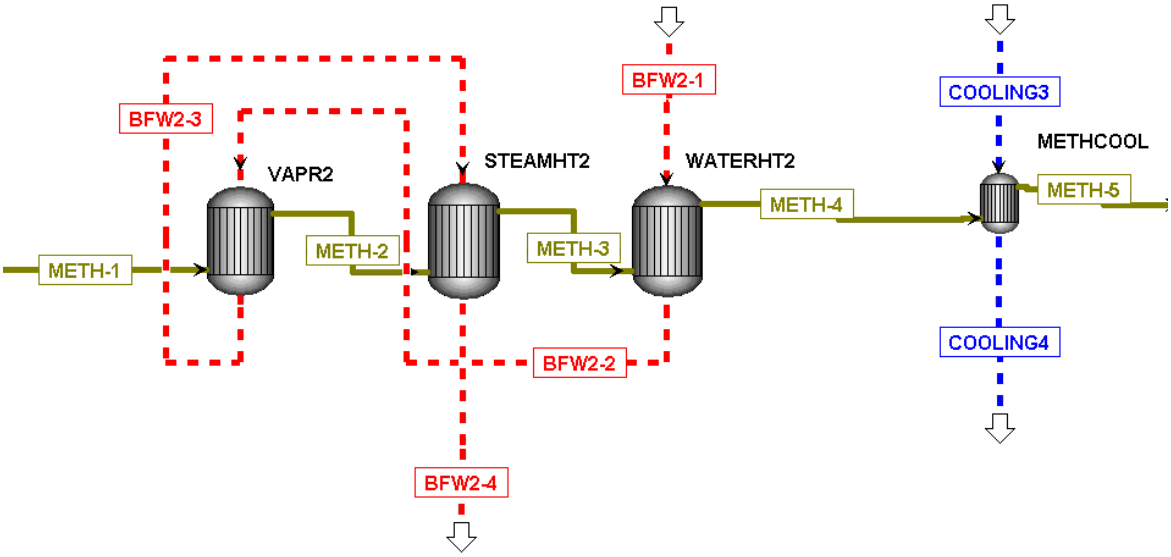

Figure 3.10 Steam generator configuration for post-methanol reactor cooling.

The BFW is heated to 95°C in the first heat exchanger (WATERHT2). It is then vaporized to 100°C in the second heat exchanger (VAPR2). In the third (STEAMHT2), the newly formed steam is heated to 140°C. This steam (BFW2-4) will be considered for heating the CO_2 capture amine reboiler in Chapter 4.

The methanol stream is cooled overall to 142°C (METH-4). Since the hot methanol stream must be cooled to 40°C, an additional stream of cold water (COOLING3) at 20°C and 1 atm is added to cool the methanol stream in the heat exchanger METHCOOL. This further cools the methanol stream to the desired 40°C. This stream must be at 40°C for when it enters the distillation columns in the purification section immediately after.

3.6.3 Fired Heater

This section describes an additional hot stream used for heat integration, but one that is different from the two mentioned in the previous section. This is the hot stream used in the fired heater in the adiabatic pre-reforming section before the ATR (described in Section 3.3.2 and shown in Figure 3.5). This hot stream is not composed of steam like the two hot streams generated from the cooling sections. Instead, this hot stream was generated from combustion of natural gas. While some of its heat was used up in the fired heater, the leftover heat is still valuable for heating other sections of the process.

Natural gas (NG-FIRE) and air (AIR-FIRE) are fed into a combustor at 30°C and 1 atm. The minimum possible amount of natural gas is fed in order to minimize the CO_2 emissions, while still generating the required combustion heat for the fired heater. This is 18.03 kmol/hr of natural gas. Air is fed into the combustor such that there is 3% total oxygen in the combustor when the natural gas and air is mixed (~18% excess air). The combustor (COMBUSTR) burns the natural gas and air, producing a hot stream (HOTIN) at 1,823°C and 1 atm. This is fed to the fired heater (FIRE) and is used to heat the natural gas and natural gas/steam mixture streams on

their way to the pre-reformer and ATR. Exchanging heat in the fired heater cools the hot stream down to 681°C. This stream (HOTOUT) can now be used in heat balancing to supply heat.

3.6.4 Heating Sections

There are three sections aside from the fired heater (described in the previous section) that require simple heating. This is where the heat acquired from heat balancing will go. These three heating sections are listed below along with their heat exchanger label in the Aspen Plus simulation.

1. O_2 heating (O2-HEAT1)
2. O_2/steam mixture heating (O2-HEAT2)
3. Recycle heating (REC-HEAT)

The O_2 recycle heating involves the stream of oxygen produced from the electrolyser (O2-1). This stream must be heated from 40°C at 35 atm to 360°C at 35 atm.

The O_2/steam mixture heating involves the oxygen feed stream after it has been mixed with steam (O2STEAM1). It is further heated from 362°C as much as possible just before it is fed into the ATR. The more it can be preheated, the less natural gas combustion is required to preheat the ATR feed streams, therefore reducing CO_2 emissions.

The recycle heating is the recycle loop from the methanol reactor (RECYCLE2). After a portion of the recycle stream is bled off, the rest must be heated before being fed back into the methanol reactor. This stream must be heated from 40°C at 70 atm to 231°C at 70 atm.

3.7 CO_2 Capture

A simplified version of the amine reboiler in the stripper column of a MEA-based post-combustion CO_2 capture was simulated in this work. Figure 3.11 shows the Aspen simulation of the amine reboiler and the steam generator used to heat it.

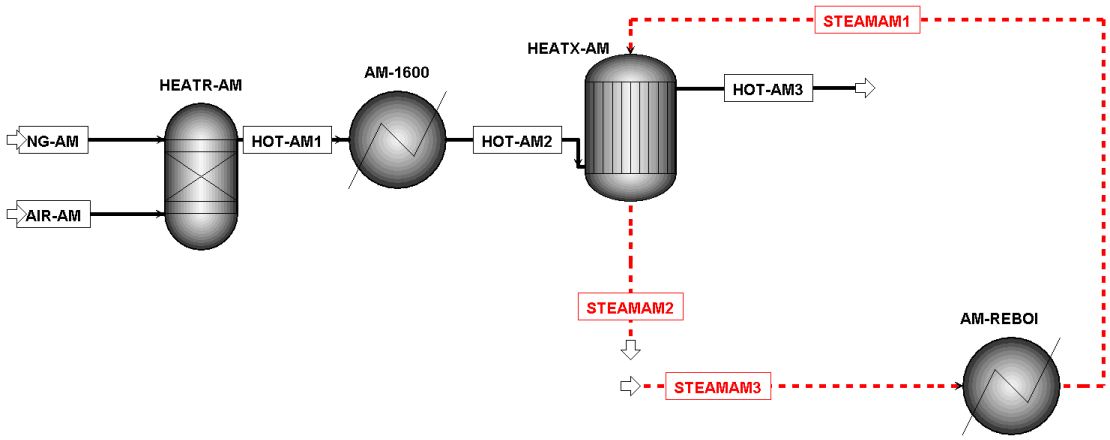

Figure 3.11 Amine reboiler and steam generator simulation in Aspen Plus.

There are two parts to this simulation: the amine reboiler and the steam generator section. The amine reboiler (AM-REBOI) represents the heating need of an amine reboiler in the stripper column of a MEA-based post-combustion CO_2 capture unit. The heating need will change based on the amount of CO_2 that needs to be captured. This will be determined in Section 4.4. This heating need will be represented by the heat duty of AM-REBOI. This heating need will be met by the steam feed to AM-REBOI. The steam enters via the stream STEAMAM3 at 130°C and 1 atm. AM-REBOI exchanges heat with the steam, cooling it to 120°C and 1 atm (STEAMAM1). The flowrate of the steam feed (STEAMAM3) will be determined by the amount of heat duty needed in AM-REBOI based on the CO_2 capture requirement. Once the steam feed flowrate is determined, any heat in the process that has not yet been integrated will be used to supply this steam. However, if there is not enough unintegrated heat to fully meet the amine reboiler heating requirement, then the steam generator will be used.

The second part of the simulation is the steam generator section. This section will be used to make heat in the form of steam if the unintegrated heat from the overall process does not fully meet the heating requirement of the amine reboiler. This section is made up of a combustor (HEATR-AM), and two heat exchangers (AM-1600 and HEATX-AM). Natural gas (NG-AM) and air (AIR-AM) are fed into the combustor at 30°C and 1 atm where they are burned to make the hot stream HOT-AM1. The natural gas flowrate will depend on the required steam output, as it will be minimized to keep emissions as low as possible. The air flowrate is such that the mix of air and natural gas has 3% oxygen (approximately 18% excess air). AM-1600 is used to cap the hot stream temperature at 1,600°C (HOT-AM2). The hot stream is then fed into the heat exchanger HEATX-AM where it is used to heat steam. The steam enters (STEAMAM1) at 120°C and 1 atm and leaves (STEAMAM2) at 130°C and 1 atm. This is the steam that will be used to heat the amine reboiler if the unintegrated heat is deemed insufficient. Again, the flowrate of this steam will depend on the heat duty requirement of the amine reboiler.

Chapter 4: Simulation Results

4.1 ATR Section

This section describes the simulation results of the ATR section.

In the Aspen simulation, there are four key design requirements from the autothermal reforming section:

1. The heat duty of the autothermal reformer has to be approximately 0 kW.
2. The syngas ratio (M) has to equal approximately 2.
3. The steam-to-carbon (S/C) ratio has to equal approximately 0.6.
4. The final methanol production should be as close to 230 MTPD (300 kmol/hr) as possible.

The heat duty requirement was due to the autothermal nature of the ATR, meaning that all heat required for the reactor must come from the heat of the reaction itself without outside heating. Zero heat duty indicates that no added heat is required for the reactor either. In Aspen, positive heat duty means that heat needs to be added to the reactor, while negative duty means that heat needs to be removed from the reactor.

The syngas ratio, describe in Section 3.1, is a molar ratio of the hydrogen, carbon dioxide, and carbon monoxide input to the methanol synthesis section. For stoichiometric reasons, this ratio must equal approximately 2, as shown below.

$$M = \frac{H_2 - CO_2}{CO + CO_2} = 2 \qquad \text{Equation 4.1}$$

This ratio is determined at the stream made up of the syngas product of the ATR mixed with the hydrogen and carbon dioxide feedstock streams (SYNGAS-7 in Figure 3.5). Therefore, it is important that the ATR is properly specified such that its syngas product maintains this ratio.

The steam-to-carbon (S/C) ratio is the ratio of the steam entering the ATR to the methane entering the ATR. As described in Section 2.3.1, a lower S/C ratio is desired, and a ratio of 0.6 has been industrially demonstrated. For this reason, 0.6 was chosen as the desired S/C ratio.

For each change made to the ATR and its surrounding operating conditions, the total end methanol production was also considered. AChT was looking into the design of a pilot plant that manufactured 230 MTPD of methanol. Therefore, the methanol production should be as close as possible to 230 MTPD (300 kmol/hr).

These four requirements influenced design decisions in the syngas production section, which are described in this section.

4.1.1 Steam-to-Carbon Ratio Design Specification

The S/C ratio was made effectively constant by the addition of a design specification in Aspen on the separator STMSEP-1 (see Figure 3.3). STMSEP-1 determined how much steam was sent to the ATR feed and how much steam was sent to heat integration. This design specification was programmed to change the amount of steam sent to the ATR until the ratio of steam and methane in the streams entering the ATR (MIXTOATR and O2STEAM2) equals 0.6. In the stream MIXTOATR, other hydrocarbons are present (C_2H_6, C_3H_8, and C_2H_4), but they are in negligible amounts compared to CH_4 and do not impact on the calculation of the S/C ratio.

The results of this design specification are shown in Table 4.1. It shows what percentage of the steam was sent to heat integration (STEAM-H1) and what percentage was sent to the ATR feeds (STEAM-2).

Table 4.1 STMSEP-1 steam separation results (380°C, 35 atm).

Stream Name	**Stream Split**	**Mole Flow (kmol/hr)**
Steam to heat integration (STEAM-H1)	0.725	461
Steam to ATR (STEAM-2)	0.275	174

The resultant molar flows of methane and steam to the ATR are shown in Table 4.2.

Table 4.2 Combined steam and methane flow to the ATR.

Stream Name	**Component**	**Mole Flow (kmol/hr)**
MIXTOATR	CH_4	263.81
MIXTOATR	H_2O	123.43
O2STEAM2	H_2O	34.90

From this, the resultant S/C ratio can be determined.

$$S/C\ Ratio = \frac{123.43 + 34.90}{263.81} = 0.60$$

With this design specification established, the S/C is essentially fixed at 0.6 from this point.

4.1.2 CO_2 to ATR

One parameter that could affect the ATR heat duty, syngas ratio, and/or methanol output was the amount of CO_2 sent through the ATR vs. the amount of CO_2 bypassed around the ATR. This occurs in the simulation at the separator CO2SEP (see Figure 3.3). The sensitivity of the ATR heat duty, syngas ratio, and methanol output to the split at CO2SEP was simulated and the results are shown in Table 4.3.

Table 4.3 CO_2 bypassing ATR vs. ATR heat duty, syngas ratio, and methanol output.

Percentage of CO2BYPAS (%)	ATR Heat Duty (kW)	Syngas Ratio	Methanol Output (kmol/hr)
0	1774	2.06	298
20	1370	2.07	294
40	959	2.07	290
60	538	2.08	286
80	108	2.08	284
100	-332	2.08	278

Figure 4.1 graphs the heat duty results. Given that the desired ATR heat duty is approximately 0 kW, it appears that 88% CO_2 bypassing the ATR would give the optimal result.

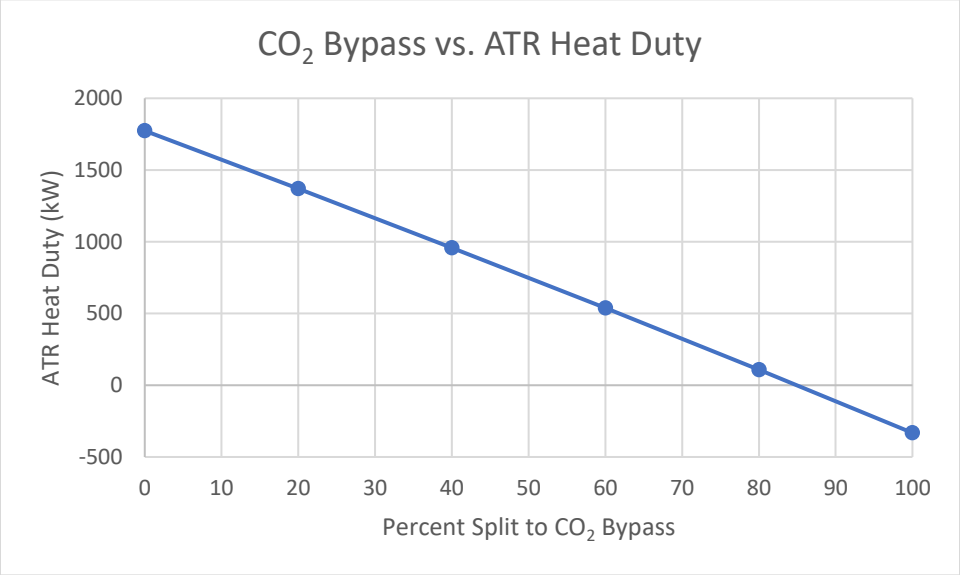

Figure 4.1 CO2 bypass percentage vs. ATR heat duty.

Figure 4.2 graphs the syngas ratio results. This shows that the syngas ratio is mostly unaffected by the CO_2 bypass percentage.

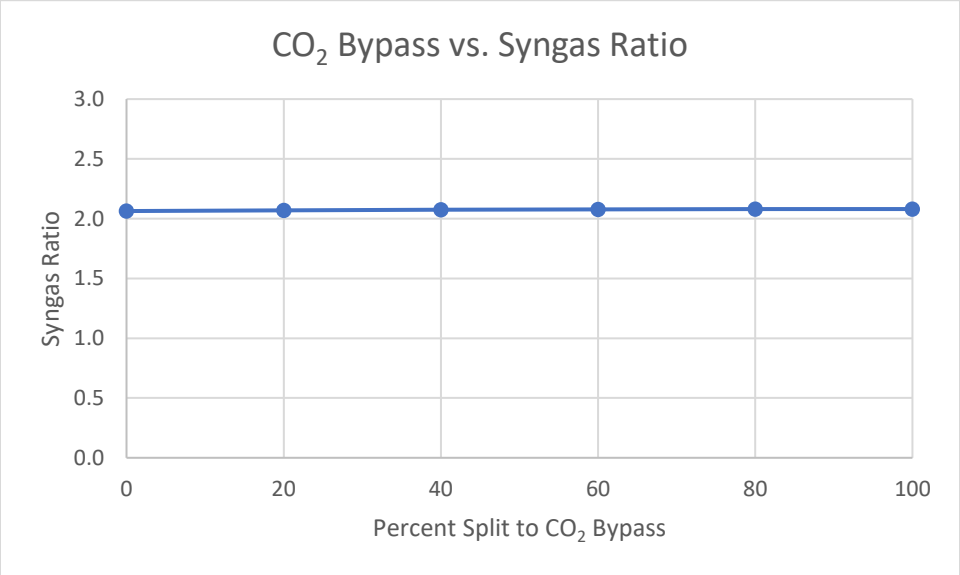

Figure 4.2 CO_2 bypass percentage vs. syngas ratio.

Figure 4.3 shows how the CO_2 bypass change affected total methanol output. Directing more CO_2 through the ATR lead to an increase in overall methanol production, while bypassing the ATR lead to a 6.8% decline in methanol output from 0% bypass and 100% bypass.

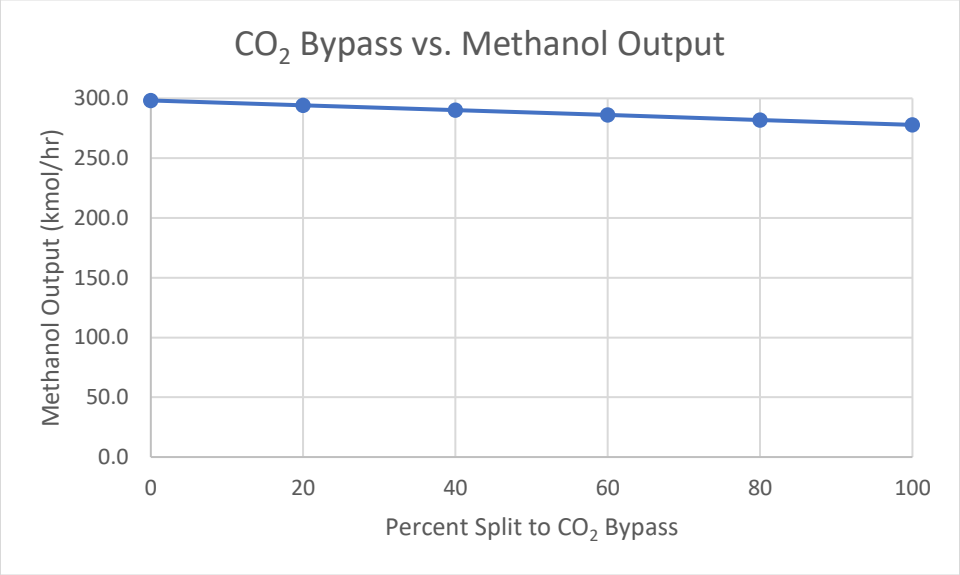

Figure 4.3 CO2 bypass percentage vs. methanol output.

88% CO_2 bypass was tested because it leads to nearly zero ATR heat duty, and the results are shown in Table 4.4.

Table 4.4 Test with 88% CO_2 bypass.

Percentage of CO2BYPAS (%)	ATR Heat Duty (kW)	Syngas Ratio	Methanol Output (kmol/hr)
88	1.18	2.08	282

88% CO_2 bypass was found to meet both the ATR heat duty requirement (approximately 0 kW) and the syngas ratio requirement (approximately 2). One drawback is a 5.8% decrease in methanol production when compared to 0% CO_2 bypass. Based on these results, the CO_2 bypass percentage of 88% was chosen for the simulation.

4.1.3 ATR Syngas Stream Results

Once the ATR design requirements were met, a final stream of syngas was produced from the ATR. Figure 4.4 shows the syngas stream (SYNGAS-1) before it goes to the methanol reactor.

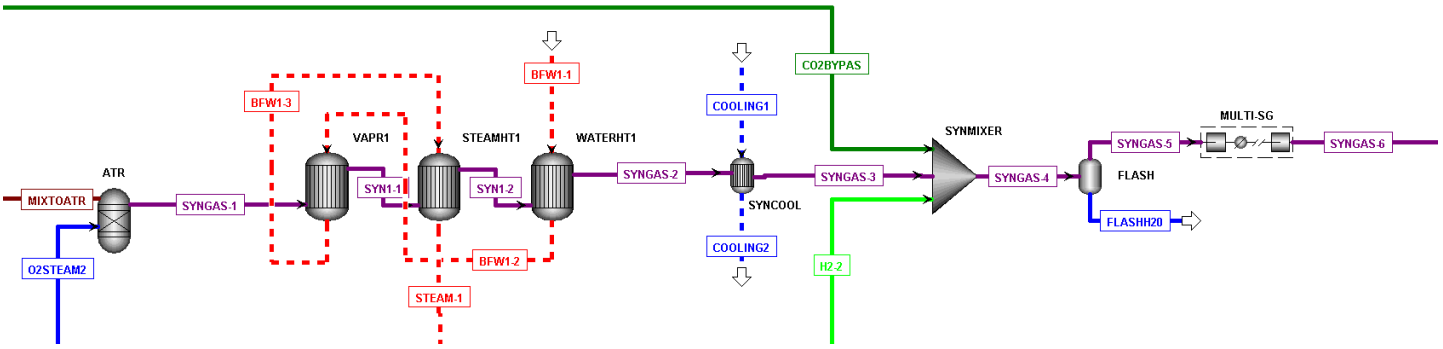

Figure 4.4 ATR syngas result stream.

The syngas goes through a 3-part steam generator (VAPR1, STEAMHT1, and WATERHT1) to cool it, as described in Sections 3.5 and 4.4. The syngas is then further cooled by cooling water in the heat exchanger SYNCOOL. The syngas is then mixed with the CO_2 that bypassed the ATR (CO2BYPASS) and the hydrogen generated from the electrolyser (H2-2). The syngas stream SYNGAS-4 has water removed in FLASH. It is then pressurized from 40 atm to 70 atm in the multistage compressor MULTI-SG. 70 atm is the operating pressure of the methanol reactor. This leads to the stream SYNGAS-6, which is ready to be sent to the methanol reactor section. It is here that the syngas ratio is calculated to be 2. The composition of this stream is shown in Table 4.5. The temperature of the stream is 231°C and the pressure is 70 atm.

Table 4.5 SYNGAS-6 stream composition at 231°C and 70 atm.

Component	Flowrate (kmol/hr)	Mole Fraction
H_2	802	0.686
CH_4	10.8	0.00928
H_2O	2.58	0.00221
CO	229	0.196
CO_2	120	0.102
CH_4O	1.23E-05	1.06E-08
O_2	0	0
N_2	4.76	0.00407
C_2H_6	3.64E-04	3.11E-07
C_3H_8	3.34E-08	2.86E-11
C_2H_4	5.05E-04	4.32E-07
Total	**1169**	**1**

4.2 Methanol Reactor Section

Now that the syngas is delivered to the methanol reactor section as describe in Section 4.1.3, the methanol reactor is simulated. This section describes the simulation results. Figure 4.5 shows the simulation of the methanol reactor section.

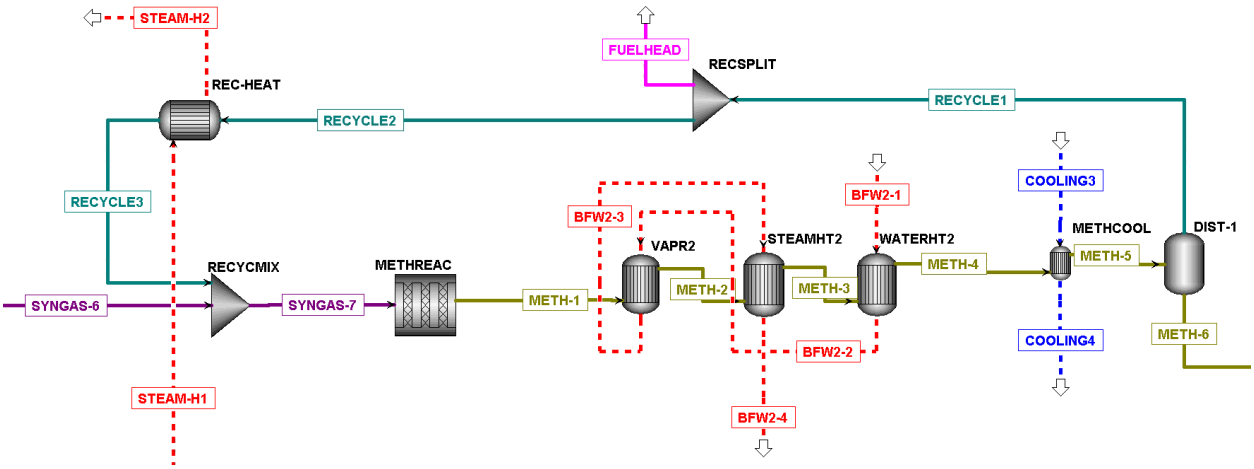

Figure 4.5 Methanol reactor section.

The syngas stream from the ATR section, SYNGAS-6, enters and is mixed with the recycle stream (RECYCLE3) at the mixer RECYCMIX. It then enters the methanol reactor (METHREAC). The output stream of the methanol reactor (METH-1) enters a 3-part steam generator (VAPR2, STEAMHT2, and WATERHT2) where it is cooled as described in Sections

3.5 and 4.3. The methanol output stream is further cooled at METHCOOL. Unreacted reactants are removed at DIST-1. The output METH-6 goes to the methanol distillation section, and the unreacted material is recycled through the RECYCLE1 stream. The recycle stream has a split where some amount of waste (FUELHEAD) is removed permanently. The rest (RECYCLE2) is reheated at REC-HEAT and mixed back with the syngas.

4.2.1 Methanol Recycle

At the methanol reactor, there is a recycle loop that recycles unreacted material (RECYCLE-1 in Figure 4.5). There is a separator at the start of this loop (RECSPLIT in Figure 4.5) that determines what percentage of the recycle stream is actually recycled and what percentage is permanently bled off as waste. This waste stream exists so as to prevent the buildup of looping recycled material. The split percentage at this separator affects some performance aspects of the methanol reactor.

First, initial tests using a broad range methanol recycle split percentages were conducted to see how they generally affect reactor performance. The tested factors were:

1. Overall methanol output (kmol/hr)
2. Total methanol recycle flow rate (kmol/hr)
3. Reactor conversion (%)

Changing the methanol recycle split percentage so that less material is recycled and more is removed as waste will result in less reactant entering the methanol reactor. Clearly, this will have an impact on the overall methanol production rate, with more methanol produced being desired.

The entire purpose of having a recycle split is to prevent excessive buildup of looping recycled materials. Therein exists a tension where on one hand, more recycled material leads to greater methanol production, and on the other hand, recycling a large amount of material could lead to impractical flowrates in the recycle loop. To monitor this, the flow rate of the recycle stream was observed.

Reactor conversion was also monitored to observe how much unreacted material was looping through the methanol reactor. It was calculated using the conversion of hydrogen:

$$H_2\ Conversion = \frac{H_2in - H_2out}{H_2in} \times 100\% \qquad \text{Equation 4.2}$$

Where H_2in and H_2out are the inlet and outlet molar flowrates of hydrogen to the methanol reactor (kmol/hr).

Methanol recycle split percentages were tested against the three factors mentioned above, with emphasis on the 90-99% range due to the desire for high methanol output. The results are shown in Table 4.6.

Table 4.6 Methanol recycle split percentage test results.

RECSPLIT to recycle	Methanol out (kmol/hr)	Methanol recycle stream flowrate (kmol/hr)	H_2in (kmol/hr)	H_2out (kmol/hr)	H_2 Conversion
0.20	170	144	910	544	40%
0.40	186	346	1067	666	38%
0.60	207	666	1326	875	34%
0.80	240	1308	1874	1341	28%
0.90	269	2055	2548	1941	24%
0.91	273	2178	2662	2045	23%
0.92	277	2320	2794	2166	22%
0.93	282	2487	2948	2309	22%
0.94	286	2687	3135	2483	21%
0.95	291	2936	3368	2702	20%
0.96	297	3264	3674	2993	19%
0.97	304	3732	4109	3410	17%
0.98	312	4507	4826	4107	15%
0.99	321	6338	6497	5754	11%

Figures 4.6, 4.7, and 4.8 graph these results.

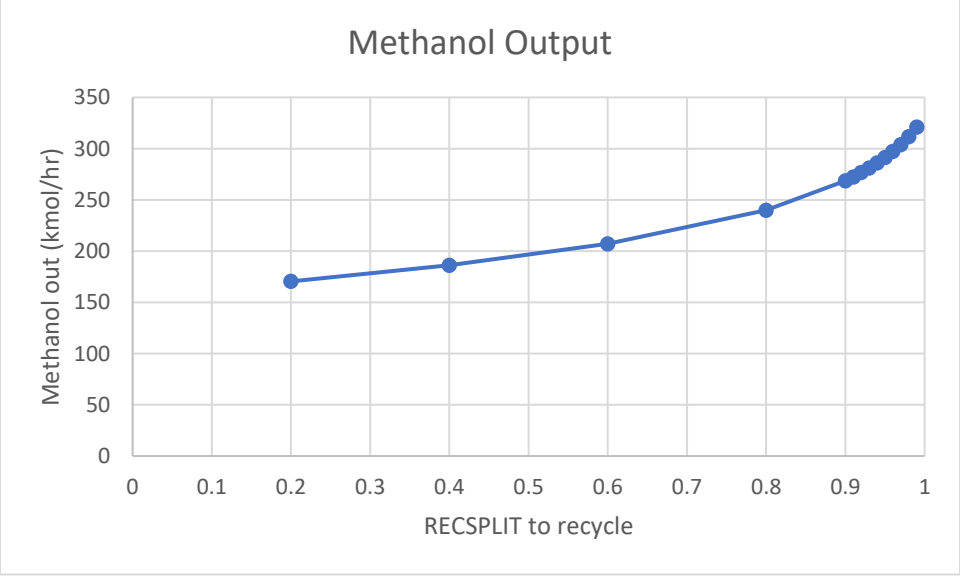

Figure 4.6 Methanol output vs. methanol recycle split to recycle.

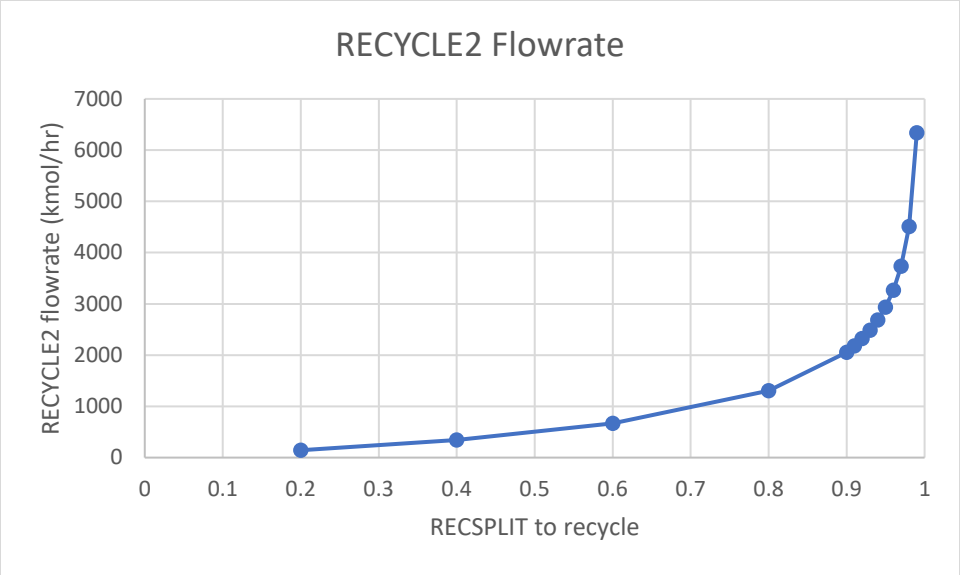

Figure 4. 7 Recycle stream flowrate vs. methanol recycle split to recycle.

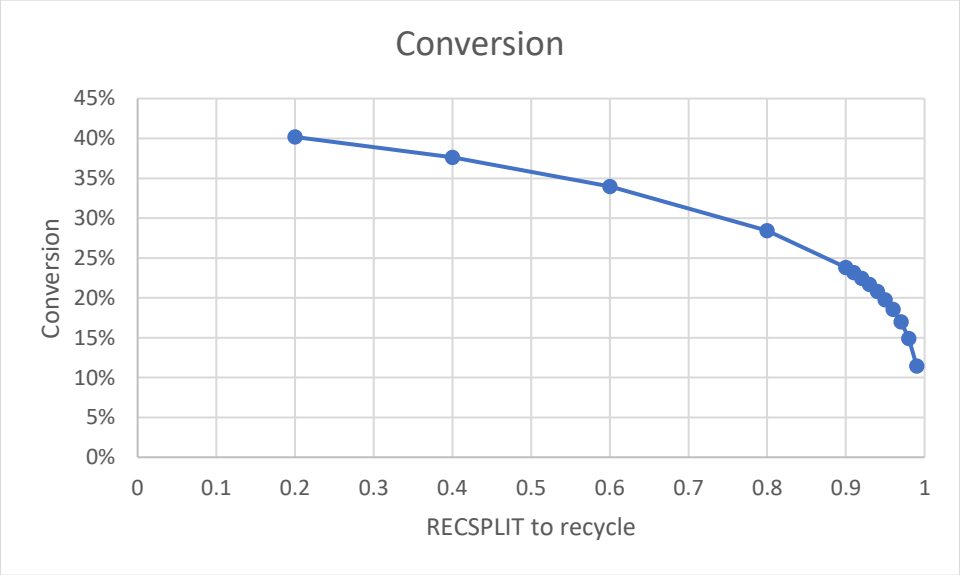

Figure 4. 8 Reactor conversion vs. methanol recycle split to recycle.

Figure 4.6 shows the relationship between the split to recycle and the methanol output: more recycling leads to greater methanol production. This positive relationship means that more recycle is desired. Figures 4.7 and 4.8 show the negative impacts of a large recycle split. Shortly beyond 90% split to recycle, the recycle flowrate expands greatly for each 1% increase in split. This large increase in looping of unreacted material also leads to a decline in reactor conversion, shown in Figure 4.8. These negative relationships indicate that a split to recycle under approximately 94% is desired. Based on these results, a recycle split of 93% and 7% to waste was chosen.

4.2.2 Hydrogen Recycle

The methanol reactor section was initially designed with one single recycle loop, shown in Figure 4.5. When running this version of the simulation, it was found that the makeup of the recycle stream (RECYCLE1), and therefore the waste stream (FUELHEAD), was mostly hydrogen. Table 4.7 shows the molar flow rate and mole fraction composition of the methanol stream, the recycle stream, and the waste stream.

Table 4.7 Molar flow and mole fraction composition of methanol, recycle, and waste streams.

	METH-6		**RECYCLE1**		**FUELHEAD**	
	Flowrate (kmol/hr)	Mole fraction	Flowrate (kmol/hr)	Mole fraction	Flowrate (kmol/hr)	Mole fraction
H_2	1.02E-04	2.50E-07	2217	0.846	155	0.846
CH_4	7.21	0.0177	51.9	0.0198	3.63	0.0198
H_2O	71.3	0.175	0.814	0.000311	0.0570	0.000311
CO	1.86	0.00457	96.7	0.0369	6.77	0.0369
CO_2	38.1	0.0935	184	0.0703	12.9	0.0703
CH_4O	288	0.707	12.6	0.00480	0.880	0.00480
N_2	0	0	0	0	0	0

This shows that 85% of the recycle stream, and therefore the waste stream, is made up of hydrogen. The hydrogen content of FUELHEAD is 155 kmol/hr. The hydrogen input to the entire process from the electrolyser is 288.6 kmol/hr (H2-1 in Figure 3.3). This means that 54% of the hydrogen input to the system is being lost through the waste stream. Since hydrogen is expensive to produce, recycling this hydrogen could be a valuable proposition. This would require a method of separating or purifying the hydrogen from the waste stream, namely pressure swing adsorption (PSA) here.

4.2.3 Pressure Swing Adsorption

Pressure swing adsorption (PSA) is a popular method of industrial-scale hydrogen purification [34] [35]. PSA technology has been around since the 1960s, and today produces hydrogen at a purity of 99.99+% [35]. It operates at high pressures and can deal with a variety of impurities such as water, carbon oxides, methane, nitrogen, and hydrocarbons [35]. Hydrogen recovery is typically around 80-90% [34] [35].

Though it is outside the scope of this work to simulate a detailed PSA process, a simplified version of the PSA was simulated in order to see how it would affect the process.

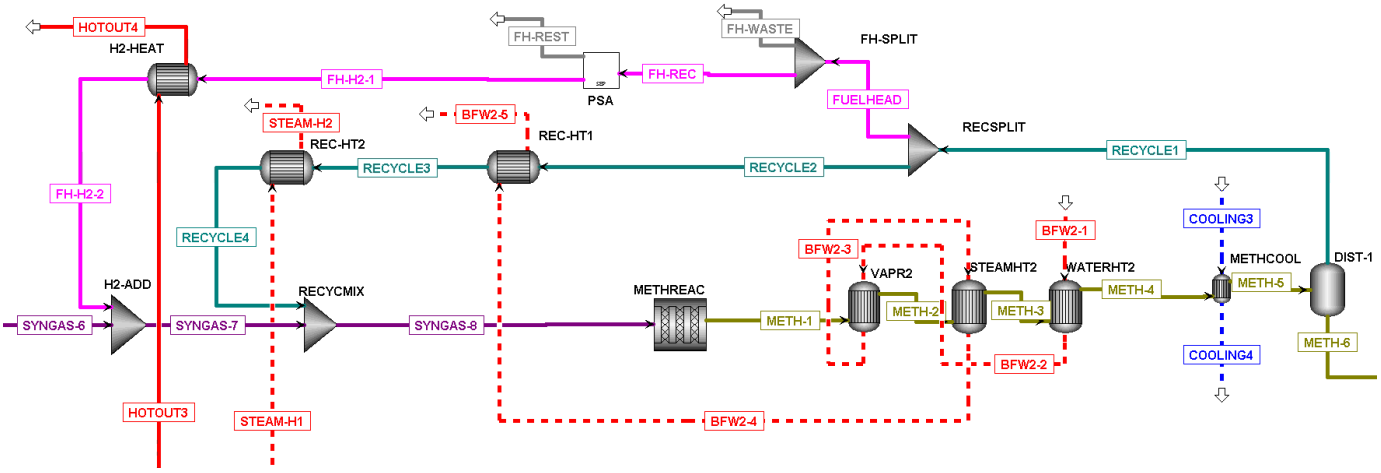

Figure 4.9 Methanol synthesis section with PSA hydrogen recovery

Shown in Figure 4.9, the FUELHEAD stream is further split at the separator FH-SPLIT, where some amount goes to hydrogen recovery, and some amount is split off as waste to prevent recycle buildup. This split is determined in Section 4.2.5. Then the stream FH-REC goes through the simplified PSA unit, where 90% of the H_2 in the stream is separated from the rest of the stream. The remainder of the stream leaves as waste (FH-REST), and the recovered hydrogen is reheated and recycled to the start of the methanol synthesis process. If this hydrogen is simply added back into the system, it results in greater methanol production. Otherwise, this hydrogen can be recovered and sold (described in the next section, 4.2.4).

4.2.4 Electrolyser Hydrogen Recovery

The hydrogen that is recovered from the PSA hydrogen recycle can replace part of the feedstock hydrogen produced by the electrolyser. The simulation of this is shown in Figure 4.10.

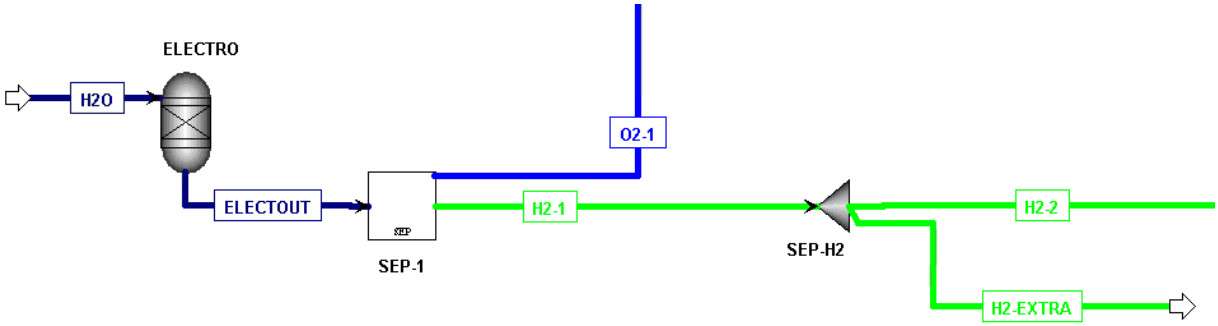

Figure 4. 10 Recovery of electrolyser hydrogen.

Figure 4.10 shows that the stream of hydrogen from the electrolyser, H2-1, is split. H2-2 is the hydrogen that goes to the ATR, while H2-EXTRA is removed at the same rate as the hydrogen being recycled in the PSA. A design specification in Aspen is programmed to ensure this.

The benefit of recovering the electrolytic hydrogen is that it is extremely pure in content, as it was generated by electrolysis. Hydrogen produced this way is valuable to sell, so separating it early and selling it generates extra value while getting the same amount of methanol.

4.2.5 Hydrogen Recycle Split Percentage

When PSA hydrogen recovery is implemented, a second waste stream split is made. As described in Section 4.2.3, the waste stream is split a second time (FH-SPLIT in Figure 4.9) before having the hydrogen in this stream recycled. This split determines what percentage of the waste stream goes to hydrogen recycle loop, and what percentage is permanently removed as waste in order to prevent recycle buildup.

With the methanol recycle split was chosen to be 93%, a sensitivity study was conducted to assess the effect of the hydrogen recycle split. Table 4.8 shows the results of those tests.

Table 4.8 Results of hydrogen recycle split percentage tests.

Methanol split to recycle	Hydrogen split to recycle	Methanol out (kmol/hr)	Methanol recycle stream flowrate (kmol/hr)	Hydrogen recycle stream flowrate (kmol/hr)	H_2in (kmol/hr)	H_2out (kmol/hr)	Conversion
0.93	0.20	282	2,489	29	2,951	2,312	21.65%
0.93	0.40	282	2,490	58	2,953	2,314	21.63%
0.93	0.60	282	2,491	88	2,956	2,318	21.60%
0.93	0.80	282	2,496	117	2,962	2,324	21.55%
0.93	0.90	282	2,494	132	2,961	2,323	21.55%
0.93	0.91	282	2,494	133	2,961	2,323	21.55%
0.93	0.92	282	2,498	135	2,966	2,327	21.52%
0.93	0.93	282	2,498	136	2,965	2,327	21.53%
0.93	0.94	282	2,498	138	2,965	2,327	21.53%
0.93	0.95	282	2,497	139	2,964	2,326	21.53%
0.93	0.96	282	2,496	141	2,964	2,325	21.53%
0.93	0.97	282	2,499	142	2,966	2,328	21.52%
0.93	0.98	282	2,497	144	2,965	2,327	21.52%
0.93	0.99	282	2,499	145	2,967	2,329	21.51%
0.93	1.00	282	2,497	147	2,965	2,327	21.52%

From these results, and as expected, it is apparent that the hydrogen recycle split has no impact on many of these factors. Methanol output, methanol recycle stream flowrate, and conversion all remain effectively unchanged as the hydrogen recycle split is altered. The only impact is a positive one on the hydrogen recycled. This positive relationship is displayed in Figure 4.11. Since more hydrogen recycled means more hydrogen from electrolysis can potentially be sold (see Section 4.2.4), this is a desirable change.

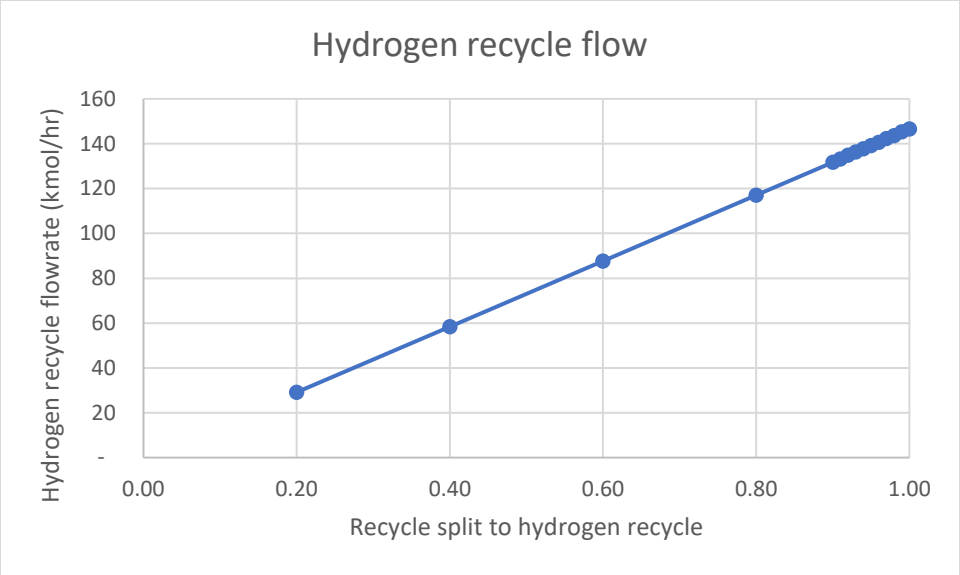

Figure 4.11 Recycle split to hydrogen recycle vs. hydrogen recycle flowrate.

One question is why the flowrate of the hydrogen recycle stream does not greatly increase in the 95%-100% recycle range as it does with the methanol recycle stream. This is due to the fact that the hydrogen separation process (PSA) only recycles 90% of the hydrogen in the waste stream and ejects the rest to waste. This prevents the buildup of unreacted material looping through the recycle. In this way, it was found that the PSA hydrogen separation makes a hydrogen recycle split unnecessary. It was therefore decided that the hydrogen recycle split would be 100% to recycle in order to recycle the maximum amount of hydrogen.

4.3 Heat Integration

In Section 3.6, three heat generating areas were described:

1. Post-ATR cooling section
2. Post-methanol reactor cooling section
3. Fired heater

This section quantifies how the hot streams from each of these three areas were organized to provide heat to the four heating sections.

4.3.1 Post-ATR Cooling Section

Figure 4.12 shows the post-ATR heating pathway. The dotted red line shows where the steam from the post-ATR steam generator (STEAM-H1) connects to the recycle heater (REC-HEAT). The steam that is allocated to mix with the oxygen and natural gas feeds to the ATR is split off at the separator (STMSEP-1), shown as the gray-coloured stream (STEAM-2).

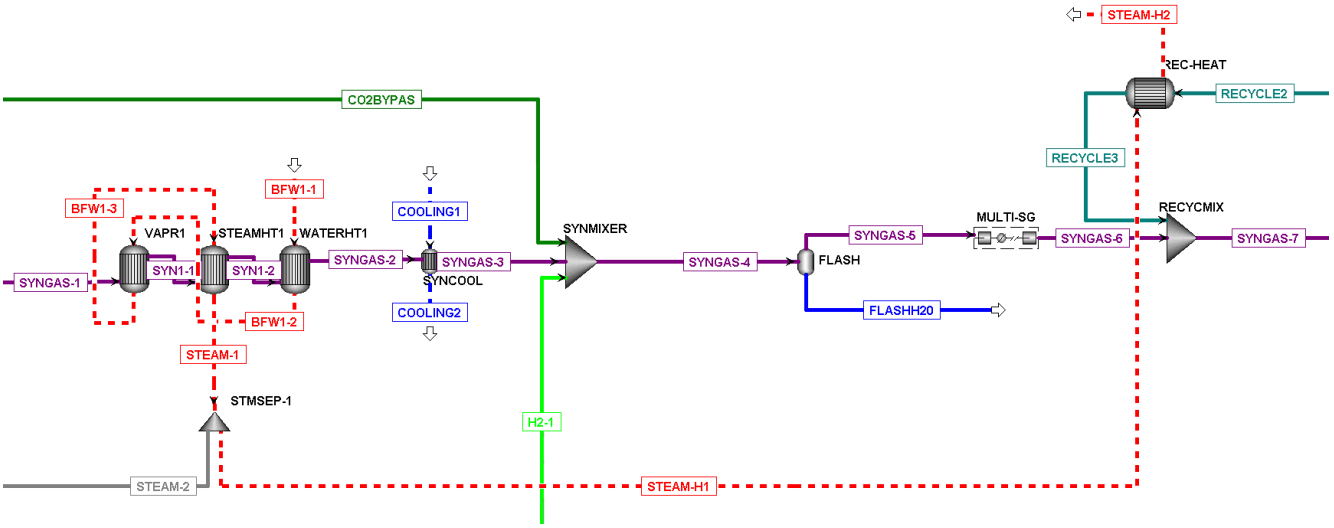

Figure 4. 12 Heat integration of the steam generated from the post-ATR cooling section.

The BFW (BFW1-1) enters the steam generation area at 121°C and 35 atm. The hot syngas stream from the ATR (SYNGAS-1) enters at 1050°C and 35 atm. The BFW is heated from water to steam (STEAM-1), exiting at 380°C and 35 atm. This steam is split at the separator STMSEP-1, with some going to mix with the ATR feeds (STEAM-2) and some going to heat integration (STEAM-H1). This split was determined in Section 4.1.1.

The heat integration steam heads to the Recycle Heating section (REC-HEAT), where it is able to heat the cold recycle stream (RECYCLE2) from 40°C to 231°C. This reduces the steam's temperature to 243°C and vapour fraction to 23%.

4.3.2 Post-Methanol Reactor Cooling Section

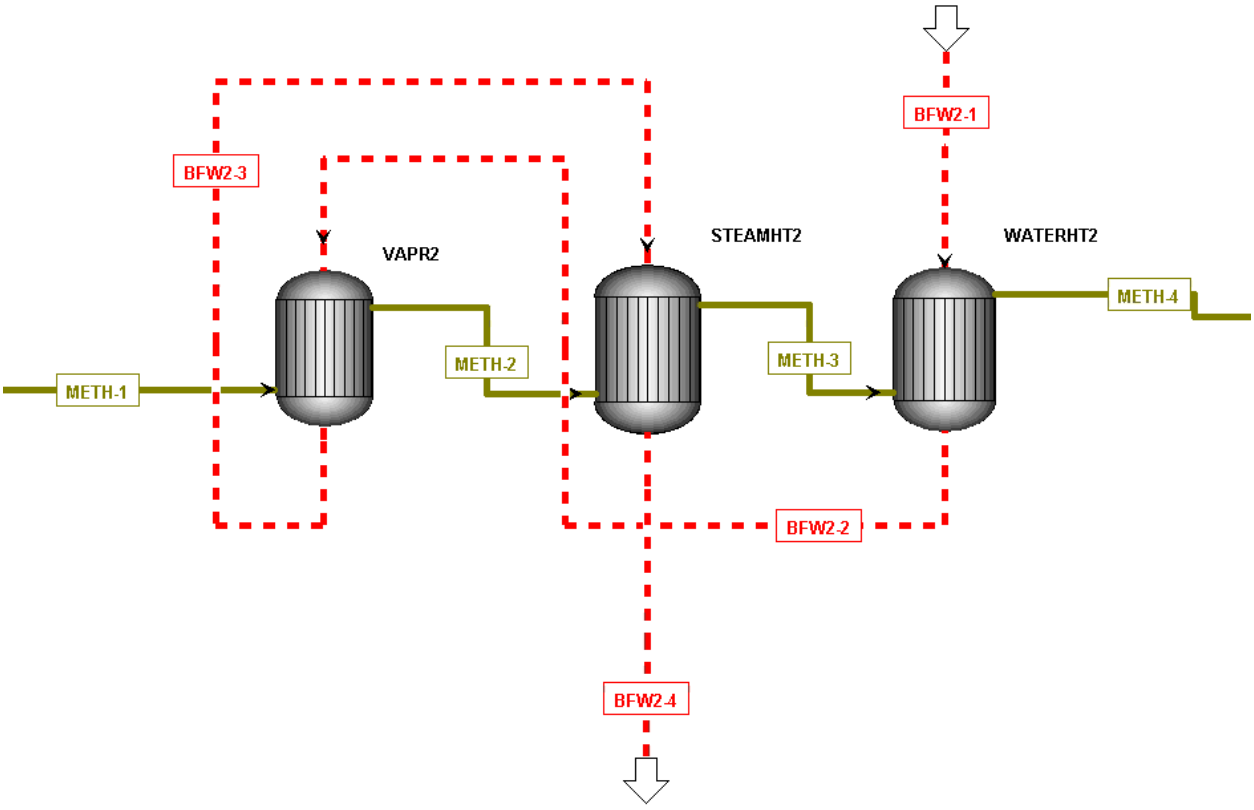

Figure 4. 13 Steam generator configuration for post-methanol reactor cooling.

Figure 4.13 shows the heat integration configuration for the post-methanol cooling section. The BFW (BFW2-1) enters the steam generation area at 50°C and 1 atm. The hot methanol stream from the methanol reactor (METH-1) enters the steam generation area at 251°C and 70 atm. The BFW is heated into steam (BFW2-4) at 140°C and 1 atm. The methanol stream is cooled to 142°C (METH-4).

4.3.3 Fired Heater Section

Figure 4.14 shows the heat integration pathway for the fired heater section. Following the solid red lines labelled HOTOUT1, HOTOUT2, and HOTOUT3 shows the fired heater outlet being used to heat oxygen in the heater O2-HEAT1, then being used to heat the oxygen/steam mixture in the heater O2-HEAT2.

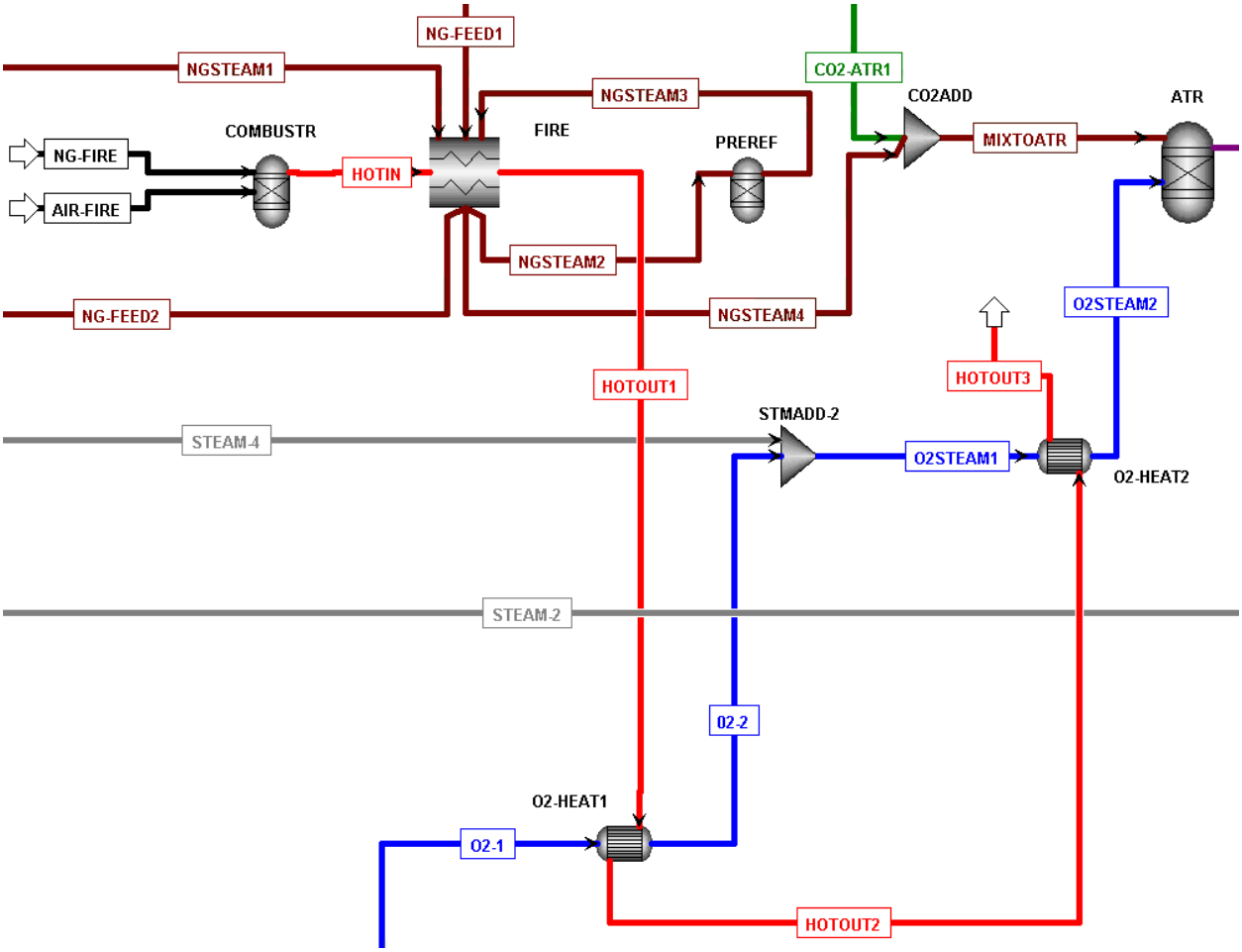

Figure 4. 14 Heat integration of the fired heater hot stream.

Natural gas and air (NG-FIRE and AIR-FIRE, respectively) are fed into a combustor (COMBUSTR) at 30°C and 1 atm. The minimum possible amount of natural gas is fed in order to minimize the CO_2 emissions, while still generating the required heat for the fired heater. Air is fed into the combustor such that there is 3% total oxygen in the combustor when the natural gas and air is mixed. The combustor burns the natural gas and air, producing a hot stream (HOTIN) at 1,823°C and 1 atm.

The hot stream is fed to the fired heater (FIRE) and is used to heat the natural gas (NG-FEED1) and natural gas/steam mixture (NGSTEAM1 and NGSTEAM3) streams on their way to the pre-reformer (PREREF) and ATR. This cools the hot stream down to 681°C.

From here, the hot stream heats the O_2 heating section (O2-HEAT1), which cools the hot stream to 490°C (HOTOUT2). It is able to heat the oxygen from 40°C (O2-1) to 360°C (O2-2).

After that, the hot stream (HOTOUT2) is fed to the O_2/steam heating section (O2-HEAT2), where it is able to heat the oxygen/steam mixture from 362°C (O2STEAM1) to 427°C (O2STEAM2). This cools the hot stream down to 437°C (HOTOUT3).

4.3.4 Remaining Hot Streams

With the heating requirements of the process met, there is still some hot streams remaining. These streams could potentially be used to help heat a CO_2 capture unit. These remaining hot streams are described in Table 4.9.

Table 4.9 Remaining hot streams.

Heat Integration Section	Stream Name	Temperature (°C)	Pressure (atm)	Flowrate (kmol/hr)
1. Post-ATR steam	STEAM-H2	243	35	461
2. Post-methanol reactor steam	BFW2-4	140	1	250
3. Fired heater hot stream	HOTOUT3	431	1	219

Note that STEAM-H2 is 23% vapour steam and 77% liquid water, BFW2-4 is pure steam, and HOTOUT3 is a mix of combustion products (N_2, O_2, CO_2, and H_2O) from combustion of natural gas and air. However, while there are differences in composition, pressure, and temperature between the three hot streams, the flowrates will give a sense of scale when the steam requirement of the CO_2 reboiler in the capture unit is determined in Section 4.4. As shown in Section 4.4, the heating requirement for the CO_2 reboiler is far greater than the amount of heat that can be recovered from these remaining hot streams. It is therefore necessary for the CO_2 capture unit to have its heat supplied by a dedicated natural gas combustion steam generator.

4.3.5 Hydrogen Recycle Heat Integration

A situation was tested where hydrogen was recycled using a PSA unit (described in Section 4.2.3) in order to make more methanol. This is also described in Section 5.2 as scenario 2. Due to the increase in production, recycle flow rates increase. This requires more heating in both the regular recycle and hydrogen recycle streams.

Shown in Figure 4.15, the heating in the regular recycle stream was supplemented by BFW2-4. In the exchanger REC-HT1, RECYCLE2 is heated from 40°C to 100°C at 70 atm, while BFW2-4 is cooled from 140°C to 93°C at 1 atm. In the process, BFW2-4 is also completely cooled from vapour to liquid.

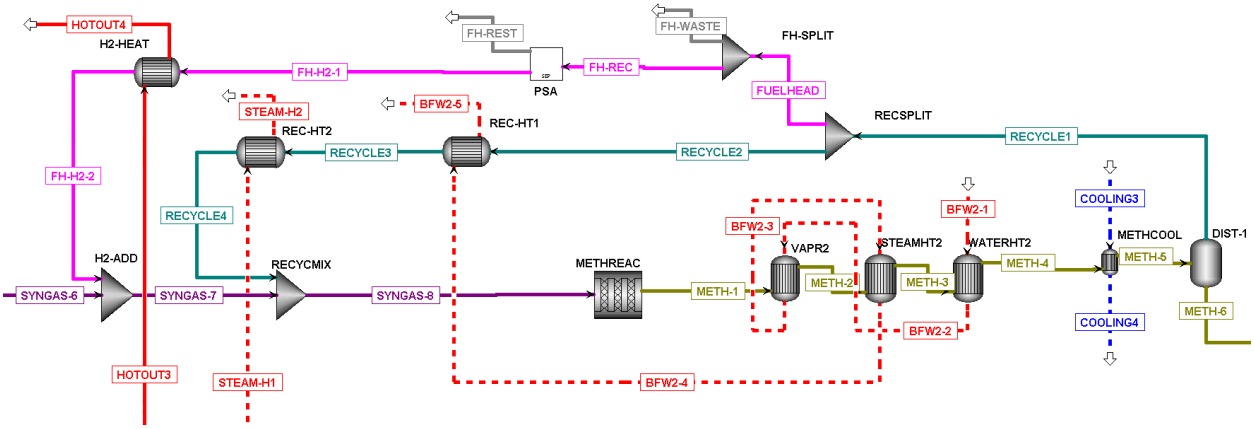

Figure 4.15 Hydrogen recycle heat integration.

In the second recycle heat exchanger (REC-HT2) the recycle stream (RECYCLE3) is heated from 100°C to 230°C at 70 atm. At the same time, the steam from the post-ATR cooling section (STEAM-H1) is cooled from 380°C to 116°C at 35 atm. It is also cooled completely from vapour to liquid.

The hydrogen recycle stream is heated using the remaining hot stream from the fired heater (HOTOUT3). In the exchanger H2-HEAT, the hydrogen recycle stream is heated from 40°C to 230°C at 1 atm. At the same time, HOTOUT3 is cooled from 431°C to 129°C at 1 atm.

4.4 CO_2 Capture

A simplified version of the amine reboiler in the stripper column of a MEA-based post-combustion CO_2 capture unit was simulated in this work. This section will describe the testing to determine the overall CO_2 capture requirements and the amine reboiler steam generator simulation results.

4.4.1 CO_2 Emitted by the Methanol Process

In order to determine the requirements of a CO_2 capture method, the amount of CO_2 to be captured must first be determined. There are three sources of CO_2 in this process: the CO_2 feedstock from the nearby plant, the natural gas combustion products in the pre-reforming fired heater, and the natural gas combustion products from the steam generator that heats the amine reboiler in the CO_2 capture unit.

The first two sources produce a known amount of CO_2. The third source is from the CO_2 capture unit itself. Since the amine reboiler of the CO_2 capture unit is heated by burning natural gas, it emits CO_2. The more CO_2 that needs to be captured, the more natural gas that needs to be burned in order to heat the amine reboiler. As more natural gas is burned, the overall CO_2 emissions increases. As the CO_2 emissions increase, more natural gas must be burned, and so on. This is a loop that needs to be iterated upon until it converges at a point where the CO_2 capture unit is able to sufficiently capture all CO_2 emissions, including its own. This iteration loop is shown in Figure 4.16.

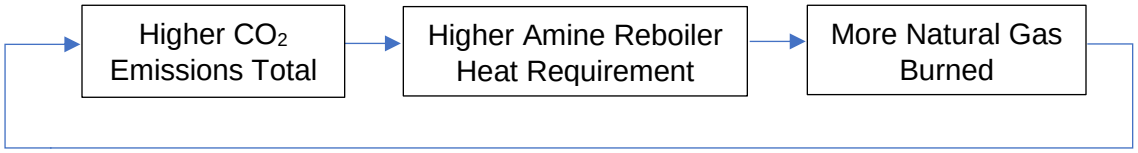

Figure 4.16 Amine reboiler steam generator iteration loop.

The three sources of CO_2 emissions are described in Table 4.10.

Table 4.10 CO_2 emissions per CO_2 source.

Source of CO_2 Emission	**Amount of CO_2 Emission (kmol/hr)**
Nearby plant CO_2	58.2
Fired heater	18
Amine reboiler steam generator	To be determined

4.4.2 Amine Reboiler Steam Generator

Iterative simulations were needed to determine the requirements of the steam generator that heats the amine reboiler. Simulation of an entire post-combustion MEA-based CO_2 capture system was outside the scope of this work, and was not required (except eventually to assess total economics). Instead, a very basic simulation of a reboiler in the stripper column of a CO_2 capture unit was done in Aspen, shown in Figure 4.17.

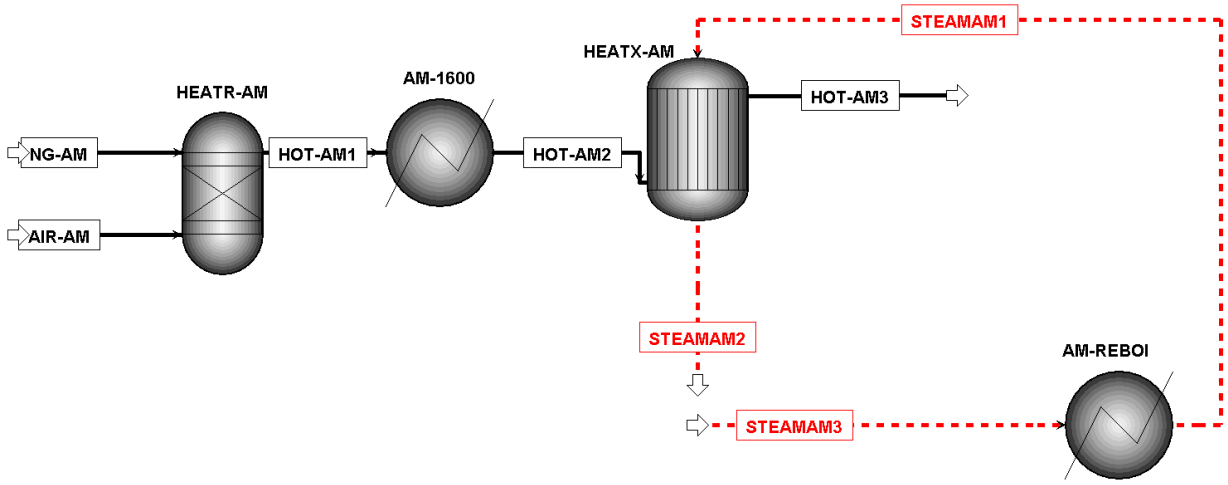

Figure 4.17 Amine reboiler and steam generator simulation in Aspen Plus.

A heat exchanger was created to represent the amine reboiler (AM-REBOI). A natural gas combustor (HEATR-AM) was also created to burn natural gas, which was then fed to an exchanger (HEATX-AM) where the boiler feed water was heated into steam. This steam is what was used to heat the amine reboiler. The CO_2 emitted from the natural gas combustion is what needed to be considered in the iterative simulation. This CO_2 quantity was checked at the stream HOT-AM3.

In terms of design specifics, the steam in the steam loop represented by the red dotted stream lines (STEAMAM1, STEAMAM2, and STEAMAM3) was heated to 130°C and 1 atm via HEATX-AM, and then cooled via AM-REBOI to 120°C and 1 atm. This was chosen to replicate the process of steam heating in an amine reboiler. Additionally, the hot stream from the natural gas combustor (HOT-AM1) was capped at 1600°C using the heater AM-1600.

One unknown was the heating requirement of the reboiler in terms of the amount of CO_2 captured. In literature, the heat duty requirement of an amine reboiler in a large-scale MEA-based CO_2 capture plant was determined on a basis of kilowatts of heat duty per kilomoles of CO_2 captured. This would effectively be a conversion rate: input the CO_2 capture requirement in kmol/hr, and it produced the reboiler heat duty in kW. This conversion rate was found from literature, described in Table 4.11.

Table 4.11 CO_2 capture to heat duty conversion rates found from literature.

Source	CO_2 Capture to Heat Duty Conversion Rate (kWh/kmol of CO_2 captured)
Manaf et al., 2015 [36]	-49
He, 2017 [37]	-62
Nittaya et al., 2014 [38]	-50

The heat duty requirement chosen was from Manaf et al.: -49 kWh/kmol of CO_2 captured. This number allows for a given CO_2 capture requirement to be easily converted into a heat duty requirement for the amine reboiler.

This conversion rate was applied to the kmol/hr CO_2 emissions from the two constant sources of CO_2 emissions in this process (see Table 4.10). An assumption of 90% CO_2 recovery was applied, so this number was also multiplied by 0.9. This resulted in a single heat duty requirement needed to capture the CO_2 emissions from the feedstock to the ATR and the fired heater.

$$Feed\ to\ ATR\ CO_2 + Fired\ heater\ CO_2 = Total\ initial\ CO_2\ emission$$

$$58.2\ kmol/hr\ + 18\ kmol/hr\ = 76.2\ kmol/hr\ CO_2\ emissions \qquad \text{Equation 4.2}$$

$$Conversion\ rate \times Total\ inital\ CO_2\ emissions \times 90\%\ CO_2\ recovery = Heat\ duty\ requirement$$

$$\frac{-49\ kW}{kmol/hr} \times 76.2\ kmol/hr\ \times 0.9 = -3{,}360\ kW\ Heat\ duty \qquad \text{Equation 4.3}$$

A design specification was programmed to change the flow rate of steam in the stream STEAMAM3 until the heat duty of AM-REBOI reached the desired amine reboiler heat duty. For the first iteration, that desired heat duty was -3,360 kW. A second design specification was programmed to change the flow rate of natural gas in the stream NG-AM until the outlet hot stream of HEATX-AM, labelled HOT-AM3, reached the exit temperature of 280°C. This temperature was chosen because it was sufficiently low to ensure effective heat exchange, while not too low so as to cause any state change in the hot stream. A third design specification changed the flow rate of the air inlet stream, AIR-AM, so that the combined natural gas and air stream would have an oxygen mole fraction of 3% (approximately 18% excess air).

For the first iteration, the heat duty in the amine reboiler is set to -3,360 kW. From this, the first design specification determines the amount of steam needed to reach that heat duty. Then, the second design specification determines the amount of natural gas needed to heat that amount of steam. The third design specification then determines the amount of air input. Recall that this first iteration does not include the CO_2 produced from the stream HOT-AM3 in this very process. From here, the CO_2 emitted in HOT-AM3 is then added to the total CO_2 emissions. Now that the total CO_2 emissions is larger, the amine reboiler heat duty requirement increases. This new amine reboiler heat duty is calculated from the conversion rate from literature and input into ASPEN. From here, the process repeats. This iteration loop is illustrated in Figure 4.16.

This iteration loop eventually converges at a point where the CO_2 capture process is able to capture all of the CO_2 emitted from all three emission sources in the overall process. The results of this are shown in Table 4.12.

Table 4.12 Final CO_2 capture iteration results.

Amine boiler heat duty requirement	-4,564 kW
Steam input requirement	47,603 kmol/hr
CO_2 emitted from HOT-AM3	27.3 kmol/hr

This completes Table 4.10 from earlier. Table 4.13 is the completed table.

Table 4.13 Total CO_2 captured.

Source of CO_2	**Amount of CO_2 (kmol/hr)**
Feedstock to ATR	58.2
Fired heater	18
Amine reboiler steam generator	27.3
Total CO_2 captured	103.5

These results can be confirmed using the conversion factor found from literature.

$$Conversion\ rate \times Total\ inital\ CO_2\ emissions \times 90\%\ CO_2\ recovery = Heat\ duty\ requirement$$

$$\frac{-49\ kW}{kmol/hr} \times 103.5\ kmol/hr\ \times 0.9 = -4{,}564\ kW\ Heat\ duty$$

-4,564 kW was also the heat duty requirement at the start of this iteration (see Table 4.12), meaning that no further steam and natural gas is required to capture the total CO_2 emissions from the process.

4.4.3 Reboiler Steam Requirement

Table 4.12 shows that the steam required to heat the amine reboiler is 47,603 kmol/hr at 130°C and 1 atm. Table 4.9 shows the flowrates of the hot streams that could be used to help meet this steam requirement. Table 4.14 compares the requirement to the hot stream availability.

Table 4.14 Remaining hot streams vs. reboiler steam requirement.

Stream Name	**Temperature (°C)**	**Pressure (atm)**	**Flowrate (kmol/hr)**
STEAM-H2	243	35	461
BFW2-4	140	1	250
HOTOUT3	431	1	219
Reboiler steam requirement	140	1	47,603

From this table, it is clear that the reboiler steam requirement is much greater than the heat that the process itself can provide. For this reason, heat integration was not applied to the CO_2 capture unit.

4.4.4 CO_2 Solutions Capture Unit Simulation

The company CO_2 Solutions (CO2Solutions.com) has developed a method of CO_2 capture using an enzyme-based solvent that requires approximately 50% less heat duty for the amine reboiler than the conventional amine process. This was simulated using the same process that was applied to the conventional MEA-based post-combustion CO_2 capture, but the conversion factor from CO_2 capture requirement to heat duty was lowered by 50% from 49 to 24.5. The results of this simulation are shown in Table 4.15.

Table 4.15 CO_2 Solutions capture results.

Heat duty requirement	-1,936 kW
Steam input requirement	20,193 kmol/hr
CO_2 emitted from HOT-AM3	11.6 kmol/hr

When compared to the traditional results in Table 4.12, there is a 57.6% reduction in required heat duty, a 57.6% reduction in steam input requirement, and a 57.6% reduction in CO_2 emitted from the steam generator. Given these results, this is a promising method of capturing CO_2.

Chapter 5: Economic Evaluation

This section looks at the economics of the process. The first section looks into the evaluation of the overall cost of the initial process compared to a process with added hydrogen recycle. The second section looks into maintenance shutdown for the electrolyser based on hourly electricity pricing.

5.1 Capital and Operating Cost Comparison with and without PSA Hydrogen Recycling

Section 4.2.2 detailed how large amounts of hydrogen were being emitted as waste. Given that hydrogen is a valuable feedstock to the methanol process, a method of capturing and recycling hydrogen was researched and simulated. It involved recycling hydrogen using a pressure swing adsorption (PSA) unit in order to produce more methanol. This section looks at the economics of the process without hydrogen recycling and with hydrogen recycling.

There are two available scenarios when it comes to hydrogen recycling:

Scenario 1: No pressure hydrogen recycling (base case).
Scenario 2: PSA hydrogen recycling.

Both scenarios were simulated in Aspen. The final amounts of methanol produced for both scenarios are shown in Table 5.1. This shows that scenario 1 produces less overall methanol, and that scenario 2 produces more methanol, but at the cost of installing and operating the hydrogen recycle unit.

Table 5.1 Simulation results with and without hydrogen recycling.

	Methanol output (kmol/hr)	**Methanol output (MTPD)**
1. No hydrogen recycle	282	217
2. PSA hydrogen recycle	324	249

The overall capital (CAPEX) and operating (OPEX) costs of both scenarios will be calculated and compared in this section. All costs were calculated in Canadian Dollars (CAD) per metric tonne (MT) of methanol produced (MeOH), or CAD/MT MeOH. Some key economic parameters are listed in Table 5.2.

Table 5.2 Key economic parameters.

Parameter	Value	Unit
Plant lifetime	20	Years
Discount rate	7.5	%
Operating days per year	354	Days/year
Operating hours per day	24	Hours/day
Operating hours per year	8,496	Hours/year
Dollars year	2019	Year
Price of natural gas	$3.50	CAD/MMBTU HHV
Price of electricity	$0.033	CAD/kWh
Price of water	$0.25	CAD/m^3

5.1.1 CAPEX of Scenario 1

This section looks at the CAPEX of scenario 1, the initial process design without hydrogen recycling. The CAPEX of this process is made up of three components. They are the CO_2 capture unit CAPEX, the electrolyser CAPEX, and the CAPEX of the rest of the plant.

First the CO_2 capture unit was calculated based on literature [39]. The CAPEX value was scaled using the CO_2 feeds of both capture plants and a scaling exponent factor of 0.6. Additionally, the CAPEX was converted from 2001 USD to 2019 CAD using an inflation calculator [40], and an exchange rate of 1.34 CAD/USD.

The CAPEX values for the electrolyser and the rest of the plant were taken from internal AChT documents. Table 5.3 shows the total CAPEX for scenario 1.

Table 5.3 Scenario 1 CAPEX values.

CAPEX	Value	Unit
Electrolyser CAPEX	$38.00	CAD million
Other CAPEX	$149.00	CAD million
CO_2 capture CAPEX	$12.99	CAD million
Total CAPEX	**$199.99**	**CAD million**

These values were annualized using the plant lifetime and discount rate shown in Table 5.2. The results are shown in Table 5.4.

Table 5.4 Scenario 1 annualized CAPEX values.

CAPEX	Value	Unit
Electrolyser CAPEX	$3,730,000	CAD/year
Other CAPEX	$14,600,000	CAD/year
CO2 CAPEX	$1,270,000	CAD/year
Total CAPEX	**$19,600,000**	**CAD/year**

These were then converted into cost of methanol rates using the methanol production rate for this scenario (217 MTPD of methanol). This is shown in Table 5.5.

Table 5.5 Scenario 1 CAPEX cost of methanol values.

CAPEX	**Value**	**Unit**
Electrolyser CAPEX	$47	CAD/MT MeOH
Other CAPEX	$185	CAD/MT MeOH
CO2 CAPEX	$16	CAD/MT MeOH
Total CAPEX	**$248**	**CAD/MT MeOH**

5.1.2 OPEX of Scenario 1

The OPEX was composed of four costs. They were natural gas costs, electricity costs, electrolyser water costs, and miscellaneous costs.

Natural gas is input at three points in the process: as a feed to the ATR (NG-FEED1 at 132°C and 35 atm), as a feed to the fired heater (NG-FIRE at 30°C and 1 atm), and as a feed to the amine reboiler (NG-AM at 30°C and 1 atm). From the simulation, the total flow of these streams was found, shown in Table 5.6. The cost of natural gas used was $3.50 CAD/MMBTU HHV of natural gas.

Table 5.6 Scenario 1 natural gas cost.

Natural Gas Stream	**Flowrate (L/hr)**	**Flowrate (HHV MMBTU/hr)**	**Flowrate (HHV MMBTU/MT MeOH)**	**Cost (CAD/MT MeOH)**
NG-FEED1	252,410	230	25.5	$89
NG-FIRE	447,676	15.6	1.7	$7
NG-AM	668,169	23.9	2.7	$9
Total		**269.5**	**29.9**	**$105**

From Table 5.6, the final natural gas cost in terms of methanol production was $105 CAD/MT MeOH.

The electricity costs are further broken into three components: syngas compressor electricity, CO_2 compressor electricity, and electrolyser electricity. From the Aspen simulation, the work required at the syngas compressor (MULTI-SG) and the CO_2 compressor (MULTICO2) was found. The electricity requirement for the electrolyser was found using internal AChT research. This is all shown in Table 5.7. The price of electricity used was $0.033 CAD/kWh.

Table 5.7 Scenario 1 cost of electricity.

Component	Power requirement (MW)	Power requirement (kWh/MT MeOH)	Electricity Cost (CAD/MT MeOH)
Syngas compressor	1.17	130	$4
CO_2 compressor	0.393	43.6	$1
Electrolyser	31.6	3,495	$116
Total	**33.2**	**3,669**	**$121**

From Table 5.7, the final cost of electricity in terms of methanol production was $121 CAD/MT MeOH.

From the Aspen simulation, the flowrate of water to the electrolyser (stream name H2O) was 5.22 m^3/hr. In terms of methanol production, it was 0.579 m^3/MT MeOH. The cost of water used was $0.25 CAD/$m^3$, based on internal AChT research. This is shown in Table 5.8.

Table 5.8 Scenario 1 cost of water to electrolyser.

Component	Flowrate (m^3/MT MeOH)	Cost (CAD/MT MeOH)
Water to electrolyser	0.579	$0.14

From Table 5.8, the cost of water to the electrolyser was found to be $0.14 CAD/MT MeOH.

The miscellaneous costs included other estimated expenses, personnel, plant maintenance, and electrolyser maintenance. Other estimated expenses and personnel costs were estimated. Maintenance of the plant was estimated at 1.5% of plant CAPEX (total CAPEX without the electrolyser) per year. Maintenance of the electrolyser was estimated at 3% of electrolyser CAPEX per year. The estimation results of all miscellaneous costs are shown in Table 5.9.

Table 5.9 Scenario 1 miscellaneous costs.

Component	Cost (CAD/MT MeOH)
Other expenses	$7
Personnel	$20
Plant maintenance	$32
Electrolyser maintenance	$15
Total	**$74**

From Table 5.9, the total miscellaneous costs were estimated to be $74 CAD/MT MeOH.

With all components of the OPEX calculated, the total OPEX is shown in Table 5.10.

Table 5.10 Scenario 1 total OPEX.

OPEX Component	Cost (CAD/MT MeOH)
Natural gas	$105
Electricity	$121
Water to electrolyser	$0.14
Miscellaneous	$74
Total OPEX	**$300**

5.1.3 Total Scenario 1 Costs

The total CAPEX and OPEX costs for scenario 1 are shown in Table 5.11.

Table 5.11 Scenario 1 total costs.

Component	**Cost (CAD/MT MeOH)**
CAPEX	$248
OPEX	$300
Total	**$548**

From Table 5.11, the total combined CAPEX and OPEX cost in terms of methanol production is $548. For reference, the methanol manufacturing company Methanex lists their 2019 sell price of methanol at $579 CAD/MT MeOH [41]. If sold at that price, scenario 1 would profit at a rate of $31 CAD/MT MeOH based on this work.

5.1.4 CAPEX of Scenario 2

The CAPEX of scenario 2 is the same as scenario 1, except for two differences: the methanol production is higher, and the CAPEX of the PSA unit is included.

As shown in Table 5.1, the simulation results of both scenarios show the methanol production increasing from 217 MTPD in scenario 1, to 249 MTPD in scenario 2. As all final costs in this section are in terms of MT of methanol produced, this change in methanol production will affect all costs that are brought over from scenario 1 to scenario 2.

A study of literature was done to determine the CAPEX of the PSA hydrogen recycle unit [42] [43] [44]. From this, the CAPEX was found to be approximately $6.50 million CAD. Using a 20-year plant life and a 7.5% discount rate, this was annualized to $637,600 CAD/year. In terms of methanol production, the PSA CAPEX was found to be $7 CAD/MT MeOH. The capital costs found for scenario 1 were put in terms of the new methanol production rate for scenario 2 and added along with the PSA CAPEX. This is shown in Table 5.12.

Table 5.12 Scenario 2 CAPEX.

CAPEX	**Value**	**Unit**
Electrolyser CAPEX	$41	CAD/MT MeOH
Other CAPEX	$161	CAD/MT MeOH
CO2 CAPEX	$14	CAD/MT MeOH
PSA CAPEX	$7	CAD/MT MeOH
Total CAPEX	**$223**	**CAD/MT MeOH**

From Table 5.12, the total CAPEX for scenario 2 was found to be $223 CAD/MT MeOH.

5.1.5 OPEX of Scenario 2

The OPEX of scenario 2 is the same as the OPEX of scenario 1, except for two main changes. First, the costs are all in terms of the new, higher methanol production rate. Instead of producing 217 MTPD, scenario 2 produces 249 MTPD. As mentioned previously, this changes all costs brought over from scenario 1. Second, the operating cost of the PSA hydrogen recycle unit is included.

The PSA OPEX was found through literature [42] [43] [44]. It was found to be approximately $1,910 CAD/year. When put in terms of the methanol production rate for scenario 2, it was found to be $0.02 CAD/MT MeOH. To note, this is fairly negligible when compared to the other OPEX requirements. Table 5.13 shows this incorporated to the total OPEX for scenario 2.

Table 5.13 Scenario 2 OPEX

OPEX Component	**Cost (CAD/MT MeOH)**
Natural gas	$91
Electricity	$120
Water to electrolyser	$0.13
Miscellaneous	$69
PSA hydrogen recycle	$0.02
Total OPEX	**$280**

From Table 5.13, the total OPEX for scenario 2 was found to be $280.

5.1.6 Total Scenario 2 Costs

The total CAPEX and OPEX costs for scenario 2 are shown in Table 5.14.

Table 5.14 Scenario 2 total costs.

Component	**Cost (CAD/MT MeOH)**
CAPEX	$223
OPEX	$280
Total	**$503**

From Table 5.14, the total combined CAPEX and OPEX cost in terms of methanol production is $503. As mentioned before, the methanol manufacturing company Methanex lists their 2019 sell price of methanol at $579 CAD/MT MeOH [41]. If sold at that price, scenario 2 would profit at a rate of $76 CAD/MT MeOH based on this work.

5.1.7 Scenario 1 and 2 Comparison

Table 5.15 shows the comparison of the scenario 1 and 2 total costs. Profit is based off of Methanex's 2019 sell price of methanol of $579/MT MeOH [41].

Table 5.15 Scenarios 1 and 2 total cost comparison.

Component	**Scenario 1 Costs (CAD/MT MeOH)**	**Scenario 2 Costs (CAD/MT MeOH)**
CAPEX	$248	$223
OPEX	$300	$280
Total Cost	**$548**	**$503**
Profit	**$31**	**$76**

Table 5.15 shows that the total costs of scenario 2 are less than that of scenario 1, and the profit margin is greater in scenario 2 over scenario 1. Scenario 2 costs 8.2% less overall than scenario 1, and scenario 2 makes 2.5 times the profit of scenario 1.

These results indicate that the PSA hydrogen recycle system makes enough added methanol to make up for its added installed and operating costs. The hydrogen recycle system shown in scenario 2 is therefore a good investment.

5.2 Payback Period

The payback period of a project is an estimate of how long it will take for the project to recoup its initial costs with an assumed interest rate of zero [45]. It is calculated using the equation shown below [45].

$$Payback\ period = \frac{Initial\ costs}{Annual\ profit} \qquad Equation\ 5.1$$

For both scenario 1 and scenario 2, the payback period was calculated using the CAPEX as the initial costs. For the annual profit, the yearly OPEX cost was subtracted from the annual revenue based on the yearly methanol output and Methanex's 2019 sell price of methanol ($579/MT) [41].

5.2.1 Scenario 1 Payback Period

For scenario 1, the payback period calculation is shown in Table 5.16. The annual profit is calculated as the difference between the revenue and the OPEX. From there, the payback period is calculated based on Equation 5.1.

Table 5.16 Scenario 1 payback period calculation.

Component	**Value**	**Unit**
CAPEX (Initial Costs)	$200	Million CAD
OPEX	$23.0	Million CAD/year
Revenue	$44.4	Million CAD/year
Annual Profit	$21.4	Million CAD/year
Payback Period	**9.35**	**years**

5.2.2 Scenario 2 Payback Period

For scenario 2, the payback period calculation is shown in Table 5.17. The annual profit is calculated as the difference between the revenue and the OPEX. From there, the payback period is calculated based on Equation 5.1.

Table 5.17 Scenario 2 payback period calculation.

Component	**Value**	**Unit**
CAPEX (Initial Costs)	$206	Million CAD
OPEX	$24.8	Million CAD/year
Revenue	$51.1	Million CAD/year
Annual Profit	$26.3	Million CAD/year
Payback Period	**7.83**	**years**

5.2.3 Payback Period Comparison

For scenario 1, the payback period was found to be 9.35 years. For scenario 2, the payback period was found to be 7.83 years. Based on the overall project lifetime of 20 years, and the fact that a smaller payback period is more desirable, it is clear that scenario 2 is the better investment when it comes to payback period.

5.3 Internal Rate of Return

Internal rate of return (IRR) is an indicator used to show the expected returns on an investment in terms of an interest rate [45]. The IRR is the interest rate at which the project breaks exactly even [45]. It is calculated by solving the following equation for i* using trial and error [45].

$$\sum_{t=0}^{T} \frac{(R_t - D_t)}{(1 + i^*)^t} = 0 \qquad Equation\ 5.2$$

Where

- R_t is the cash inflow in period t
- D_t is the cash outflow in period t
- T is the number of time periods
- i* is the internal rate of return (IRR)

For both scenario 1 and scenario 2, the IRR was calculated using two methods: first, by hand using interest factor tables from Fraser et. Al [45] and linear interpolation; second, using the IRR function in Microsoft Excel. These results are shown in Table 5.18.

Table 5.18 IRR calculations for scenarios 1 and 2.

Scenario	IRR (By Hand)	IRR (From Excel)
Scenario 1	8.43%	8.65%
Scenario 2	11.1%	11.2%

Based on these results, it is clear that scenario 2 has a greater IRR than scenario 1. Since a greater IRR is desired, scenario 2 is more economically viable based on this indicator.

5.4 Sensitivity Analysis

In order to determine the sensitivity of the CAPEX and OPEX to each individual pricing component, a sensitivity analysis was done for both scenario 1 and scenario 2. This was conducted by adjusting each cost component by a range of +/- 50% and calculating the new resultant CAPEX or OPEX. When compared on a graph, the cost components that more heavily impacted the CAPEX or OPEX would be displayed with a steeper slope than those components that did not impact the CAPEX or OPEX as heavily.

For scenario 1, the CAPEX components were the electrolyser CAPEX, the “other” CAPEX, and the CO_2 capture CAPEX. The OPEX components were the natural gas price, the electricity price, and the water price.

For scenario 2, the cost components were the same as scenario 1, but there was also a PSA cost added to both the CAPEX and the OPEX.

5.4.1 Scenario 1 Sensitivity Analysis

When each component of the CAPEX and OPEX for scenario 1 were adjusted at a range of +/- 50%, the results of the impact on the CAPEX and OPEX are shown in figures 5.1 and 5.2.

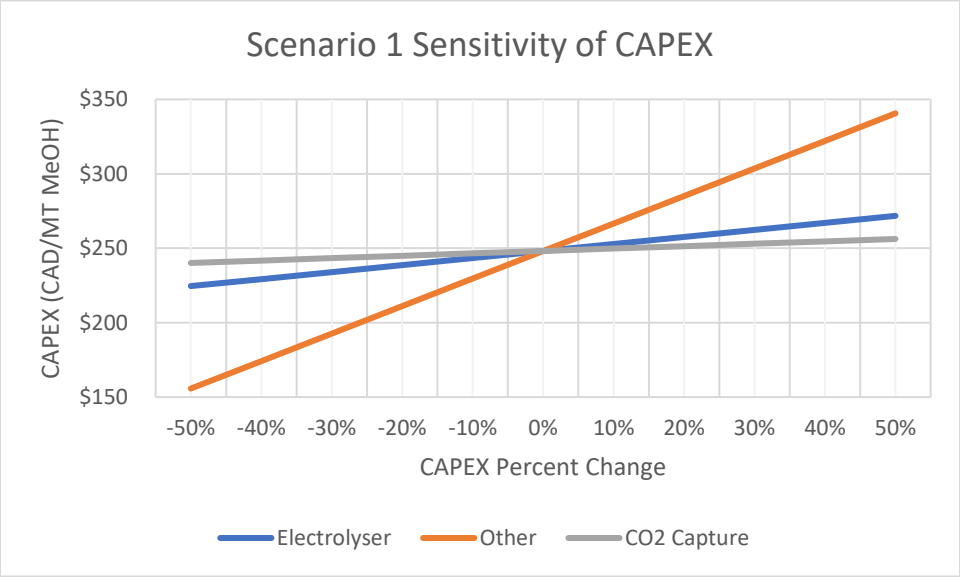

Figure 5.1 Scenario 1 sensitivity of CAPEX.

This shows that the scenario 1 CAPEX is highly dependent on the other CAPEX, while being only somewhat sensitive to the CAPEX of the electrolyser and CO_2 capture system.

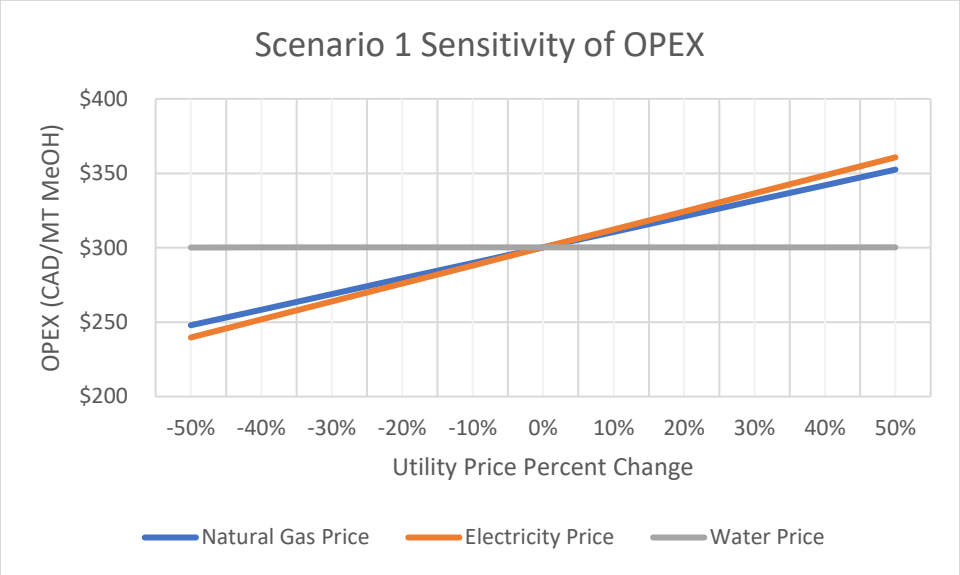

Figure 5.2 Scenario 1 sensitivity of OPEX.

This shows that the scenario 1 OPEX is highly sensitive to both the natural gas price and the electricity price, while being essentially nonreactive to the change in the water price.

5.4.1 Scenario 2 Sensitivity Analysis

When each component of the CAPEX and OPEX for scenario 2 were adjusted at a range of +/- 50%, the results of the impact on the CAPEX and OPEX are shown in figures 5.3 and 5.4.

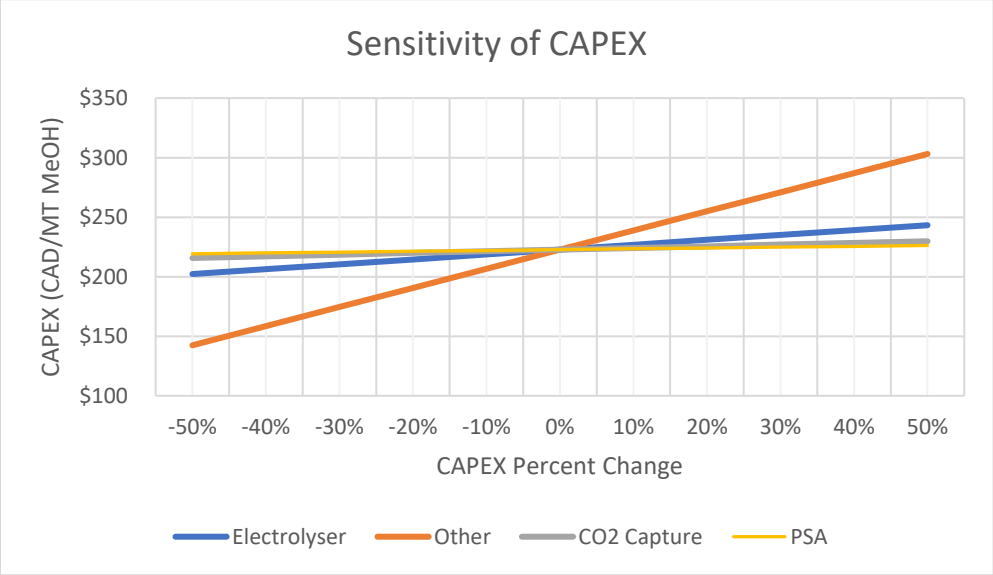

Figure 5.3 Scenario 2 sensitivity of CAPEX.

This shows that in scenario 2, the CAPEX is highly sensitive to a change in the “other” CAPEX. It is less sensitive to a change in the electrolyser CAPEX, while being nearly unaffected by a change in the CO_2 capture and PSA CAPEX.

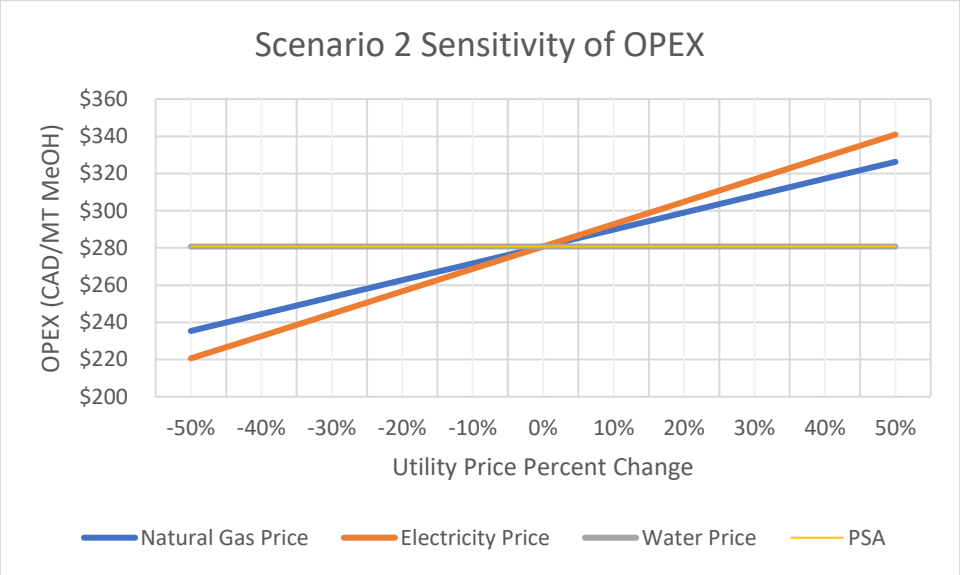

Figure 5.4 Scenario 2 sensitivity of OPEX.

This shows that the scenario 2 OPEX is highly sensitive to changes in both the natural gas price and the cost of electricity. It also shows that it is nearly unaffected by changes to the water price or cost of operating the PSA.

5.5 Electrolyser Shutdown

The plant is scheduled to operate 354 days per year, meaning there is a scheduled 11-day consecutive shutdown every year. When the plant is shut down, no electricity is consumed. Table 5.7 shows that over 95% of the electricity costs in the plant come from the electrolyser, so shutdown should be planned around the needs of the electrolyser. With hourly pricing data, the 11-day shutdown can be planned to avoid the greatest electricity cost.

The OPEX costs in section 5.1 were calculated using an estimated electricity price of $0.033/kWh, however, in practice the price of electricity varies from hour to hour. The Hourly Ontario Electricity Price (HOEP) data for Ontario in 2018 was obtained from the Independent Electricity System Operator (IESO) [46]. Using this data, the average HOEP of every consecutive 11-day period in 2018 was calculated. This is graphed in Figure 5.5.

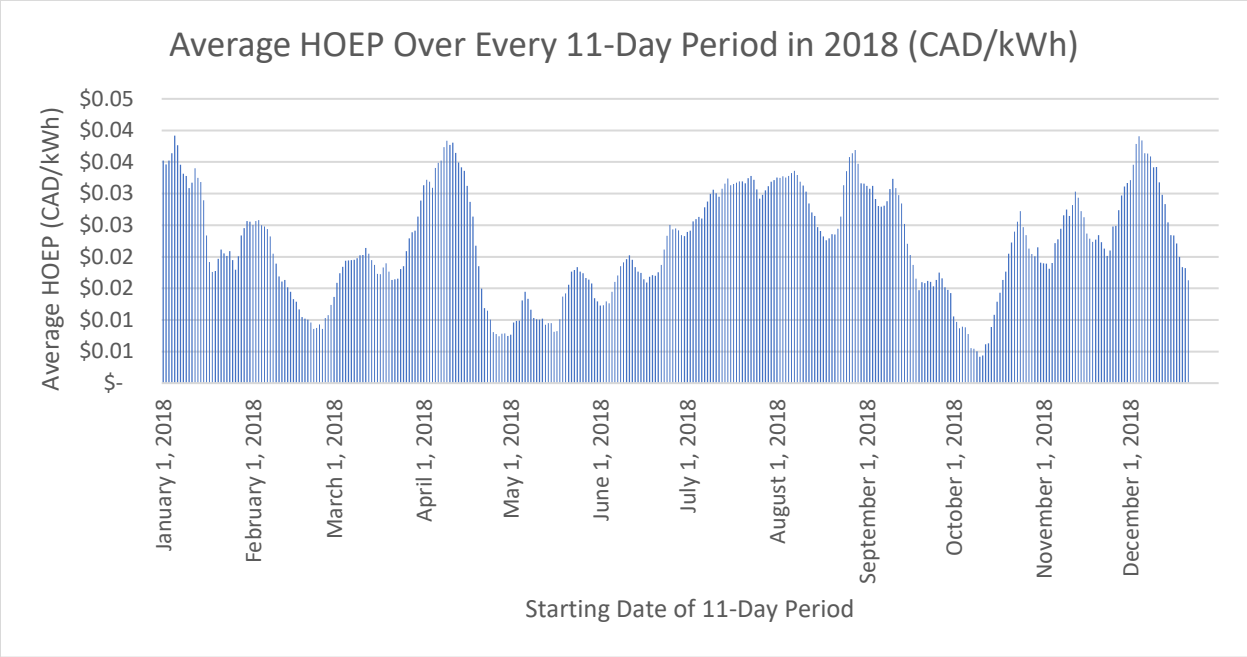

Figure 5.5 Average HOEP of every consecutive 11-day period in 2018.

From Figure 5.5, the consecutive 11-day period that had the highest average HOEP in 2018 started on January 5th. Peaks also occurred starting on December 4th, December 5th, April 9th, and April 11th. Based on this data, it would be best to begin the 11-day shutdown on one of those days.

Chapter 6: Conclusions and Recommendations

6.1 Conclusions

The AChT Green Methanol Process was simulated in Aspen Plus. The syngas production method was changed over from POX to ATR, the heat in the system was successfully integrated, and an economic analysis was done.

Work was also completed on simulating the CO_2 capture heat requirement of the process, which was found to be -4,564 kW of heat duty in the amine reboiler. This amounted to a requirement of 47,603 kmol/hr of steam at 130°C and 1 atm to heat the amine reboiler. It was also found that through heat integration, the process itself generated a far lower amount of steam than the reboiler requirement, indicating that a dedicated natural gas combustor would be needed to generate the heat for the CO_2 capture amine reboiler.

An economic analysis was done of two design scenarios: the original methanol process (scenario 1), and the same process with a PSA hydrogen recycle unit added (scenario 2). According to the Aspen Plus simulations, scenario 1 produced 217 MTPD of methanol, and scenario 2 produced 249 MTPD of methanol.

For scenario 1, the overall CAPEX was found to be $248 CAD/MT MeOH and the overall OPEX was found to be $300 CAD/MT MeOH. The total cost for scenario 1 was, therefore, $548 CAD/MT MeOH.

For scenario 2, the overall CAPEX was found to be $223 CAD/MT MeOH and the overall OPEX was found to be $280 CAD/MT MeOH. The total cost for scenario 2 was therefore $503.

When compared to the 2019 sell price of methanol of $579 CAD/MT MeOH, the profit from scenario 1 was $31, while the profit from scenario 2 was $76. It was, therefore, determined that the PSA hydrogen recycle unit applied to scenario 2 was a good investment.

Additionally, a plan was developed for shutting down the plant during 11 consecutive maintenance days. Using the Ontario hourly electricity pricing data from 2018, the most expensive 11-day period was found to start on January 5th. It was therefore recommended that the shutdown start on that day.

6.2 Recommendations

Some recommendations for future work on this process:

- Develop different methanol reactor kinetics, that takes into account the large amount of CO_2 involved. The kinetics used in the methanol reactor here are based on conventional syngas composition which contains significantly less CO_2. This would involve experimental verification, and possibly develop alternative kinetics parameters.

- Optimize the amount of CO_2 that is sent directly to the ATR vs. bypassed the ATR. It was found that bypassing the ATR with more CO_2 lowered the amount of methanol output, but also lowered the ATR heat duty. An optimization study could be done to determine if the extra methanol made from not bypassing the ATR with the CO_2 feed was worth having to heat the ATR by burning natural gas in order to make up for the increased heat duty.

- Further develop the electricity pricing plan, specifically with regards to the electrolyser. Based on existing HOEP data, a future study could estimate the most economically advantageous times each year to shut down the electrolyser on a programmed schedule, beyond scheduled maintenance days.

References

[1] A. Alarifi, A. Elkamel and E. Croiset, Modeling, Analysis and Optimization of the Gas-Phase Methanol Synthesis Process, 2016.

[2] L. van de Water, S. Wilkinson, R. Smith and M. Watson, Understanding methanol synthesis from CO/H2 feeds over Cu/O2 catalysts, 2018.

[3] The Methanol Institute, "Methanol Price," 2019. [Online]. Available: https://www.methanol.org/methanol-price-supply-demand/. [Accessed 2 May 2019].

[4] S. A. Al-Sobhi, A. Elkamel, F. S. Erenay and M. A. Shaik, Simulation-Optimization Framework for Synthesis and Design of Natural Gas Downstream Utilization Networks, 2018.

[5] Seidel, Jorke, Vollbrecht, Seidel-Morgenstern and Kienle, Kinetic modeling of methanol synthesis from renewable resources, 2017.

[6] Lalitornasate and Croiset, Combined Catalytic Partial Oxidation and CO2 Reforming for the Green Methanol Part I: Techno-Economic Study of the Green Methanol Process Using Aspen Plus, Technologie Convergence Inc. Ontario Centre of Excellence. University of Waterloo., 2010.

[7] Aasberg-Petersen, Christensen, Dybkjaer, Sehested, Ostberg, Coertzen, Keyser and Steynberg, Fischer-Tropsch Technology Chapter 4: Synthesis gas production for FT synthesis, Haldor Topsoe, Steynberg & Dry (Editors), 2004.

[8] T. C. Inc., "Methanol Production Process". United States Patent 20040171701, 2 September 2004.

[9] Lee, Methanol Synthesis Technology, CRC Press Inc., 1990.

[10] Waugh, Methanol Synthesis, 2012.

[11] A. Abbas, D. Milani and M. T. Luu, Analysis of CO2 utilization for methanol synthesis integrated with enhanced gas recovery, 2015.

[12] Li and Jens, Low-Temperature and Low-Pressure Methanol Synthesis in the Liquid Phase Catalyzed by Copper Alkoxide Systems, 2019.

[13] C.-S. Li, G. Melaet, W. Ralston, K. An, C. Brooks, Y. Ye, Y.-S. Liu, J. Zhu, J. Guo, S. Alayoglu and G. Somorjai, High-performance hybrid oxide catalyst of manganese and cobalt for low-pressure methanol synthesis, 2014.

[14] L. Clausen, N. Houbak and B. Elmegaard, Technoeconomic analysis of a methanol plant based on gasification of biomass and electrolysis of water, 2010.

[15] Fulton and Fair, Manufacture of Methanol and Substitue Natural Gas; Preliminary Design and Economic Evaluation, St. Louis, Missouri: Corporate Engineering Department, Monsanto Company, 1974.

[16] F. G. Uctug, S. Agrali, Y. Arikan and E. Avcioglu, Deciding between carbon trading and carbon capture and sequestration: An optimisation-based case study for methanol synthesis from syngas, 2013.

[17] E. Supp, How to Produce Methanol from Coal, Springer-Verlag Berlin Heidelberg BmbH, 1990.

[18] H. Liu, Analysis of the Large Scale Centralized Hydrogen Production and the Hydrogen Demand from Fuel Cell Vehicles in Ontario, 2009.

[19] de Levie, The electrolysis of water, Department of Chemistry, Bowdoin College, Bruswick, USA, 1999.

[20] A. Alsubaie, Implementation of Power-to-Gas to Reduce Carbon Intensity and Increase Renewable Content in Liquid Petroleum Fuels, 2017.

[21] I. Vincent and D. Bessarabov, Low cost hydrogen production by anion exchange membrane electrolysis: A review, 2017.

[22] S. S. Al-Zakwani, Allocation of Hydrogen Produced via Power-to-Gas Technology to Various Power-to-Gas Pathways, 2018.

[23] P.-H. Huang, J.-K. Kuo and Z.-D. Wu, Applying small wind turbines and a photovoltaic system to facilitate electrolysis hydrogen production, 2015.

[24] S. D. Ebbesen, J. Hogh, K. A. Nielsen, J. U. Nielsen and M. Mogensen, Durable SOC stacks for production of hydrogen and synthesis gas by high temperature electrolysis, 2011.

[25] Guerra, Moura, Rodrigues, Gomes, Puna, Bordado and Santos, Synthesis gas production from water electrolysis, using the Electrocracking concept, 2017.

[26] J. Baltrusaitis and W. L. Luyben, Methane Conversion to Syngas for Gas-to-Liquids (GTL): Is Sustainable CO2 Reuse via Dry Methane Reforming (DMR) Cost Competitive with SMR and ATR Processes?, 2015.

[27] W. Maqbool and E. S. Lee, Syngas Production Process Development and Economic Evaluation for Gas-to-Liquid Applications, 2014.

[28] Chan and Wang, Carbon monoxide yield in natural gas autothermal reforming process, 2001.

[29] Hoang and Chan, Experimental investigation on the effect of natural gas composition on performance of autothermal reforming, 2006.

[30] Rau, Herrmann, Krause, Fino and Trimis, Efficiency of a pilot-plant for the autothermal reforming of biogas, 2018.

[31] Hydrogenics, "Cost Reduction Potential for Electrolyser Technology," 18 June 2018. [Online]. Available: http://europeanpowertogas.com/wp-content/uploads/2018/06/20180619_Hydrogenics_EU-P2G-Platform_for-distribution.pdf. [Accessed 9 April 2019].

[32] T. S. Christensen, Adiabatic prereforming of hydrocarbons - an important step in syngas production, 1996.

[33] N. Lieberman and E. Lieberman, A Working Guide to Process Equipment, McGraw-Hill, 1997.

[34] J. A. Delgado, M. A. Uguina, V. I. Agueda, J. L. Sotelo, P. Brea and C. A. Grande, Adsorption and Diffusion of H2, CO, CH4, and CO2 in BPL Activated Carbon and 13X Zeolite: Evaluation of Performance in Pressure Swing Adsorption Hydrogen Purification by Simulation, 2014.

[35] W. Elseviers, P. F. Hassett, J.-L. Navarre and M. Whysall, 50 Years of PSA Technology for H2 Purification, 2015.

[36] N. A. Manaf, A. Cousins, P. Feron and A. Abbas, Dynamic modelling, identification and preliminary control analysis of an amine-based post-combustion CO2 capture plant, 2015.

[37] Z. He, Modelling, Scheduling, and Control of Pilot-Scale and Commercial-Scale MEA-based CO2 Capture Plants, 2017.

[38] T. Nittaya, P. L. Douglas, E. Croiset and L. A. Ricardez-Sandoval, Dynamic modelling and control of MEA absorption processes for CO2 capture from power plants, 2013.

[39] D. J. Singh, Simulation of CO2 Capture Strategies for an Existing Coal Fired Power Plant: MEA Scrubbing versus O2/CO2 Recycle Combustion, Waterloo, Ontario, Canada, 2001.

[40] Official Data Foundation, "Inflation Calculator," 2019. [Online]. Available: http://www.in2013dollars.com/2001-dollars-in-2018. [Accessed 5 May 2019].

[41] Methanex, Methanex Methanol Price Sheet, April 29, 2019, 2019.

[42] G. Di Marcoberardino, D. Vitali, F. Spinelli, M. Binotti and G. Manzolini, Green Hydrogen Production from Raw Biogas: A Techno-Economic Investigation of Conventional Porcesses Using Pressure Swing Adsorption Unit, 2018.

[43] L. Riva, I. Martinez, M. Martini, F. Gallucci, M. van Sint Annaland and M. C. Romano, Techno-economic analysis of the Ca-Cu process integrated in hydrogen plants with CO2 capture, 2018.

[44] S. Peramanu, B. Cox and B. Pruden, Economics of hydrogen recovery processes for the purification of hydroprocessor purge and off-gases, 1999.

[45] N. M. Fraser, E. M. Jewkes, I. Bernhardt and M. Tajima, Engineering Economics in Canada Third Edition, 2006.

[46] Independent Electricity System Operator, "Hourly Ontario Energy Price (HOEP)," 2019. [Online]. Available: http://www.ieso.ca/en/Power-Data/Price-Overview/Hourly-Ontario-Energy-Price. [Accessed 1 May 2019].

[47] A. Guiliano, M. Poletto and D. Barletta, Pure hydrogen co-production by membrane technology in an IGCC power plant with carbon capture, 2018.

Appendix A: Scenario 1 ASPEN Stream Results

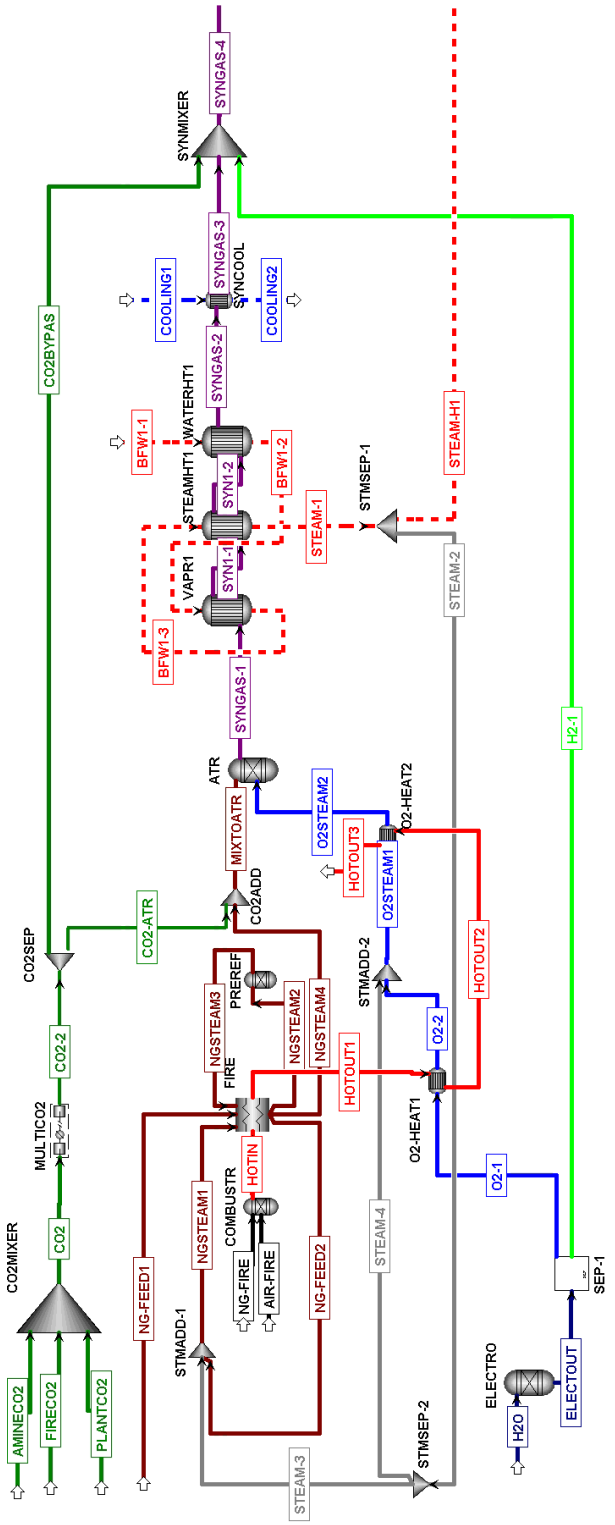

Figure A.1 Scenario 1 Aspen simulation part 1: Electrolyser and ATR section

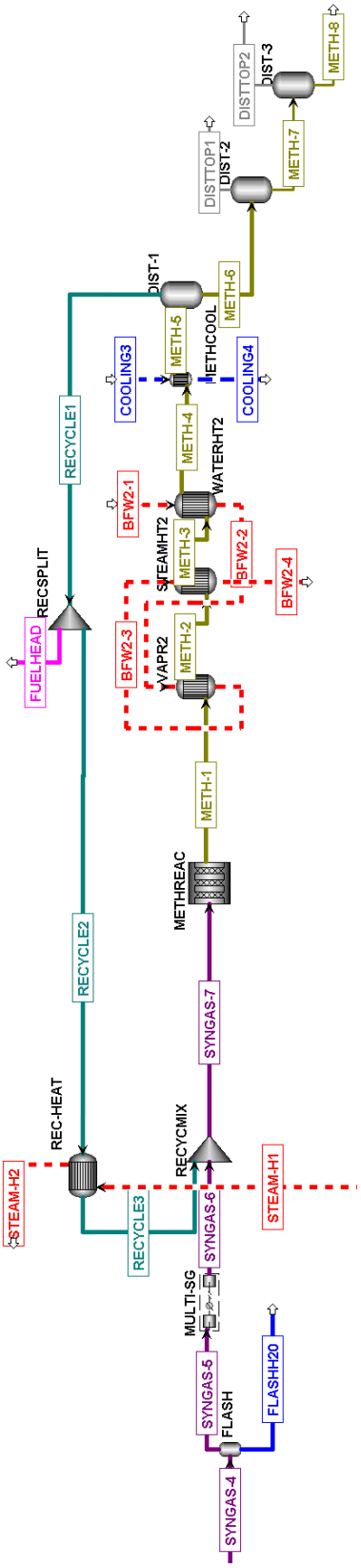

Figure A.2 Scenario 1 Aspen simulation part 2: Methanol reactor section

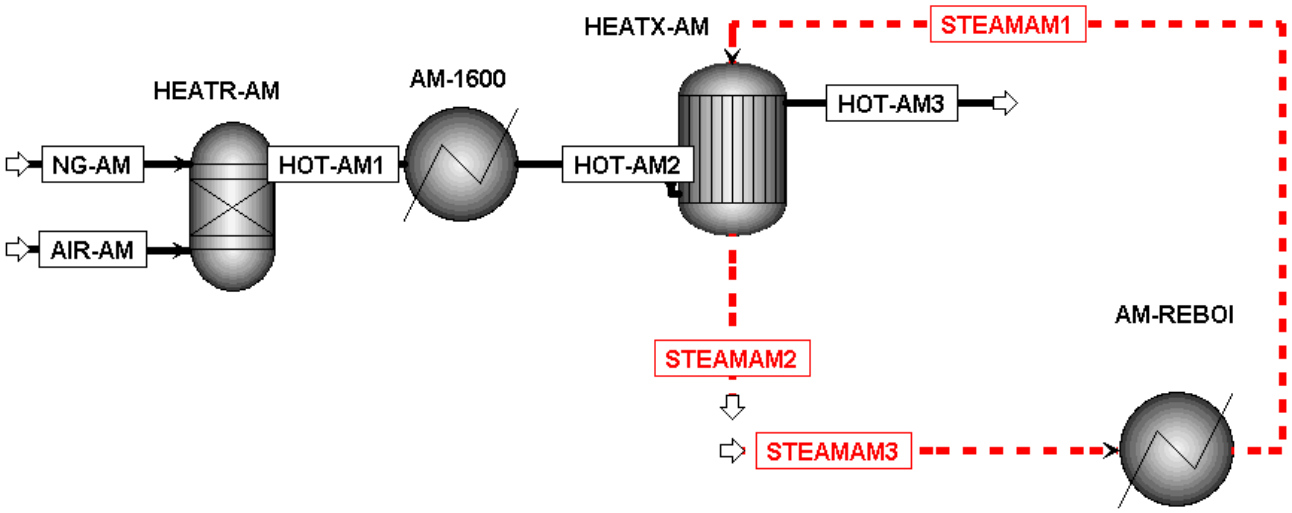

Figure A.3 Scenario 1 Aspen simulation part 3: Amine reboiler

Table A.1 Scenario 1 Aspen simulation results.

	AIR-AM	AIR-FIRE	AMINECO2	BFW1-1	BFW1-2
Mole Frac					
H2	0	0	0	0	0
CH4	0	0	0	0	0
H2O	0	0	0	1	1
CO	0	0	0	0	0
CO2	0	0	1	0	0
CH4O	0	0	0	0	0
O2	0.21152	0.21152	0	0	0
N2	0.78848	0.78848	0	0	0
C2H6	0	0	0	0	0
C3H8	0	0	0	0	0
C2H4	0	0	0	0	0
Total Flow kmol/hr	308.4558	200.2361	27.3	635	635
Temperature °C	30	30	30	121	240
Pressure atm	1	1	1	35	35
Vapor Frac	1	1	1	0	0

	BFW1-3	BFW2-1	BFW2-2	BFW2-3	BFW2-4
Mole Frac					
H2	0	0	0	0	0
CH4	0	0	0	0	0
H2O	1	1	1	1	1
CO	0	0	0	0	0
CO2	0	0	0	0	0
CH4O	0	0	0	0	0
O2	0	0	0	0	0
N2	0	0	0	0	0
C2H6	0	0	0	0	0
C3H8	0	0	0	0	0
C2H4	0	0	0	0	0
Total Flow kmol/hr	635	250	250	250	250
Temperature °C	243.3371	50	95	99.99782	140
Pressure atm	35	1	1	1	1
Vapor Frac	1	0	0	1	1

	CO2	CO2-2	CO2-ATR	CO2BYPAS	COOLING1
Mole Frac					
H2	0	0	0	0	0
CH4	0	0	0	0	0
H2O	0	0	0	0	1
CO	0	0	0	0	0
CO2	1	1	1	1	0
CH4O	0	0	0	0	0
O2	0	0	0	0	0
N2	0	0	0	0	0
C2H6	0	0	0	0	0
C3H8	0	0	0	0	0
C2H4	0	0	0	0	0
Total Flow kmol/hr	103.5	103.5	12.42	91.08	3252.038
Temperature °C	30	40	40	40	20
Pressure atm	1	35	35	35	1
Vapor Frac	1	1	1	1	0

	COOLING2	COOLING3	COOLING4	DISTTOP1	DISTTOP2
Mole Frac					
H2	0	0	0	2.33E-06	0
CH4	0	0	0	0.137291	0
H2O	1	1	1	0.009533	0
CO	0	0	0	0.041466	0
CO2	0	0	0	0.651753	0
CH4O	0	0	0	0.141156	0
O2	0	0	0	0	0
N2	0	0	0	0.018788	0
C2H6	0	0	0	4.51E-06	0
C3H8	0	0	0	3.06E-10	0
C2H4	0	0	0	6.40E-06	0
Total Flow kmol/hr	3252.038	7689.754	7689.754	43.70073	0
Temperature °C	59.99852	20	60.05059	34.12198	
Pressure atm	1	1	1	1.5	1.5
Vapor Frac	0	0	0	1	

	ELECTOUT	FIRECO2	FLASHH2O	FUELHEAD	H2-1
Mole Frac					
H2	0.666667	0	1.02E-07	0.84584	1
CH4	0	0	0.004501	0.020101	0
H2O	0	0	0.908886	0.00031	0
CO	0	0	0.012852	0.037075	0
CO2	0	1	0.073553	0.070457	0
CH4O	0	0	5.18E-07	0.004802	0
O2	0.333333	0	0	0	0
N2	0	0	0.000206	0.021414	0
C2H6	0	0	3.29E-07	4.10E-07	0
C3H8	0	0	7.85E-11	1.61E-11	0
C2H4	0	0	3.67E-07	6.66E-07	0
Total Flow kmol/hr	432.9	18	188.9628	182.931	288.6
Temperature °C	25	30	40	40	25
Pressure atm	35	1	35	70	35
Vapor Frac	1	1	0	1	1

	H2O	HOT-AM1	HOT-AM2	HOT-AM3	HOTIN
Mole Frac					
H2	0	0.000543	0.000543	0.000543	0.000541
CH4	0	3.43E-20	3.43E-20	3.43E-20	3.47E-20
H2O	1	0.164181	0.164181	0.164181	0.162916
CO	0	0.001311	0.001311	0.001311	0.001331
CO2	0	0.081051	0.081051	0.081051	0.081999
CH4O	0	1.70E-20	1.70E-20	1.70E-20	1.72E-20
O2	0	0.030106	0.030106	0.030106	0.029941
N2	0	0.722809	0.722809	0.722809	0.723272
C2H6	0	0	0	0	4.36E-38
C3H8	0	0	0	0	1.17E-55
C2H4	0	2.30E-31	2.30E-31	2.30E-31	2.37E-31
Total Flow kmol/hr	288.6	336.4809	336.4809	336.4809	218.7309
Temperature °C	30	1823.316	1600	277.0988	1823.456
Pressure atm	1	1	1	1	1
Vapor Frac	0	1	1	1	1

	HOTOUT1	HOTOUT2	HOTOUT3	METH-1	METH-2
Mole Frac					
H2	0.000541	0.000541	0.000541	0.731769	0.731769
CH4	3.47E-20	3.47E-20	3.47E-20	0.019809	0.019809
H2O	0.162916	0.162916	0.162916	0.023778	0.023778
CO	0.001331	0.001331	0.001331	0.032694	0.032694
CO2	0.081999	0.081999	0.081999	0.073588	0.073588
CH4O	1.72E-20	1.72E-20	1.72E-20	0.099558	0.099558
O2	0.029941	0.029941	0.029941	0	0
N2	0.723272	0.723272	0.723272	0.018804	0.018804
C2H6	4.36E-38	4.36E-38	4.36E-38	4.54E-07	4.54E-07
C3H8	1.17E-55	1.17E-55	1.17E-55	2.44E-11	2.44E-11
C2H4	2.37E-31	2.37E-31	2.37E-31	7.07E-07	7.07E-07
Total Flow kmol/hr	218.7309	218.7309	218.7309	3020.797	3020.797
Temperature °C	681.2507	481.0283	431.8665	251.5976	152.5774
Pressure atm	1	1	1	70	70
Vapor Frac	1	1	1	1	1

	METH-3	METH-4	METH-5	METH-6	METH-7
Mole Frac					
H2	0.731769	0.731769	0.731769	2.50E-07	1.42E-14
CH4	0.019809	0.019809	0.019809	0.017939	0.003598
H2O	0.023778	0.023778	0.023778	0.174317	0.194117
CO	0.032694	0.032694	0.032694	0.004591	0.00016
CO2	0.073588	0.073588	0.073588	0.093684	0.026627
CH4O	0.099558	0.099558	0.099558	0.707403	0.775442
O2	0	0	0	0	0
N2	0.018804	0.018804	0.018804	0.002065	5.52E-05
C2H6	4.54E-07	4.54E-07	4.54E-07	7.34E-07	2.80E-07
C3H8	2.44E-11	2.44E-11	2.44E-11	7.83E-11	5.10E-11
C2H4	7.07E-07	7.07E-07	7.07E-07	9.73E-07	3.21E-07
Total Flow kmol/hr	3020.797	3020.797	3020.797	407.392	363.6913
Temperature °C	149.2314	140.9725	40	40	34.12198
Pressure atm	70	70	70	70	1.5
Vapor Frac	1	1	0.865135	0	0

	METH-8	MIXTOATR	NG-AM	NG-FEED1	NG-FEED2
Mole Frac					
H2	1.42E-14	0.056687	0	0	0
CH4	0.003598	0.600975	1	0.950525	0.950525
H2O	0.194117	0.281176	0	0	0
CO	0.00016	0.000579	0	0	0
CO2	0.026627	0.049612	0	0.00501	0.00501
CH4O	0.775442	9.64E-09	0	0	0
O2	0	6.13E-31	0	0.000193	0.000193
N2	5.52E-05	0.010929	0	0.017736	0.017736
C2H6	2.80E-07	4.15E-05	0	0.024226	0.024226
C3H8	5.10E-11	1.82E-08	0	0.00231	0.00231
C2H4	3.21E-07	1.01E-08	0	0	0
Total Flow kmol/hr	363.6913	438.9611	27.71321	270.5	270.5
Temperature °C	34.12195	640.3123	30	132	380
Pressure atm	1.5	35	1	35	35
Vapor Frac	0	1	1	1	1

	NG-FIRE	NGSTEAM1	NGSTEAM2	NGSTEAM3	NGSTEAM4
Mole Frac					
H2	0	0	0	0.058338	0.058338
CH4	0.950525	0.626992	0.626992	0.618474	0.618474
H2O	0	0.340373	0.340373	0.289363	0.289363
CO	0	0	0	0.000596	0.000596
CO2	0.00501	0.003305	0.003305	0.021939	0.021939
CH4O	0	0	0	9.92E-09	9.92E-09
O2	0.000193	0.000127	0.000127	6.31E-31	6.31E-31
N2	0.017736	0.011699	0.011699	0.011248	0.011248
C2H6	0.024226	0.01598	0.01598	4.28E-05	4.28E-05
C3H8	0.00231	0.001524	0.001524	1.87E-08	1.87E-08
C2H4	0	0	0	1.04E-08	1.04E-08
Total Flow kmol/hr	18.03	410.0799	410.0799	426.5411	426.5411
Temperature °C	30	378.6687	450	450	655
Pressure atm	1	35	35	35	35
Vapor Frac	1	1	1	1	1

	O2-1	O2-2	O2STEAM1	O2STEAM2	PLANTCO2
Mole Frac					
H2	0	0	0	0	0
CH4	0	0	0	0	0
H2O	0	0	0.194732	0.194732	0
CO	0	0	0	0	0
CO2	0	0	0	0	1
CH4O	0	0	0	0	0
O2	1	1	0.805268	0.805268	0
N2	0	0	0	0	0
C2H6	0	0	0	0	0
C3H8	0	0	0	0	0
C2H4	0	0	0	0	0
Total Flow kmol/hr	144.3	144.3	179.195	179.195	58.2
Temperature °C	25	360	362.3701	421.8633	30
Pressure atm	35	35	35	35	1
Vapor Frac	1	1	1	1	1

	RECYCLE1	RECYCLE2	RECYCLE3	STEAM-1	STEAM-2
Mole Frac					
H2	0.84584	0.84584	0.84584	0	0
CH4	0.020101	0.020101	0.020101	0	0
H2O	0.00031	0.00031	0.00031	1	1
CO	0.037075	0.037075	0.037075	0	0
CO2	0.070457	0.070457	0.070457	0	0
CH4O	0.004802	0.004802	0.004802	0	0
O2	0	0	0	0	0
N2	0.021414	0.021414	0.021414	0	0
C2H6	4.10E-07	4.10E-07	4.10E-07	0	0
C3H8	1.61E-11	1.61E-11	1.61E-11	0	0
C2H4	6.66E-07	6.66E-07	6.66E-07	0	0
Total Flow kmol/hr	2613.3	2430.369	2430.369	635	174.4749
Temperature °C	40	40	231	380	380
Pressure atm	70	70	70	35	35
Vapor Frac	1	1	1	1	1

	STEAM-3	STEAM-4	STEAM-H1	STEAM-H2	STEAMAM1
Mole Frac					
H2	0	0	0	0	0
CH4	0	0	0	0	0
H2O	1	1	1	1	1
CO	0	0	0	0	0
CO2	0	0	0	0	0
CH4O	0	0	0	0	0
O2	0	0	0	0	0
N2	0	0	0	0	0
C2H6	0	0	0	0	0
C3H8	0	0	0	0	0
C2H4	0	0	0	0	0
Total Flow kmol/hr	139.5799	34.89498	460.5251	460.5251	47603.31
Temperature °C	380	380	380	243.3371	130
Pressure atm	35	35	35	35	1
Vapor Frac	1	1	1	0.225545	1

	STEAMAM2	STEAMAM3	SYN1-1	SYN1-2	SYNGAS-1
Mole Frac					
H2	0	0	0.524474	0.524474	0.524474
CH4	0	0	0.012105	0.012105	0.012105
H2O	1	1	0.178276	0.178276	0.178276
CO	0	0	0.236912	0.236912	0.236912
CO2	0	0	0.043326	0.043326	0.043326
CH4O	0	0	1.13E-07	1.13E-07	1.13E-07
O2	0	0	5.37E-17	5.37E-17	5.37E-17
N2	0	0	0.004906	0.004906	0.004906
C2H6	0	0	4.46E-07	4.46E-07	4.46E-07
C3H8	0	0	5.08E-11	5.08E-11	5.08E-11
C2H4	0	0	6.01E-07	6.01E-07	6.01E-07
Total Flow kmol/hr	47603.31	47603.31	977.8607	977.8607	977.8607
Temperature °C	140	140	423.6451	314.9345	1050
Pressure atm	1	1	35	35	35
Vapor Frac	1	1	1	1	1

	SYNGAS-2	SYNGAS-3	SYNGAS-4
Mole Frac			
H2	0.524474	0.524474	0.590378
CH4	0.012105	0.012105	0.008719
H2O	0.178276	0.178276	0.128415
CO	0.236912	0.236912	0.170652
CO2	0.043326	0.043326	0.0983
CH4O	1.13E-07	1.13E-07	8.13E-08
O2	5.37E-17	5.37E-17	3.87E-17
N2	0.004906	0.004906	0.003534
C2H6	4.46E-07	4.46E-07	3.21E-07
C3H8	5.08E-11	5.08E-11	3.66E-11
C2H4	6.01E-07	6.01E-07	4.33E-07
Total Flow kmol/hr	977.8607	977.8607	1357.541
Temperature °C	153.5672	40	35.53131
Pressure atm	35	35	35
Vapor Frac	0.972352	0.812605	0.859858

	SYNGAS-5	SYNGAS-6	SYNGAS-7
Mole Frac			
H2	0.685844	0.685844	0.793889
CH4	0.009402	0.009402	0.016627
H2O	0.002211	0.002211	0.000927
CO	0.196169	0.196169	0.088733
CO2	0.102302	0.102302	0.080797
CH4O	1.07E-08	1.07E-08	0.003243
O2	0	0	0
N2	0.004072	0.004072	0.015783
C2H6	3.20E-07	3.20E-07	3.81E-07
C3H8	2.98E-11	2.98E-11	2.05E-11
C2H4	4.44E-07	4.44E-07	5.94E-07
Total Flow kmol/hr	1168.578	1168.578	3598.947
Temperature °C	40	231.3724	231.0847
Pressure atm	35	70	70
Vapor Frac	1	1	1

Appendix B: Scenario 2 Aspen Simulation Results

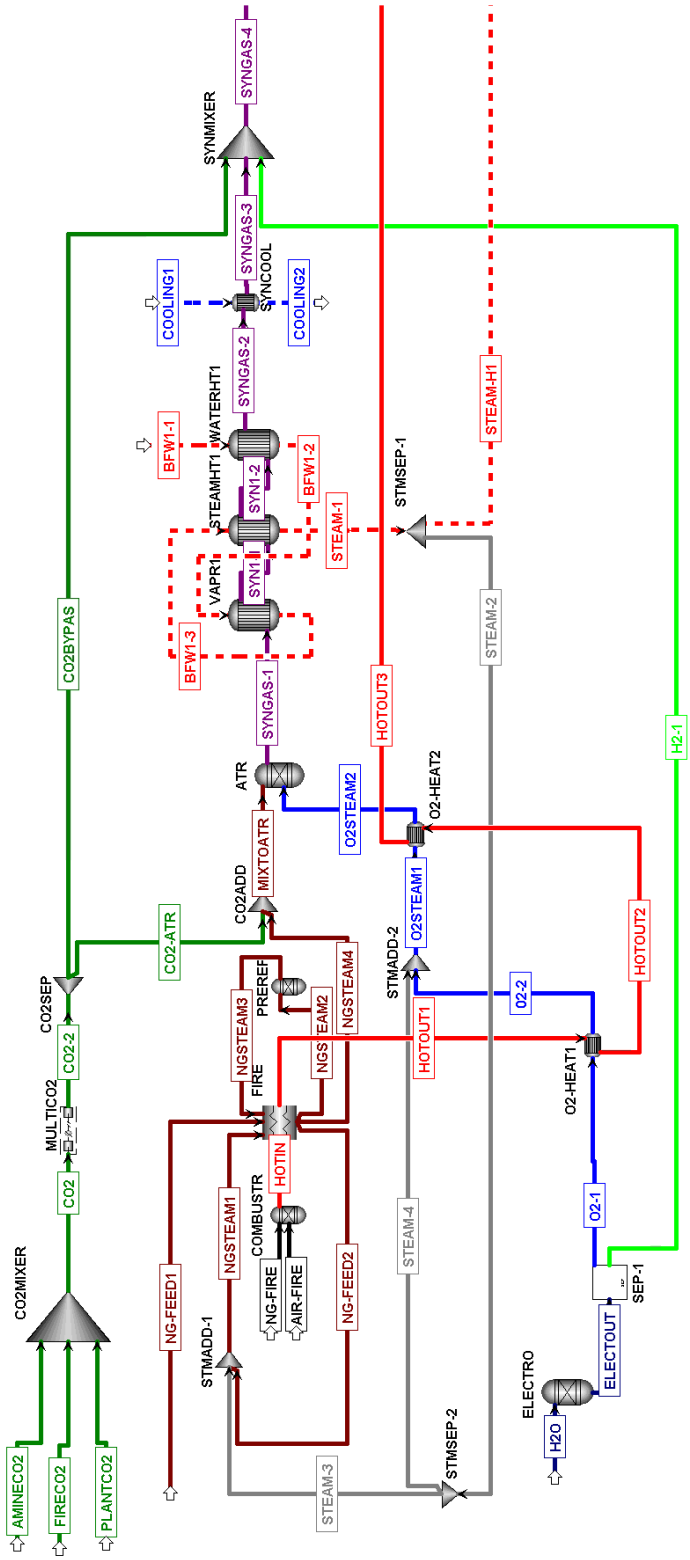

Figure B.1 Scenario 2 Aspen simulation with PSA part 1: Electrolyser and ATR section.

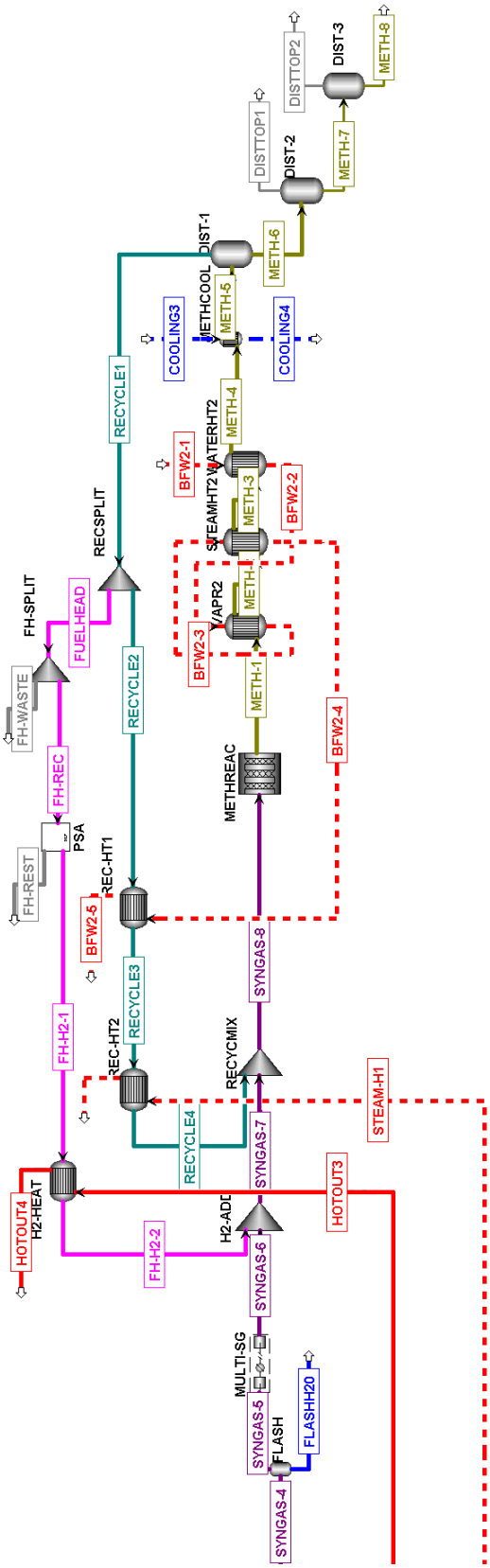

Figure B.2 Scenario 2 Aspen simulation with PSA part 2: Methanol reactor section.

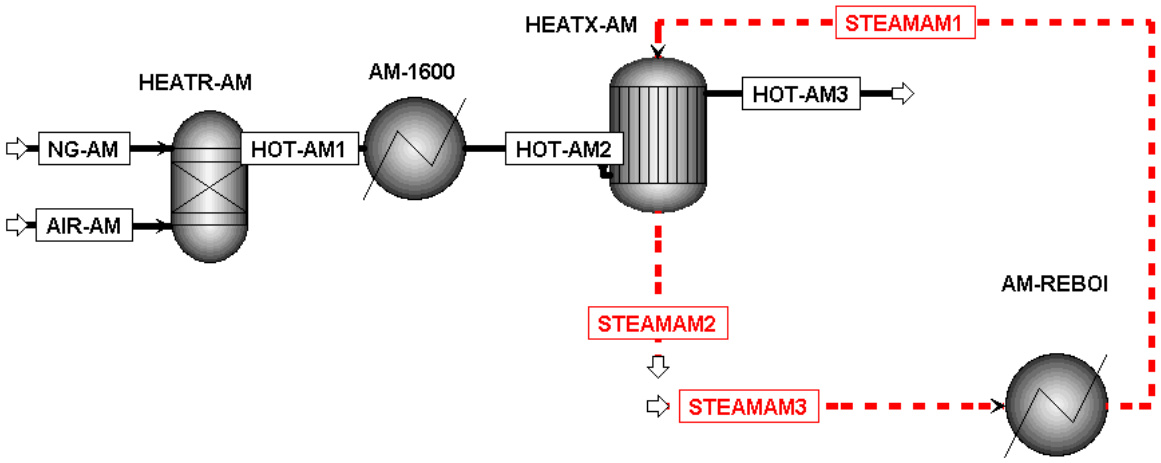

Figure B.3 Scenario 2 Aspen simulation with PSA part 3: Amine reboiler section.

Table B.1 Scenario 2 Aspen simulation stream results

	AIR-AM	AIR-FIRE	AMINECO2	BFW1-1	BFW1-2
Mole Frac					
H2	0	0	0	0	0
CH4	0	0	0	0	0
H2O	0	0	0	1	1
CO	0	0	0	0	0
CO2	0	0	1	0	0
CH4O	0	0	0	0	0
O2	0.21152	0.21152	0	0	0
N2	0.78848	0.78848	0	0	0
C2H6	0	0	0	0	0
C3H8	0	0	0	0	0
C2H4	0	0	0	0	0
Total Flow kmol/hr	308.3032	200.2361	27.3	650	650
Temperature °C	30	30	40	121	240
Pressure atm	1	1	1	35	35
Vapor Frac	1	1	1	0	0

	BFW1-3	BFW2-1	BFW2-2	BFW2-3	BFW2-4
Mole Frac					
H2	0	0	0	0	0
CH4	0	0	0	0	0
H2O	1	1	1	1	1
CO	0	0	0	0	0
CO2	0	0	0	0	0
CH4O	0	0	0	0	0
O2	0	0	0	0	0
N2	0	0	0	0	0
C2H6	0	0	0	0	0
C3H8	0	0	0	0	0
C2H4	0	0	0	0	0
Total Flow kmol/hr	650	250	250	250	250
Temperature °C	243.3371	50	95	99.99782	140
Pressure atm	35	1	1	1	1
Vapor Frac	1	0	0	1	1

	BFW2-5	CO2	CO2-2	CO2-ATR	CO2BYPAS
Mole Frac					
H2	0	0	0	0	0
CH4	0	0	0	0	0
H2O	1	0	0	0	0
CO	0	0	0	0	0
CO2	0	1	1	1	1
CH4O	0	0	0	0	0
O2	0	0	0	0	0
N2	0	0	0	0	0
C2H6	0	0	0	0	0
C3H8	0	0	0	0	0
C2H4	0	0	0	0	0
Total Flow kmol/hr	250	103.5	103.5	12.42	91.08
Temperature °C	93	40.00001	40	40	40
Pressure atm	1	1	35	35	35
Vapor Frac	0	1	1	1	1

	COOLING1	COOLING2	COOLING3	COOLING4	DISTTOP1
Mole Frac					
H2	0	0	0	0	2.04E-05
CH4	0	0	0	0	0.29567
H2O	1	1	1	1	0.015441
CO	0	0	0	0	0.083862
CO2	0	0	0	0	0.374405
CH4O	0	0	0	0	0.172727
O2	0	0	0	0	0
N2	0	0	0	0	0.057855
C2H6	0	0	0	0	7.27E-06
C3H8	0	0	0	0	3.89E-10
C2H4	0	0	0	0	1.12E-05
Total Flow kmol/hr	3037.591	3037.591	16665.08	16665.08	6.296491
Temperature °C	20	59.96944	20	59.93146	39.32131
Pressure atm	1	1	1	1	1.5
Vapor Frac	0	0	0	0	1

	DISTTOP2	ELECTOUT	FH-H2-1	FH-H2-2	FH-REC
Mole Frac					
H2	0	0.666667	1	1	0.947187
CH4	0	0	0	0	0.012573
H2O	0	0	0	0	0.000396
CO	0	0	0	0	0.011404
CO2	0	0	0	0	0.014204
CH4O	0	0	0	0	0.004594
O2	0	0.333333	0	0	0
N2	0	0	0	0	0.00964
C2H6	0	0	0	0	2.81E-07
C3H8	0	0	0	0	1.20E-11
C2H4	0	0	0	0	4.46E-07
Total Flow kmol/hr	0	432.9	382.4657	382.4657	448.6566
Temperature °C		25	40	230	40
Pressure atm	1.5	35	70	70	70
Vapor Frac		1	1	1	1

	FH-REST	FH-WASTE	FIRECO2	FLASHH2O	FUELHEAD
Mole Frac					
H2	0.642024	0	0	1.02E-07	0.947187
CH4	0.085222	0	0	0.004476	0.012573
H2O	0.002688	0	0	0.908887	0.000396
CO	0.077297	0	0	0.012845	0.011404
CO2	0.096281	0	1	0.073585	0.014204
CH4O	0.031141	0	0	5.15E-07	0.004594
O2	0	0	0	0	0
N2	0.065342	0	0	0.000206	0.00964
C2H6	1.91E-06	0	0	3.25E-07	2.81E-07
C3H8	8.13E-11	0	0	7.72E-11	1.20E-11
C2H4	3.02E-06	0	0	3.63E-07	4.46E-07
Total Flow kmol/hr	66.19097	0	18	189.7908	448.6566
Temperature °C	40		40	40	40
Pressure atm	70		1	35	70
Vapor Frac	0.964188		1	0	1

	H2-1	H2O	HOT-AM1	HOT-AM2	HOT-AM3
Mole Frac					
H2	1	0	0.000546	0.000546	0.000546
CH4	0	0	3.50E-20	3.50E-20	3.50E-20
H2O	0	1	0.164252	0.164252	0.164252
CO	0	0	0.001319	0.001319	0.001319
CO2	0	0	0.08108	0.08108	0.08108
CH4O	0	0	1.73E-20	1.73E-20	1.73E-20
O2	0	0	0.030028	0.030028	0.030028
N2	0	0	0.722775	0.722775	0.722775
C2H6	0	0	0	0	0
C3H8	0	0	0	0	0
C2H4	0	0	2.37E-31	2.37E-31	2.37E-31
Total Flow kmol/hr	288.6	288.6	336.3301	336.3301	336.3301
Temperature °C	25	30	1823.916	1600	276.4679
Pressure atm	35	1	1	1	1
Vapor Frac	1	0	1	1	1

	HOTIN	HOTOUT1	HOTOUT2	HOTOUT3	HOTOUT4
Mole Frac					
H2	0.000541	0.000541	0.000541	0.000541	0.000541
CH4	3.47E-20	3.47E-20	3.47E-20	3.47E-20	3.47E-20
H2O	0.162916	0.162916	0.162916	0.162916	0.162916
CO	0.001331	0.001331	0.001331	0.001331	0.001331
CO2	0.081999	0.081999	0.081999	0.081999	0.081999
CH4O	1.72E-20	1.72E-20	1.72E-20	1.72E-20	1.72E-20
O2	0.029941	0.029941	0.029941	0.029941	0.029941
N2	0.723272	0.723272	0.723272	0.723272	0.723272
C2H6	4.36E-38	4.36E-38	4.36E-38	4.36E-38	4.36E-38
C3H8	1.17E-55	1.17E-55	1.17E-55	1.17E-55	1.17E-55
C2H4	2.37E-31	2.37E-31	2.37E-31	2.37E-31	2.37E-31
Total Flow kmol/hr	218.7309	218.7309	218.7309	218.7309	218.7309
Temperature °C	1823.456	680.1509	479.8748	431.2035	129.3373
Pressure atm	1	1	1	1	1
Vapor Frac	1	1	1	1	1

	METH-1	METH-2	METH-3	METH-4	METH-5
Mole Frac					
H2	0.885361	0.885361	0.885361	0.885361	0.885361
CH4	0.012524	0.012524	0.012524	0.012524	0.012524
H2O	0.015921	0.015921	0.015921	0.015921	0.015921
CO	0.010756	0.010756	0.010756	0.010756	0.010756
CO2	0.014595	0.014595	0.014595	0.014595	0.014595
CH4O	0.051769	0.051769	0.051769	0.051769	0.051769
O2	0	0	0	0	0
N2	0.009074	0.009074	0.009074	0.009074	0.009074
C2H6	2.99E-07	2.99E-07	2.99E-07	2.99E-07	2.99E-07
C3H8	1.54E-11	1.54E-11	1.54E-11	1.54E-11	1.54E-11
C2H4	4.62E-07	4.62E-07	4.62E-07	4.62E-07	4.62E-07
Total Flow kmol/hr	6856.835	6856.835	6856.835	6856.835	6856.835
Temperature °C	251.5546	204.1616	202.5734	198.6563	40
Pressure atm	70	70	70	70	70
Vapor Frac	1	1	1	1	0.934727

	METH-6	METH-7	METH-8	MIXTOATR	NG-AM
Mole Frac					
H2	2.87E-07	1.49E-13	1.49E-13	0.056768	0
CH4	0.011818	0.007768	0.007768	0.599831	1
H2O	0.23823	0.241409	0.241409	0.282304	0
CO	0.001474	0.000298	0.000298	0.000578	0
CO2	0.020176	0.015121	0.015121	0.049568	0
CH4O	0.727331	0.735245	0.735245	9.65E-09	0
O2	0	0	0	6.16E-31	0
N2	0.000969	0.000157	0.000157	0.010909	0
C2H6	5.44E-07	4.48E-07	4.48E-07	4.13E-05	0
C3H8	6.45E-11	5.98E-11	5.98E-11	1.80E-08	0
C2H4	6.99E-07	5.49E-07	5.49E-07	1.00E-08	0
Total Flow kmol/hr	447.5636	441.2671	441.2671	439.7645	27.71321
Temperature °C	40	39.32131	39.32132	640.3306	30
Pressure atm	70	1.5	1.5	35	1
Vapor Frac	0	0	0	1	1

	NG-FEED1	NG-FEED2	NG-FIRE	NGSTEAM1	NGSTEAM2
Mole Frac					
H2	0	0	0	0	0
CH4	0.950525	0.950525	0.950525	0.625828	0.625828
H2O	0	0	0	0.341597	0.341597
CO	0	0	0	0	0
CO2	0.00501	0.00501	0.00501	0.003299	0.003299
CH4O	0	0	0	0	0
O2	0.000193	0.000193	0.000193	0.000127	0.000127
N2	0.017736	0.017736	0.017736	0.011677	0.011677
C2H6	0.024226	0.024226	0.024226	0.015951	0.015951
C3H8	0.00231	0.00231	0.00231	0.001521	0.001521
C2H4	0	0	0	0	0
Total Flow kmol/hr	270.5	270.5	18.03	410.8427	410.8427
Temperature °C	132	380	30	378.6656	450
Pressure atm	35	35	1	35	35
Vapor Frac	1	1	1	1	1

	NGSTEAM3	NGSTEAM4	O2-1	O2-2	O2STEAM1
Mole Frac					
H2	0.058418	0.058418	0	0	0
CH4	0.617264	0.617264	0	0	0
H2O	0.290509	0.290509	0	0	0.195588
CO	0.000595	0.000595	0	0	0
CO2	0.021945	0.021945	0	0	0
CH4O	9.93E-09	9.93E-09	0	0	0
O2	6.34E-31	6.34E-31	1	1	0.804412
N2	0.011227	0.011227	0	0	0
C2H6	4.25E-05	4.25E-05	0	0	0
C3H8	1.86E-08	1.86E-08	0	0	0
C2H4	1.03E-08	1.03E-08	0	0	0
Total Flow kmol/hr	427.3445	427.3445	144.3	144.3	179.3857
Temperature °C	450	655	25	360	362.3823
Pressure atm	35	35	35	35	35
Vapor Frac	1	1	1	1	1

	O2STEAM2	PLANTCO2	RECYCLE1	RECYCLE2	RECYCLE3
Mole Frac					
H2	0	0	0.947187	0.947187	0.947187
CH4	0	0	0.012573	0.012573	0.012573
H2O	0.195588	0	0.000396	0.000396	0.000396
CO	0	0	0.011404	0.011404	0.011404
CO2	0	1	0.014204	0.014204	0.014204
CH4O	0	0	0.004594	0.004594	0.004594
O2	0.804412	0	0	0	0
N2	0	0	0.00964	0.00964	0.00964
C2H6	0	0	2.81E-07	2.81E-07	2.81E-07
C3H8	0	0	1.20E-11	1.20E-11	1.20E-11
C2H4	0	0	4.46E-07	4.46E-07	4.46E-07
Total Flow kmol/hr	179.3857	58.2	6409.381	5960.724	5960.724
Temperature °C	421.2013	40	40	40	100.4756
Pressure atm	35	1	70	70	70
Vapor Frac	1	1	1	1	1

	RECYCLE4	STEAM-1	STEAM-2	STEAM-3	STEAM-4
Mole Frac					
H2	0.947187	0	0	0	0
CH4	0.012573	0	0	0	0
H2O	0.000396	1	1	1	1
CO	0.011404	0	0	0	0
CO2	0.014204	0	0	0	0
CH4O	0.004594	0	0	0	0
O2	0	0	0	0	0
N2	0.00964	0	0	0	0
C2H6	2.81E-07	0	0	0	0
C3H8	1.20E-11	0	0	0	0
C2H4	4.46E-07	0	0	0	0
Total Flow kmol/hr	5960.724	650	175.4284	140.3427	35.08569
Temperature °C	230	380	380	380	380
Pressure atm	70	35	35	35	35
Vapor Frac	1	1	1	1	1

	STEAM-H1	STEAM-H2	STEAMAM1	STEAMAM2	STEAMAM3
Mole Frac					
H2	0	0	0	0	0
CH4	0	0	0	0	0
H2O	1	1	1	1	1
CO	0	0	0	0	0
CO2	0	0	0	0	0
CH4O	0	0	0	0	0
O2	0	0	0	0	0
N2	0	0	0	0	0
C2H6	0	0	0	0	0
C3H8	0	0	0	0	0
C2H4	0	0	0	0	0
Total Flow kmol/hr	474.5716	474.5716	47603.31	47603.31	47603.31
Temperature °C	380	116.3012	130	140	140
Pressure atm	35	35	1	1	1
Vapor Frac	1	0	1	1	1

	SYN1-1	SYN1-2	SYNGAS-1	SYNGAS-2	SYNGAS-3
Mole Frac					
H2	0.524225	0.524225	0.524225	0.524225	0.524225
CH4	0.012032	0.012032	0.012032	0.012032	0.012032
H2O	0.17885	0.17885	0.17885	0.17885	0.17885
CO	0.236569	0.236569	0.236569	0.236569	0.236569
CO2	0.043423	0.043423	0.043423	0.043423	0.043423
CH4O	1.13E-07	1.13E-07	1.13E-07	1.13E-07	1.13E-07
O2	5.41E-17	5.41E-17	5.41E-17	5.41E-17	5.41E-17
N2	0.004901	0.004901	0.004901	0.004901	0.004901
C2H6	4.41E-07	4.41E-07	4.41E-07	4.41E-07	4.41E-07
C3H8	4.99E-11	4.99E-11	4.99E-11	4.99E-11	4.99E-11
C2H4	5.94E-07	5.94E-07	5.94E-07	5.94E-07	5.94E-07
Total Flow kmol/hr	978.9319	978.9319	978.9319	978.9319	978.9319
Temperature °C	408.7962	297.3957	1050	150.2206	40
Pressure atm	35	35	35	35	35
Vapor Frac	1	1	1	0.956346	0.811987

	SYNGAS-4	SYNGAS-5	SYNGAS-6	SYNGAS-7	SYNGAS-8
Mole Frac					
H2	0.590147	0.685973	0.685973	0.763396	0.909233
CH4	0.008669	0.00935	0.00935	0.007045	0.011431
H2O	0.128868	0.00221	0.00221	0.001665	0.000659
CO	0.170457	0.19605	0.19605	0.147714	0.039553
CO2	0.098327	0.102345	0.102345	0.077112	0.027195
CH4O	8.11E-08	1.06E-08	1.06E-08	8.01E-09	0.003646
O2	3.90E-17	0	0	0	0
N2	0.003531	0.004071	0.004071	0.003067	0.008283
C2H6	3.18E-07	3.16E-07	3.16E-07	2.38E-07	2.73E-07
C3H8	3.60E-11	2.93E-11	2.93E-11	2.21E-11	1.41E-11
C2H4	4.28E-07	4.39E-07	4.39E-07	3.31E-07	4.22E-07
Total Flow kmol/hr	1358.612	1168.821	1168.821	1551.287	7512.011
Temperature °C	35.53665	40	231.3727	230.8566	230.1286
Pressure atm	35	35	70	70	70
Vapor Frac	0.859358	1	1	1	1